

**Manipulating Selectivity and Reactivity in
Palladium-Catalyzed Oxidation Reactions**

Thesis by
Zachary Kimble Wickens

In Partial Fulfillment of the Requirements for the
degree of
Doctor of Philosophy



CALIFORNIA INSTITUTE OF TECHNOLOGY

Pasadena, California

2015

(Defended June 2nd, 2015)

© 2015
Zachary Kimble Wickens
All Rights Reserved

Dedicated to my parents for never pushing me to become a scientist

Acknowledgments

The work I have the pleasure of sharing with you in this thesis would have been completely impossible without the help (both emotional and intellectual) of a tremendously large number of people. First, I want to thank my advisor, Bob Grubbs. I truly could not have asked for a more incredible thesis advisor. Since the beginning of my time at Caltech, you have subtly guided me towards the water but never forced me to drink. You have given me independence in choosing which projects to pursue and the directions these projects go, but always provided suggestions and hints along the way that have kept me on track. I know you will continue to provide great advice and strong support even long after I've left Caltech. Thanks for being my invisible safety net over the last five years.

I would have never even considered pursuing a Ph.D in chemistry in the first place if it weren't for the fantastic chemistry faculty at Macalester College. Rebecca Hoye, Ronald Brisbois, Paul Fischer, Keith Kuwata, Thomas Varberg and Katherine Splan, you were all tremendously influential in my life. You taught me how to see the exciting puzzles that are scattered throughout the field of chemistry. Becky and Ron, thanks for putting me on a track to pursue organic chemistry. I haven't looked back. In addition to the chemistry faculty, Chad Topaz in the Mathematics department also deserves special mention. You were the very first one to show me how exciting experimental research could be, how research hurdles are just challenges to solve and how satisfying it is to take even small

steps towards the research goal.

When I initially left Macalester, I thought there was no way Caltech could come anywhere close to the sense of community and belonging I felt at Mac. That assumption was rapidly dismissed. The community at Caltech is unbelievable. First, I have to thank my committee members: Brian Stoltz, Jonas Peters and Sarah Reisman. All three of you have provided excellent advice and feedback on numerous occasions and I couldn't ask for a better committee. Next, I have to thank the Grubbs group, past and present. You guys have been incredible! First, I want to thank Linda Syme. We would be a mess without you. Thanks for holding the group together. Next, I want to thank my mentors in the lab. When I first joined the group, I was paired with Dr. Guangbin Dong. I couldn't have been paired with a better mentor—you are the full package: brilliant, patient and friendly. You taught me a huge amount about chemistry, both in terms of techniques as well as understanding and philosophy. I've enjoyed watching you rapidly become a giant in the field of catalysis. Next, Dr. Bill Morandi, my mentor and palladium partner-in-crime. Discussing ideas with you (both chemistry and non-chemistry) will obviously be one of my most lasting memories from my Ph.D. I learned an unbelievably large amount from you—ranging from how to construct and write a paper to how to "do it now." As much as everyone (including us) thought our epic hallway/Red Door/turtle pond/basement/conference room/street corner conversations were a waste of time, I think they were arguably amongst my most

valuable experiences in graduate school. I hope I can somehow, some way, convince you to collaborate again in the future. I look forward to watching your independent career take shape—you are open-minded, creative and extraordinarily intelligent. I am confident you will save the world in no time. Beyond these two, I've had to good fortune to collaborate with several other incredibly talented postdocs and graduate students over the past five years: Dr. Peili Teo, Dr. Pablo Guzmán, Dr. Peter Dornan, Crystal Chu and Jiaming Li. Without you guys, I'd have nothing to put in this thesis. I greatly appreciate your insights, suggestions and hard work in the lab. Dr. Benjamín Sveinbjörnsson, Dr. Chris Daeffler, and Dr. Jean Li, thanks for making me feel welcome and answering my stupid questions when I first joined the group. Dr. Raymond Weitekamp and Brendan Quigley, you guys were an awesome cohort to share each year of the graduate school experience with. Dr. Bill Morandi, Dr. John Hartung, Dr. Keary (and Jae) Engle, Dr. Jeff Cannon, Dr. Shane Mangold, Dr. Rob "Big Mac" MacFarlane, Dr. Peter Dornan, Dr. Myles Herbert, Crystal Chu and Alice Chang, you guys have been my closest friends in the lab as well as easily amongst the closest friends I've had in my life. Thank you for the support and for pretending to enjoy long-ass discussions/arguments with me about nothing of value. Julian Edwards, Lauren Rosenbrugh, Tonia Ahmed, Dr. Vanessa Marx, Dr. Sarah Bronner, Dr. Juneyoung Lee, Dr. Pablo Guzman, Dr. Benjamin Keith Keitz, Dr. Joshua Palmer, Dr. Chris Bates, Dr. Hoyong Chung, Dr. Jeremiah Johnson, Dr. Melanie Pribisko Yen, Carl Blumenfeld, Anton Toutov, Dr.

Garret Miyake, Dr. Rosemary Conrad-Kiser, Dr. Vlad Iluc and Dr. Matthew VanWingerden you all have been excellent labmates and friends over the past years. Keep it up. As an aside, Dr. Jeremiah Johnson, you probably don't remember this but you once told me "time is money" when I was doing something stupid and time-consuming in lab. Although I can't claim to have started always spending my time wisely (see section regarding Dr. Bill Morandi), this one offhand comment from you has stuck with me, and made sure that I was always at least thinking about how I was spending my time. I have had the privilege of mentoring three exceptional undergraduates over my time here at Caltech: Kacper Skakuj, Brian Carr and Renee Sifri. You guys were awesome! All three of you were a graduate student's dream undergraduate: your work ethic and enthusiasm were unparalleled. You are talented and creative and I expect great things from each of you. I've also got to thank (not Dr.) Benjamin Suslick. Thanks for putting up with being made fun of by me for your tenure in the Grubbs lab. In a moment of honesty, I'd just like to say that I'm confident that you're going to do extraordinarily well in graduate school and in your career as a chemist.

My research at Caltech would have had a premature halt without the help of the whole department. Dave VanderVelde, thank you for keeping the NMR facility operating smoothly and for teaching me a tremendous amount about NMR hardware and physics. Mona and Naseem, thanks for putting up with me when I brought you a pile of samples for get high resolution mass spec and said "is there any chance I

can get these in the next few days?" Somehow, you two always did it. Scott Virgil, you are a unique asset to the Caltech chemistry department. You seem to know everything about everything and be willing to help anyone with anything. Thanks to Rick Gerhart for making me glassware that I dreamt up and for fixing glassware that I smashed. Finally, Joe Drew, Agnes Tong, Steve Gould and Anne Penney, thanks for keeping everything running smoothly.

Finally, I want to thank my friends outside of the lab (in particular Dr. Madeleine Kieffer, Kangway Chuang, Haoxuan Wang, Raul Navarro and Jon Rittle, as well as many others) and my parents. Last, but not least, I want to thank Natalie Khuen. I can think of lots of clichés that could apply here but I'll strive for at least slightly more originality. Thanks for your love and support over the past seven(!) years. Thanks for recognizing that "lab time" is not the same as the hours, minutes, and seconds used by normal people. Thanks for listening when I jabber on about the reclining man. Thanks for providing a place (and a beach!) for me to run away to when you lived in Santa Maria or in La Jolla and thanks for moving to LA and being there when I come home.

Abstract

Since the initial discovery of the Wacker process over half a century ago, the Wacker oxidation has become a premier reaction for the oxidation of terminal alkenes to methyl ketones. This thesis describes strategies for manipulating selectivity and reactivity in Wacker-type oxidations to provide synthetically useful transformations.

Chapter 2 describes how nitrite co-catalysts can be exploited in Wacker oxidations to reverse their typically high Markovnikov selectivity. Using these aerobic oxidation conditions, alkenes can be oxidized to aldehydes in high yield and selectivity. Preliminary mechanistic experiments are presented that are consistent with oxygen atom transfer from the nitrite catalyst to the substrate. The influence of proximal functionality on the new reaction is explored, yielding both synthetically useful transformations and further mechanistic insight.

Chapter 3 investigates how minor modifications to the nitrite-modified Wacker can interrupt the Wacker oxidation pathway, providing dioxygenated products using molecular oxygen as the terminal oxidant. A variety of functional groups are tolerated and high yields of 1,2-diacetylated products are obtained with a range of substrates. Mechanistic experiments are presented that demonstrate the kinetic competency of nitrogen dioxide to mediate the reaction and probe the nature of the reductive elimination event.

Chapter 4 details the development of a highly active Wacker-type oxidation capable of efficiently oxidizing internal alkenes, which are unreactive under

classical conditions. Under these simple and mild reaction conditions, a wide range of functional groups are tolerated and molecular oxygen can be employed as the terminal oxidant. Furthermore, the regioselectivity in unsymmetrical internal alkenes is investigated.

Chapter 5 explores the origins of innate regioselectivity in Wacker oxidations. Systematic investigations of both internal and terminal alkenes illustrate that inductive effects are sufficient to dramatically influence Wacker regioselectivity. These observations lead to the development of a simple set of reactions conditions that strongly enforces Markovnikov's rule, even with substrates that provide mixtures of aldehydes and ketones under classical conditions.

TABLE OF CONTENTS

Acknowledgments	3
Abstract	8
Table of Contents	10
Chapter 1 INTRODUCTION	12
Introduction	13
Mechanistic Overview	14
Challenges Associated with Wacker Regioselectivity	16
Conclusion	26
References	27
Chapter 2 CATALYST-CONTROLLED ALDEHYDE-SELECTIVE WACKER ENABLED BY CO-CATALYTIC NITRITE	31
Abstract	32
<i>Aldehyde-Selective Wacker Oxidation of Unbiased Alkenes</i>	
Introduction	32
Results and Discussion	36
Conclusion	47
<i>Nitrite-Modified Wacker Oxidation to Access Functionalized Aldehydes</i>	
Introduction	47
Results and Discussion	50
Conclusion	58
Experimental Section	59
References	87
Chapter 3 AEROBIC PALLADIUM-CATALYZED ALKENE DIOXYGENATION ENABLED BY CO-CATALYTIC NITRITE	95
Abstract	96
Introduction	96
Results and Discussion	99
Conclusion	108
Experimental Section	108

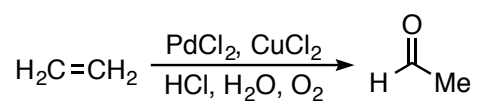
	References and Notes	121
Chapter 4	GENERAL AND PRACTICAL WACKER-TYPE OXIDATION OF INTERNAL ALKENES	125
	Abstract	126
	<i>Highly Active Wacker System for the Oxidation of Internal Alkenes</i>	
	Introduction	126
	Results and Discussion	128
	Conclusion	136
	<i>Rapid Access to Functionalized Ketones from Internal Alkenes</i>	
	Introduction	136
	Results and Discussion	138
	Conclusion	144
	Experimental Section	145
	References	172
Chapter 5	UNDERSTANDING AND MANIPULATING INNATE NUCLEOPALLADATION REGIOSELECTIVITY	176
	Abstract	177
	Introduction	177
	<i>Results and Discussion</i>	179
	Conclusion	190
	Experimental Section	190
	References	218

CHAPTER 1

INTRODUCTION

Introduction

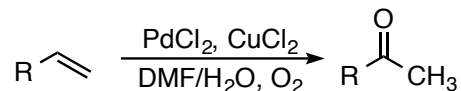
The Wacker oxidation has become a premier reaction for the catalytic oxidation of alkenes to carbonyls due to its efficiency and functional-group tolerance.¹⁻³ The stoichiometric oxidation of alkenes to carbonyl compounds by palladium salts was originally observed by Phillips in 1894.⁴ Over half a century later, Smidt and coworkers discovered that the process could be rendered catalytic in palladium by the inclusion of copper salts, which mediate the thermodynamically favorable aerobic reoxidation of Pd(0) to Pd(II).⁵ Following this discovery, the process was rapidly optimized and adopted by Wacker Chemie for the large-scale preparation of acetaldehyde from ethylene (Scheme 1.1).⁶ The total production capacity of acetaldehyde via the Wacker process reached over two million tons per year.⁶ However, these conditions were not applicable to the oxidation of heavier alkene substrates.



Scheme 1.1 Wacker process for the conversion of ethylene to acetaldehyde.

Given the potential utility of this oxidation in organic synthesis, a more general variant of these conditions was pioneered initially by Clemet⁷ and later substantially advanced by Tsuji.¹ The resultant Tsuji–Wacker conditions resemble those of the Wacker process but employ a mixed DMF and water solvent system (Scheme 1.2). These conditions provide a general and practical

catalytic reaction for the oxidation of more complex alkenes to carbonyl compounds.

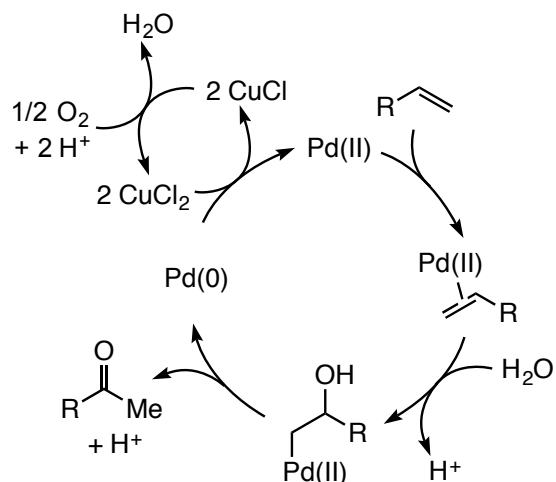


Scheme 1.2 Tsuji–Wacker oxidation.

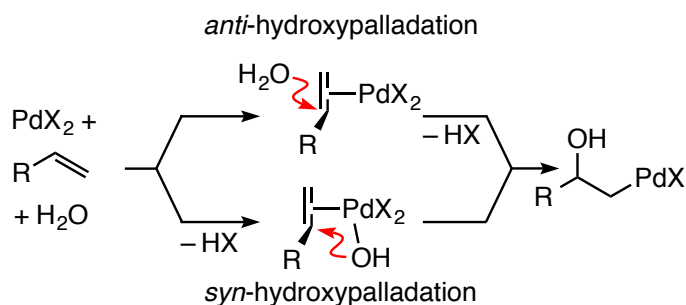
The Tsuji–Wacker oxidation has allowed alkenes to be viewed as masked methyl ketones with orthogonal reactivity (alkenes are much more stable than carbonyl compounds to typical basic and acidic conditions). In the decades following its initial development, the Tsuji–Wacker oxidation and related variants have been broadly applied in organic synthesis.^{3,8-10}

Mechanistic Overview

The Wacker oxidation mechanism has been investigated extensively both experimentally and computationally.^{3,11} A simplified mechanistic scheme aiming to highlight the key mechanistic features of the Wacker oxidation is outlined in Scheme 1.3. Under classical Wacker-type conditions, the oxygen atom is derived from water via nucleopalladation from a η^2 -Pd-alkene π -complex. However, the exact nature of this nucleopallation event has been a topic of great debate.¹¹ Depending on the exact conditions of the experiment, strong evidence has been found in favor of both inner sphere *syn*-nucleopalladation and outer sphere *anti*-nucleopalladation.



Scheme 1.3 Simplified mechanism of the Tsuji–Wacker reaction.



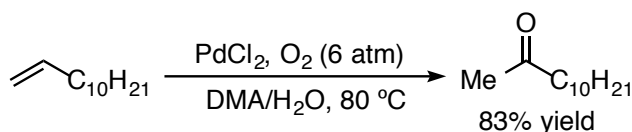
Scheme 1.4 Two possible modes of hydroxypalladation.

This mechanistic dichotomy appears to be controlled by the overall chloride concentration in the reaction mixture, with high chloride concentration favoring *anti*-nucleopalladation and low chloride concentration preferring *syn*-nucleopalladation. This specific example illustrates the more general observation that several pathways of comparable energy coexist under Wacker oxidation conditions, and as a result, the exact mechanism can change upon modification

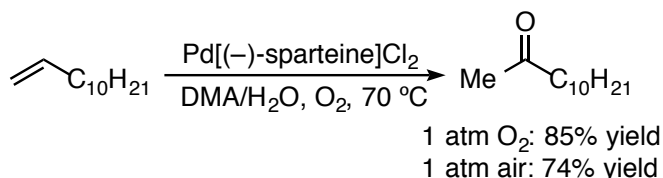
to the reaction conditions. Wacker oxidation processes are unified by nucleopalladation and subsequent decomposition of the alkylpalladium intermediate to provide a carbonyl compound.

Challenges Associated with Wacker Regioselectivity

After the development of the archetypical Tsuji–Wacker conditions, several variants have been developed based upon modifications to the solvent system, and/or the introduction of exogenous ligands and additives.^{3,12} For example, Kaneda and coworkers found that by changing the solvent to DMA, Pd(0) could be directly oxidized to Pd(II) under 6 atm of O₂ (Scheme 1.5).¹³ Sigman and coworkers were able to accomplish reoxidation using molecular oxygen under milder conditions (1 atm O₂ or even air) through use of sparteine as the ancillary ligand (Scheme 1.6).¹⁴



Scheme 1.5 Copper-free aerobic Wacker oxidation by Kaneda and coworkers.



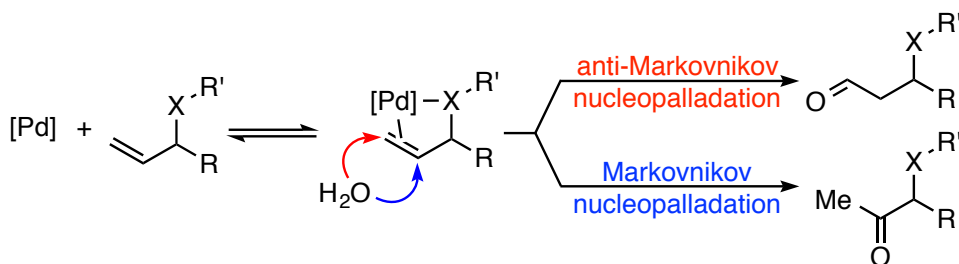
Scheme 1.6 Ligand enabled aerobic Wacker oxidation (Sigman and coworkers).

Though a wide array of Wacker oxidation variants have been reported, three key challenges remain areas of intense interest: 1) the discovery of general strategies to *control regioselectivity*; 2) the development of a highly reactive yet practical catalyst system for *internal alkene substrates*; 3) the identification of novel approaches for *direct reoxidation with molecular oxygen*.^{9,15,16} Although this thesis covers a variety of topics related to Wacker-type oxidations, the primary focus of the research described herein is to understand and control nucleopalladation regioselectivity. With this in mind, a brief overview of the topic of nucleopalladation regioselectivity is provided below.

The regioselectivity of the Tsuji–Wacker oxidation is substrate-controlled, and methyl ketone products are typically favored in accord with Markovnikov's rule. Although the Wacker oxidation has been broadly adopted, classically its reliance on substrate control introduces two substantial problems: 1) if the innate Markovnikov selectivity is perturbed by substrate properties, formation of ketone products becomes unreliable, and 2) the anti-Markovnikov aldehyde products are typically inaccessible, except in a small number of cases involving a narrow range of substrates. To address these challenges, the development of catalyst-controlled variants capable of enforcing the desired regioselectivity (i.e., Markovnikov or anti-Markovnikov) over a wide range of substrates has been a longstanding goal of Wacker research.

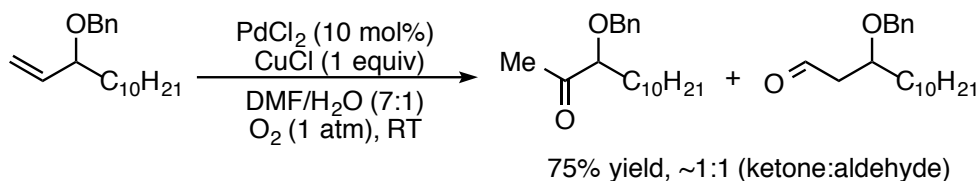
The typically reliable Markovnikov selectivity exhibited by Wacker-type oxidations is lost in substrates bearing proximal heteroatoms.¹⁷ The ratio of

aldehyde to ketone products formed from oxidation of substrates with allylic functional groups is particularly challenging to predict *a priori* and is often close to 1:1.^{8,17} Typically this effect is attributed to the coordination of the heteroatom to the palladium center, which influences the nucleopalladation regioselectivity (Scheme 1.7).



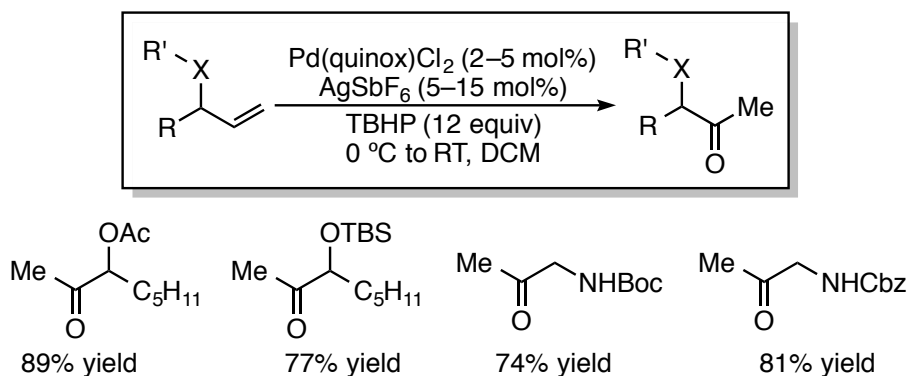
Scheme 1.7 Putative coordination by heteroatoms can influence selectivity. X = O, N or S. [Pd] = palladium(II) salt.

As a representative example of how the presence of proximal heteroatoms affects regioselectivity, Kang and coworkers attempted Tsuji–Wacker oxidation with a simple alkene bearing an allylic benzyl ether and observed an intractable 1:1 mixture of aldehyde and ketone products (Scheme 1.8).¹⁸ Although this coordination model is frequently invoked and is likely active in some cases, Chapter 5 discusses evidence that the electronic-withdrawing nature of the proximal functional groups also plays a substantial role in dictating Wacker regioselectivity.



Scheme 1.8 Tsuji–Wacker oxidation of a benzyl ether substrate produces a mixture of aldehyde and ketone products (Kang and coworkers).

To address this challenge, Sigman and coworkers developed a catalyst-controlled ketone-selective Wacker oxidation that could overcome the poor innate selectivity exhibited with these functionalized substrates.¹⁹⁻²¹ This catalytic system employs a palladium complex bearing a bidentate ligand and uses TBHP (*tert*-butyl hydroperoxide) as the nucleophile in lieu of water. This new catalytic transformation proved to be effective for a variety of functionalized alkenes (Scheme 1.9).⁸



Scheme 1.9 Selected examples from Sigman and coworkers' catalyst-controlled Markovnikov selective Wacker oxidation. X = O, N or S.

The authors suggest that these modifications result in a coordinatively saturated peroxypalladation that precludes coordination of the proximal heteroatom to the palladium center (Figure 1.1).²² As a complementary approach, we have identified an exceptionally simple Wacker-type oxidation system that exhibits predictably high Markovnikov selectivity on the basis of alkene electronic properties. This new reaction is discussed in Chapter 5.

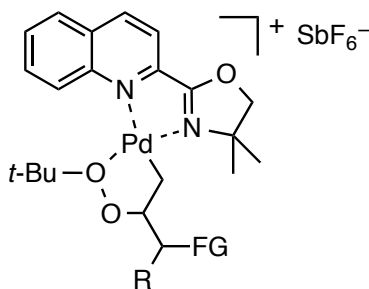
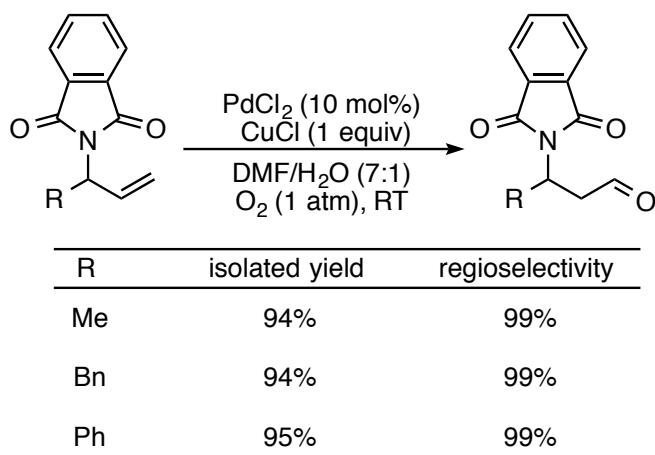


Figure 1.1 Sigman and coworkers' coordinatively saturated peroxypalladation model for Markovnikov selectivity. FG = functional group.

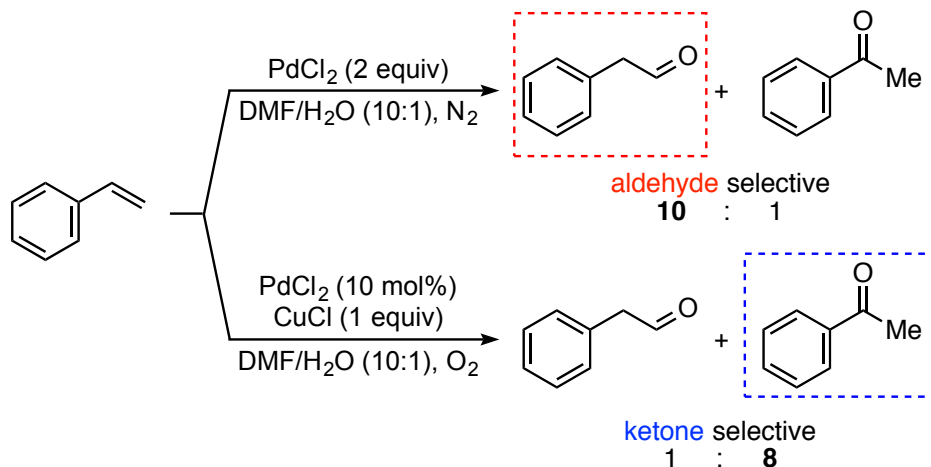
In the context of anti-Markovnikov regioselectivity, researchers have exploited specific biased alkenes to favor the aldehyde pathway.^{17,23-26} Although several isolated examples of substrate-derived aldehyde-selectivity have been observed,¹⁷ these examples are typically highly dependent on the carbon skeleton of substrate as well as the chemical identity of the directing group. In an unusually general example of aldehyde-selectivity, Feringa and coworkers

identified that a variety of allylic phthalimide substrates provided exceptionally high aldehyde selectivity under Tsuji–Wacker conditions.²⁷

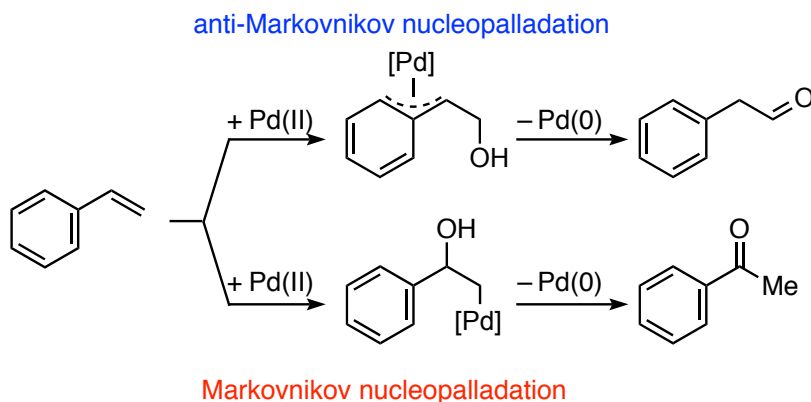
Table 1.1 Selected examples of phthalimide-directed anti-Markovnikov Wacker oxidations (Feringa and coworkers).



Oxidants can have an unexpected influence on nucleopalladation regioselectivity. For example, employing stoichiometric palladium, Spencer and coworkers observed that styrenyl substrates are predisposed to undergo anti-Markovnikov oxidation (Scheme 1.10).^{28,29} The use of traditional catalytic conditions, however, restored Markovnikov selectivity. Spencer and coworkers went on to perform a series of elegant experiments consistent with the formation of a stabilized benzylpalladium intermediate encouraging anti-Markovnikov oxidation.^{28,29} The origin of the relationship between regioselectivity and oxidant, however, was not identified (Scheme 1.11).



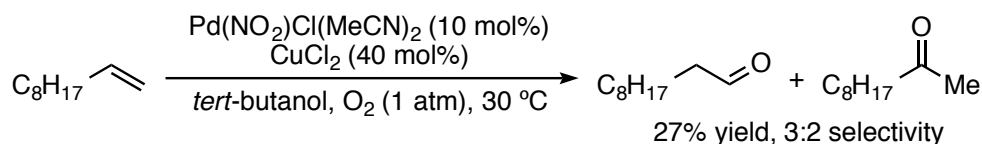
Scheme 1.10 Stoichiometric and catalytic oxidation of styrene under Tsuji—Wacker conditions (Spencer and coworkers).



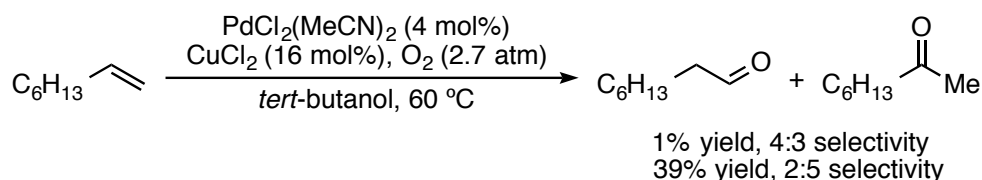
Scheme 1.11 Model to explain the unusual anti-Markovnikov selectivity observed with styrene (Spencer and coworkers).

Unfortunately, exploiting innate substrate-controlled selectivity to provide anti-Markovnikov aldehyde products is an inherently limited approach because the vast majority of alkenes are unbiased. Thus mere traces of the anti-Markovnikov aldehyde products are typically observed.^{2,17,26,30,31} A generally applicable

aldehyde-selective Wacker oxidation must fundamentally overturn the innate Markovnikov selectivity.^{32,33} In attempts to develop a catalyst system to reverse the innate Markovnikov selectivity of Wacker oxidations, the traditional DMF and water solvent mixture was replaced with a tertiary alcohol solvent.³⁴⁻³⁷ This change led to a slight preference for aldehyde formation from completely unbiased aliphatic alkenes (Schemes 1.12 and 1.13).



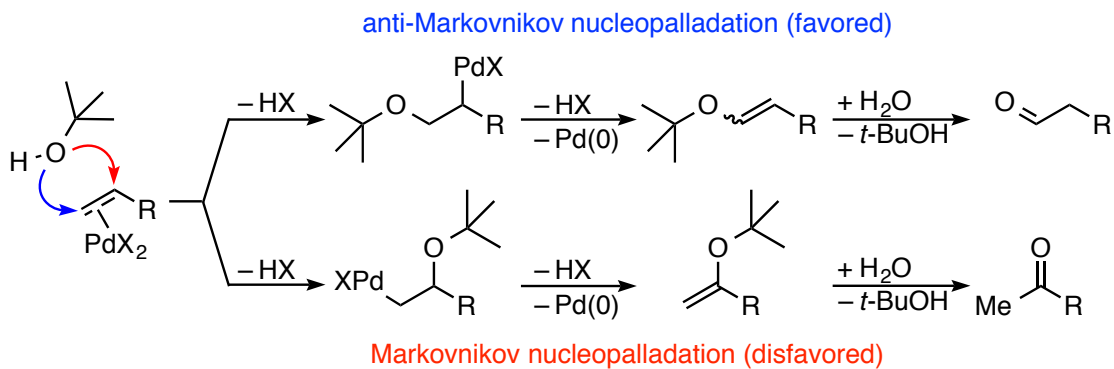
Scheme 1.12 Modest aldehyde-selectivity in the oxidation of an aliphatic alkene with a palladium nitrite catalyst in *tert*-butanol (Feringa).



Scheme 1.13 Elevated aldehyde production in the oxidation of aliphatic alkenes in *tert*-butanol (Wenzel).

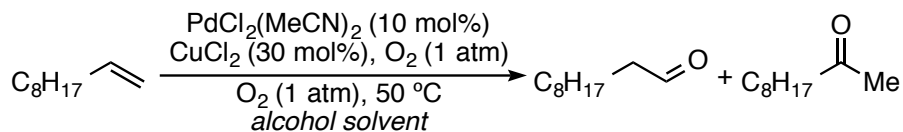
This enhanced aldehyde-selectivity was rationalized by the preference for a bulky alcohol nucleophile (typically *tert*-butanol) to attack the sterically less hindered site. Relative to water, *tert*-butanol possesses a significantly increased steric profile, which disfavors attack at the more hindered internal (Markovnikov)

position of the alkene (Scheme 1.14). Hosokawa and coworkers investigated the influence of alcohol steric bulk on Wacker oxidation regioselectivity and found results consistent with this hypothesis (Table 1.2).³⁶



Scheme 1.14 Model involving *tert*-Butanol as an alternative Wacker nucleophile to discourage Markovnikov oxidation.

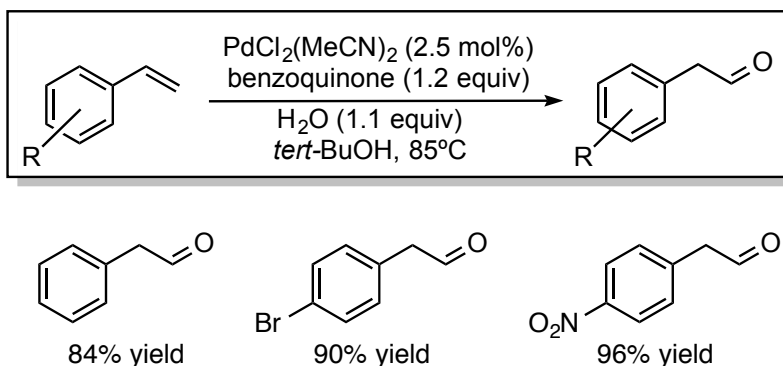
Table 1.2 Role of the steric bulk of alcohol solvents on Wacker oxidation yield and aldehyde-selectivity (Hosokawa and coworkers).



alcohol solvent	yield	aldehyde : ketone
MeOH	26	3 : 97
EtOH	22	16 : 84
<i>i</i> -PrOH	11	42 : 58
<i>t</i> -BuOH	7	84 : 16

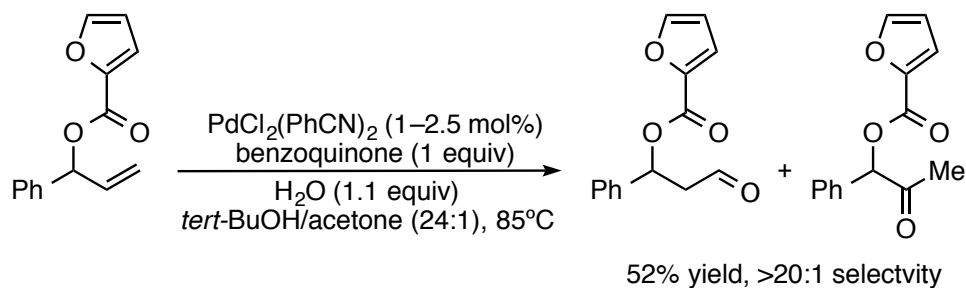
Unfortunately, despite initially promising results, low yields have plagued the use of *tert*-butanol in the oxidation of unbiased aliphatic substrates, and a synthetically useful, catalyst-controlled Wacker oxidation has yet to emerge from this strategy.²⁶

Although the *tert*-butanol strategy failed to provide a general catalytic system for aldehyde-selective oxidation of alkenes, it has proven highly effective in further encouraging anti-Markovnikov oxidation in substrates that provide mixtures of aldehydes and ketones under classical Tsuji–Wacker conditions. For example, the Grubbs group demonstrated that a catalytic system comprised of *tert*-butanol, PdCl₂(MeCN)₂, and benzoquinone efficiently oxidizes styrene derivatives with extraordinarily high anti-Markovnikov selectivity and relatively low loadings of palladium (2.5 mol%) (Scheme 1.15).^{38,39} This reaction combines the bulky *tert*-butanol nucleophile with a substrate predisposed to anti-Markovnikov oxidation (*vide supra*).



Scheme 1.15 Enhanced aldehyde-selectivity in the Wacker oxidation of styrene and other vinyl arenes in *tert*-butanol (Grubbs and coworkers).

Under similar catalytic conditions, Feringa and coworkers were able to oxidize allylic furoyl ester derivatives⁴⁰ and later a variety of allylic amines with high aldehyde selectivity (Scheme 1.16).³¹ Although these systems are not fully catalyst controlled, the use of a bulky nucleophile in place of water expands the scope of substrates that possess exploitable anti-Markovnikov selectivity. However, a general catalyst-controlled solution remains necessary to reliably obtain aldehydes from the vast majority of alkene substrates. In Chapter 2, the development of a catalyst-controlled anti-Markovnikov Wacker oxidation is discussed in detail.



Scheme 1.16 Enhanced aldehyde-selectivity in the Wacker oxidation of a furoyl esters with *tert*-butanol (Feringa and coworkers).

Conclusion

Overall, despite over half a century of extensive research and broad adoption of the Wacker oxidation by the synthetic community, the reaction remains an arena rife with opportunity. In particular, control over selectivity in Wacker-type nucleopalladation manifolds will continue to provide a myriad of synthetically

useful transformations. Thus, this thesis is focused on identifying strategies for the manipulation of selectivity and reactivity in Wacker type oxidations to solve classical challenges in palladium-catalyzed oxidations of alkenes. In Chapter 2, we develop a catalyst-controlled aldehyde-selective Wacker-type oxidation. In Chapter 3, we explore how the nitrite additives can be exploited to interrupt the Wacker oxidation and provide dioxygenated products instead of carbonyl compounds. In Chapter 4, we identify a highly active Wacker-type oxidation capable of efficiently oxidizing classically unreactive internal alkenes without sacrificing generality or practicality. In Chapter 5, we leverage the oxidation of internal alkenes to explore the origins of innate nucleopalladation regioselectivity in Wacker-type oxidations. Overall, this thesis provides a suite of synthetically useful selective alkene oxidation reactions and develops a mechanistic foundation for further study of each reaction.

References

- (1) Tsuji, J. *Synthesis* **1984**, 369.
- (2) Tsuji, J. *Palladium Reagents and Catalysts: New Perspectives for the 21st Century*, 2nd ed.; Wiley, **2004**.
- (3) Takacs, J.; Jiang, X.-T. *Curr. Org. Chem.* **2003**, *7*, 369.
- (4) Philips, F. C. *Am. Chem. J.* **1894**, 255
- (5) Smidt, J.; Hafner, W.; Sedlmeier, J.; Jira, R.; Rüttinger, R. *Angew. Chem.* **1959**, *71*, 176.

- (6) Jira, R. *Angew. Chem. Int. Ed.* **2009**, *48*, 9034.
- (7) Clement, W. H.; Selwitz, C. M. *J. Org. Chem.* **1964**, *29*, 241.
- (8) Sigman, M. S.; Werner, E. W. *Acc. Chem. Res.* **2012**, *45*, 874.
- (9) Sigman, M. S.; Cornell, C. N. *Inorg. Chem.* **2007**, *46*, 1903.
- (10) McDonald, R. I.; Liu, G.; Stahl, S. S. *Chem. Rev.* **2011**, *111*, 2981.
- (11) Keith, J. A.; Henry, P. M. *Angew. Chem. Int. Ed.* **2009**, *48*, 9038.
- (12) Gligorich, K. M.; Sigman, M. S. *Chem. Commun.* **2009**, 3854.
- (13) Mitsudome, T.; Umetani, T.; Nosaka, N.; Mori, K.; Mizugaki, T.; Ebitani, K.; Kaneda, K. *Angew. Chem. Int. Ed.* **2006**, *45*, 481.
- (14) Cornell, C. N.; Sigman, M. S. *Org. Lett.* **2006**, *8*, 4117–4120.
- (15) Piera, J.; Bäckvall, J.-E. *Angew. Chem. Int. Ed.* **2008**, *47*, 3506.
- (16) Stahl, S. S. *Angew. Chem. Int. Ed. Engl.* **2004**, *43*, 3400.
- (17) Muzart, J. *Tetrahedron* **2007**, *63*, 7505.
- (18) Kang, S.-K.; Jung, K.-Y.; Chung, J.-U.; Namkoong, E.-Y.; Kim, T.-H. *J. Org. Chem.* **1995**, *60*, 4678.
- (19) Michel, B. W.; Camelio, A. M.; Cornell, C. N.; Sigman, M. S. *J. Am. Chem. Soc.* **2009**, *131*, 6076.
- (20) Michel, B. W.; Sigman, M. S.; McCombs, J. R.; Winkler, A. *Angew. Chem. Int. Ed.* **2010**, *49*, 7312.
- (21) McCombs, J. R.; Michel, B. W.; Sigman, M. S. *J. Org. Chem.* **2011**.
- (22) Michel, B. W.; Steffens, L. D.; Sigman, M. S. *J. Am. Chem. Soc.* **2011**.
- (23) Lai, J.; Shi, X.; Dai, L. *J. Org. Chem.* **1992**, *57*, 3485.

- (24) Yamamoto, M.; Nakaoka, S.; Ura, Y.; Kataoka, Y. *Chem. Commun.* **2012**.
- (25) Choi, P. J.; Sperry, J.; Brimble, M. A. *J. Org. Chem.* **2010**, *75*, 7388.
- (26) Dong, J. J.; Browne, W. R.; Feringa, B. L. *Angew. Chem. Int. Ed.* **2015**, *54*, 734.
- (27) Weiner, B.; Baeza, A.; Jerphagnon, T.; Feringa, B. *J. Am. Chem. Soc.* **2009**, *131*, 9473.
- (28) Wright, J. A.; Gaunt, M. J.; Spencer, J. B. *Chem. Eur. J.* **2006**, *12*, 949.
- (29) Trost, B. M.; Czabaniuk, L. C. *Angew. Chem. Int. Ed.* **2014**, *53*, 2826.
- (30) Tsuji, J.; Nagashima, H.; Nemoto, H. *Org. Synth.* **1984**, *62*, 9.
- (31) Dong, J. J.; Harvey, E. C.; Fañanás-Mastral, M.; Browne, W. R.; Feringa, B. L. *J. Am. Chem. Soc.* **2014**, *136*, 17302.
- (32) Beller, M.; Seayad, J.; Tillack, A.; Jiao, H. *Angew. Chem. Int. Ed.* **2004**, *43*, 3368.
- (33) Mahatthananchai, J.; Dumas, A. M.; Bode, J. W. *Angew. Chem. Int. Ed.* **2012**, *51*, 10954.
- (34) Feringa, B. L. *Chem. Commun.* **1986**, 909.
- (35) Wenzel, T. T. *J. Chem. Soc., Chem. Commun.* **1989**, 932.
- (36) Ogura, T.; Kamimura, R.; Shiga, A.; Hosokawa, T. *Bull. Chem. Soc. Jpn.* **2005**, *78*, 1555.
- (37) Wenzel, T. T. *J. Chem. Soc., Chem. Commun.* **1993**, 862.
- (38) Teo, P.; Wickens, Z. K.; Dong, G.; Grubbs, R. H. *Org. Lett.* **2012**, *14*, 3237.

- (39) Dong, G.; Teo, P.; Wickens, Z. K.; Grubbs, R. H. *Science* **2011**, *333*, 1609.
- (40) Dong, J. J.; Fañanás-Mastral, M.; Alsters, P. L.; Browne, W. R.; Feringa, B. L. *Angew. Chem. Int. Ed.* **2013**, *52*, 5561.

CHAPTER 2

CATALYST-CONTROLLED ALDEHYDE-SELECTIVE WACKER ENABLED BY CO-CATALYTIC NITRITE

The text in this chapter was reproduced in part with permission from:

Wickens, Z. K.; Morandi, B.; Grubbs, R. H. *Angew. Chem. Int. Ed.* **2013**, *52*, 11257–11260

Copyright 2013 John Wiley and Sons

Wickens, Z.K.; Skakuj, K.; Morandi, B.; Grubbs, R. H. *J. Am. Chem. Soc.* **2014**, *136*, 890–893

Copyright 2014 American Chemical Society

Abstract

Reversal of the high Markovnikov selectivity of Wacker-type oxidations was accomplished using nitrite additives. Unbiased aliphatic alkenes can be oxidized in up to 80% yield and as high as 90% aldehyde-selectivity and several functional groups are tolerated. ^{18}O -labeling experiments indicate that the aldehydic oxygen atom is derived from the nitrite salt, providing important preliminary mechanistic insight into this anti-Markovnikov transformation. The nitrite-modified Wacker oxidation was also demonstrated to be highly effective for the aldehyde-selective oxidation of alkenes bearing diverse oxygen groups in the allylic and homoallylic position. Oxygenated alkenes were oxidized in up to 88% aldehyde yield and as high as 97% aldehyde-selectivity. The aldehyde-selective oxidation enabled the rapid, enantioselective synthesis of an important pharmaceutical agent, atomoxetine. Finally, the origin of the influence of proximal functional groups on this anti-Markovnikov reaction was explored.

Aldehyde-Selective Wacker Oxidation of Unbiased Alkenes

Introduction

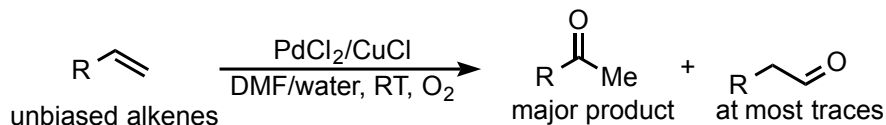
The efficient catalytic transformation of monosubstituted alkenes into valuable terminally functionalized alkanes, such as amines, alcohols, acids and aldehydes, is of critical importance to polymer science, drug discovery, chemical biology and the bulk chemical industry.^{1,2} However, these transformations require

breaking a textbook rule of organic chemistry: Markovnikov's rule.³ This rule predicts that nucleophiles will attack the more substituted carbon of an alkene. Thus, to functionalize the terminal position of unbiased alkenes with an oxygen or nitrogen nucleophile, the innate (substrate-controlled) Markovnikov selectivity must be superseded using a highly anti-Markovnikov selective catalyst-controlled process.⁴ Despite the recognition of such important transformations as top challenges in catalysis two decades ago,⁵ synthetically useful reactions that involve direct, catalytic anti-Markovnikov addition of oxygen or nitrogen to unbiased alkenes remain elusive.^{4,6}

The traditional approach to anti-Markovnikov functionalization of terminal alkenes has relied upon the ubiquitous hydroboration reaction.⁷ The widespread adoption of hydroboration in organic synthesis is due to the synthetic versatility of the alkylborane products, which can be transformed into many important functional groups. Unfortunately, this stoichiometric process generates significant waste and has limited functional-group compatibility. In theory, the catalytic introduction of a versatile functional group to the terminal position of an alkene could parallel the hydroboration reaction while bypassing its inherent limitations (Scheme 2.1).

We reasoned that the aerobic oxidation of an alkene to an aldehyde would be an ideal candidate for a catalytic alternative to hydroboration. General and efficient catalytic transformations have been developed to readily transform aldehydes into amines, alcohols and acids without generating wasteful

predominately methyl ketones are produced from the majority of terminal alkenes in accord with Markovnikov's rule (Scheme 2.2).



Scheme 2.2 Regioselectivity of the Tsuji–Wacker in unbiased alkenes.

As discussed in detail in chapter 1, many researchers have exploited specific biased alkenes to circumvent Markovnikov's rule and produce aldehydes and have achieved varying levels of success.^{31–36} Unfortunately, the utility of this approach is inherently limited because the vast majority of alkenes are unbiased, and thus mere traces of the anti-Markovnikov aldehyde products are observed.^{31,37} A generally applicable aldehyde-selective Wacker oxidation must therefore reverse the innate Markovnikov selectivity.^{4,6} Such a development would be a key advance in the field of anti-Markovnikov functionalization.^{6,38}

Despite many attempts to develop a catalyst-controlled, aldehyde-selective Wacker oxidation, such a variant has remained elusive.³¹ Unbiased substrates such as aliphatic alkenes produce, at most, mere traces of anti-Markovnikov oxidation products under standard Tsuji–Wacker conditions.³⁷ Attempts to produce aldehydes from unbiased alkenes (except ethylene) using Wacker oxidations have universally resulted in both low yield and poor selectivity.^{39–41} All methods have universally reverted to the expected ketone selectivity upon reaching synthetically relevant conversions. The inherent challenge of obtaining anti-Markovnikov regioselectivity has thus limited the

development of a synthetically viable aldehyde-selective Wacker oxidation without reliance upon substrate control.

Results and Discussion

For our work, 1-dodecene was selected as a model unbiased alkene for the development of a catalyst-controlled process, as it contains no chemical handle to reverse the Markovnikov selectivity. For example, although our previously reported conditions oxidize styrene with 97% aldehyde-selectivity in 90% yield,³⁵ 1-dodecene provided only traces of oxidation products with high ketone selectivity and considerable isomerization under these conditions (Figure 2, entry 1). Thus, these conditions are unable to provide aldehyde-selectivity without the powerful substrate-control offered by the aromatic moiety and a general catalyst-controlled solution remains to be developed.

Nearly 30 years prior to our on this topic, Feringa reported that $\text{PdNO}_2\text{Cl}(\text{MeCN})_2$, when combined with CuCl_2 in *tert*-BuOH, provided poor yields (<20%) but with encouraging aldehyde-selectivity (2.3:1).³⁹ Unfortunately, reactions which reach useful yields were reverted to Markovnikov selectivity (1:4.5) (entry 2). However, it has been suggested that under these conditions, the palladium nitrite generates *tert*-butyl nitrite.⁴⁰ We hypothesized that the poor aldehyde yield and selectivity observed under Feringa's conditions³⁹ could be due to inefficient generation of a highly aldehyde-selective species from *tert*-butyl nitrite. To test this hypothesis, we combined catalytic *tert*-butyl nitrite with PdCl_2 and CuCl_2 co-catalysts and observed significantly increased selectivity, for the

first time providing modest aldehyde selectivity above 50% conversion to oxidized products (1, entry 3). However, increasing the loading of *tert*-butyl nitrite increased the overall yield but decreased selectivity (entry 4).

We reasoned that other nitrite sources could enable more efficient access to the selective catalytic species. Of the nitrite sources evaluated, each offered similar oxidation efficiency with varying aldehyde-selectivity (entries 3-9). Catalytic AgNO₂ provided a significant improvement, leading to good anti-Markovnikov selectivity and synthetically useful yields. Interestingly, no significant difference between 12 and 6 mol% AgNO₂ was observed (entries 7 and 8). The comparable selectivity observed with NaNO₂ (entry 9) suggests that Ag(I) most likely does not play a key co-catalytic role.⁴² Furthermore, replacement of the nitrite anion with nitrate dramatically reduced oxidation yield and regioselectivity (entry 10). Attempts to deviate from metal dichloride salts or *tert*-BuOH⁴³ universally resulted in significantly decreased yield and selectivity. MeNO₂ was found to be the superior co-solvent although its omission from the optimized conditions still provided a somewhat aldehyde-selective process (entry 11). Importantly, when the palladium nitrite catalyst used by Feringa³⁹ was applied to the optimized conditions, the process was much less selective (slightly ketone-selective) than other nitrite sources (entry 12). Thus, we suspect that the nitrite anion does not simply undergo salt metathesis to form PdNO₂Cl *in situ* and that instead a more complex synergistic interaction between the metals occurs.

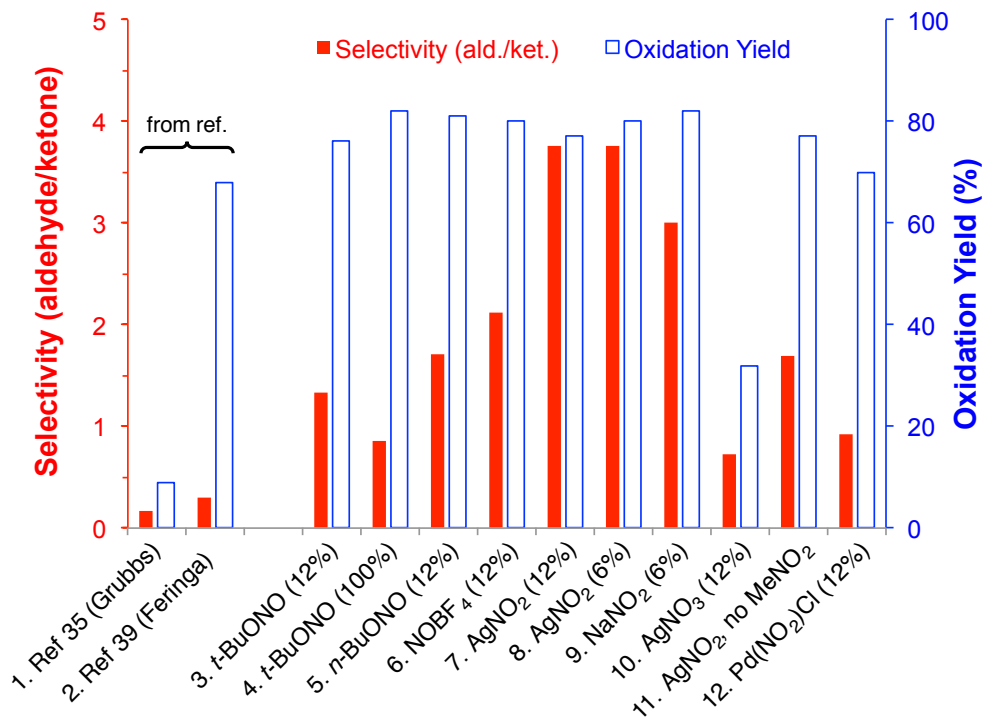
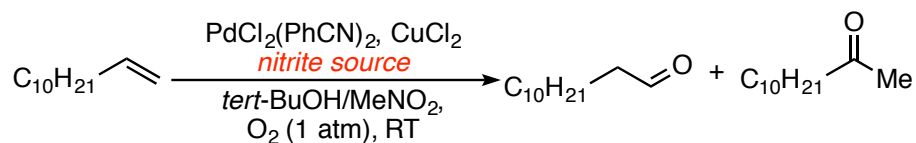


Figure 2.1 Catalyst optimization. See experimental section for details.

With optimized conditions in hand, the functional group tolerance of the transformation (Table 2.1) was explored. To avoid substrate-derived anti-Markovnikov selectivity, aliphatic substrates bearing only distal functionality were selected. These substrates provided yields comparable to those expected under Tsuji–Wacker conditions¹⁶ but with anti-Markovnikov selectivity. The reaction is compatible with a diverse array of functional groups: alkyl and aryl halides, esters, ethers, and nitro groups were all tolerated. Despite the potential challenge of using unprotected functional groups, carboxylic acids and alcohols still provided

synthetically viable yields of the corresponding aldehyde products. The reduced selectivity in these cases could be attributed to an intermolecular Markovnikov attack by these nucleophilic functionalities, producing ketones.

Table 2.1 Aldehyde-selective Wacker-type oxidation of unbiased alkenes^a

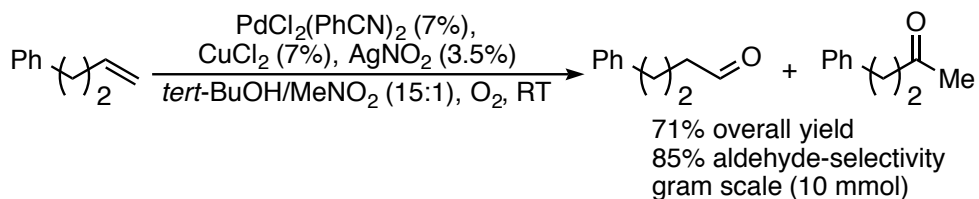
$$\text{R}-\text{CH}=\text{CH}_2 \xrightarrow[\text{tert-BuOH/MeNO}_2 (15:1), \text{O}_2, \text{RT}]{\text{PdCl}_2(\text{PhCN})_2 (12\%), \text{CuCl}_2 (12\%), \text{AgNO}_2 (6\%)} \text{R}-\text{CH}_2\text{CHO} + \text{R}-\text{C}(=\text{O})\text{Me}$$

Entry	Substrate	Oxidation Yield (Aldehyde yield ^b)	Selectivity ^c
1		80 (63) ^d	79%
2		74 (61)	79%
3		78 (70)	89%
4		72 (59)	79%
5		68 (51) ^e	67%
6		77 (65)	82%
7		70 (59)	81%
8		80 (45)	57%
9		75 (60) ^e	80%
10		77 (69)	89%
11		71 (64) ^e	90%

^a0.5 mmol alkene treated with PdCl₂(PhCN)₂ (12 mol%), CuCl₂·2H₂O (12 mol%), AgNO₂ (6 mol%), ^tBuOH/MeNO₂ (15:1) under O₂ (1 atm) at 20-25 °C. ^bYield of aldehyde by isolation. Overall yield calculated using selectivity. ^cSelectivity calculated by ¹H-NMR analysis ^dYield and selectivity both obtained by GC analysis. ^eYield determined via ¹H-NMR analysis.

Although alkene isomerization is a common problem in Wacker-type oxidations, no significant isomerization was observed with any of the substrates. All examples represent the first instances of aldehyde-selective Wacker oxidations on such substrates at synthetically relevant conversion.³¹

Next, the process scalability was assessed. Although the small scale palladium loading was comparable to Tsuji-Wacker conditions, it was reduced to 7% to accommodate a gram-scale process (Scheme 2.3). The success of this large scale reaction demonstrates that the process can maintain high yield and aldehyde-selectivity at an increased scale even with decreased catalyst-loading.



Scheme 2.3 Aldehyde-selective Wacker on 10 mmol scale

with reduced loading of catalysts.

Having demonstrated aldehyde-selectivity in unbiased aliphatic alkenes, a set of three phthalimides which upon minor carbon skeleton changes range from aldehyde to ketone-selective under traditional substrate-controlled Tsuji-Wacker conditions were next subjected to the reaction conditions (Figure 2.2). For each substrate high yield and selectivity was obtained regardless of the innate selectivity. Beyond providing preliminary evidence that this process could be a

general catalyst-controlled solution to aldehyde-selectivity, these results illustrate the efficacy of this process with proximal nitrogen functionality without reliance upon the substrate-controlled regioselectivity. Further investigation of functionalized substrates will be presented later in this chapter.

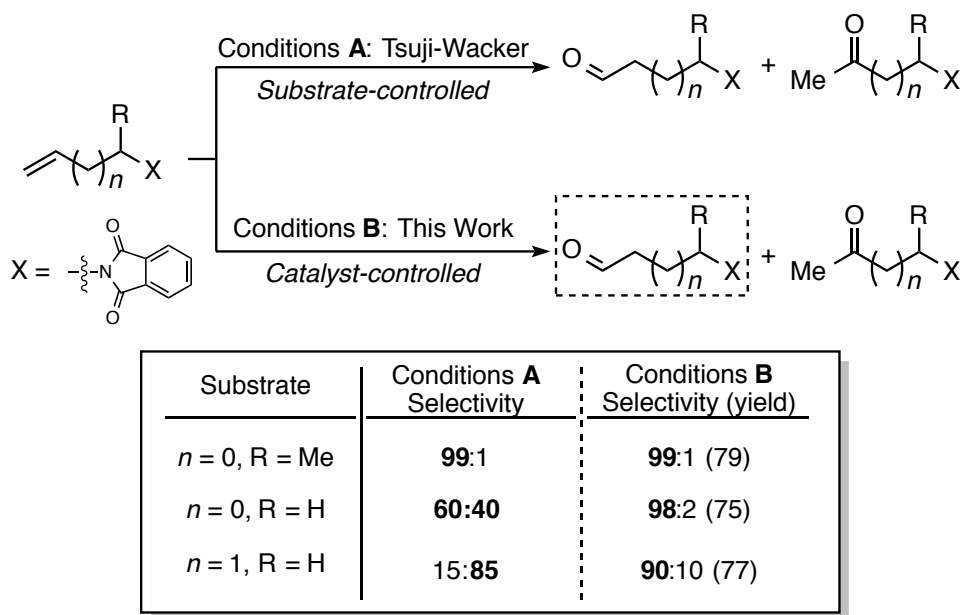


Figure 2.2. Comparison of innate selectivity (conditions A) to catalyst-controlled selectivity (conditions B). Conditions A: PdCl₂ (10-30%), CuCl (1 equiv), DMF/H₂O (7:1), RT, O₂ (1 atm). Conditions B: 0.5 mmol alkene, PdCl₂(PhCN)₂ (12%), CuCl₂ (12%), AgNO₂ (6%), *tert*-BuOH/MeNO₂ (15:1), RT, O₂ (1 atm). Aldehyde yield determined by isolation. Selectivity determined by ¹H-NMR analysis prior to purification.

Previous attempts to develop an aldehyde-selective Wacker have been plagued by low yields and loss of selectivity over the course of the reaction. Thus,

we examined the reaction profile to assess behavior of the aldehyde-selectivity (Figure 4). Upon surpassing 5% conversion, the selectivity stabilized and became relatively independent of both yield and time. This potentially suggests that, once formed, the same catalytic species remains active throughout the remainder of the reaction. The brief induction period in aldehyde-selectivity is particularly interesting, as previous systems have commonly demonstrated moderate to high aldehyde selectivity only at very low conversion.

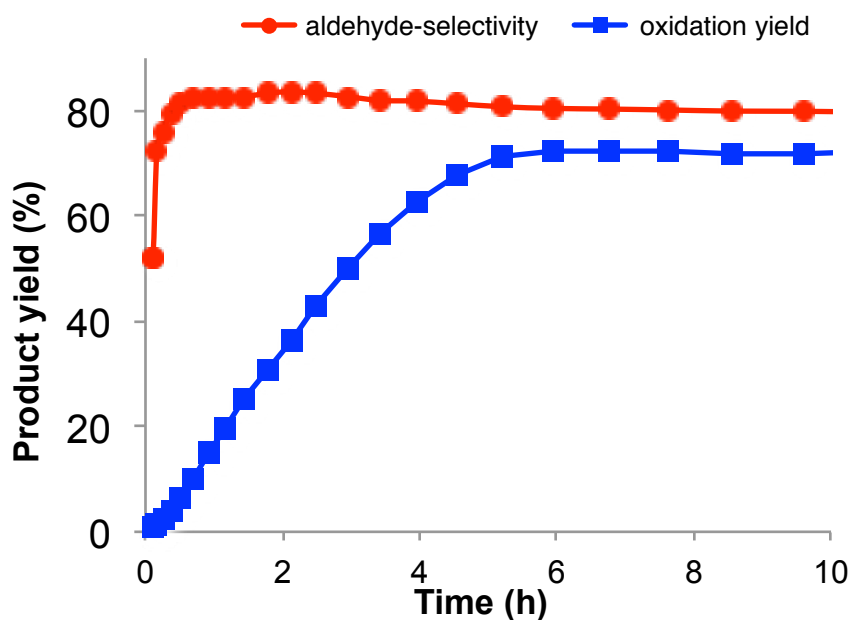


Figure 2.3. Stability of aldehyde-selective catalytically active species.

Since nitrite was the key additive found to unlock effective and aldehyde-selective oxidation, we collected detailed reaction profiles employing various quantities of AgNO_2 (Figure 2.4). Increased loading of AgNO_2 correlated with a

faster reaction, implying a rate dependence on AgNO_2 concentration. A similar overall yield of aldehyde was obtained using both 12 and 6 mol% AgNO_2 , with slightly improved aldehyde yield using 6 mol%. Interestingly, even 2 mol% AgNO_2 provided useful yields of aldehyde after a longer reaction time. Interestingly, increased amounts of AgNO_2 slightly decreased aldehyde-selectivity. However, omission of AgNO_2 led to a process not exceeding 20% overall yield, a problem that has plagued previous attempts at developing an aldehyde-selective Wacker-type oxidation of aliphatic alkenes.³¹

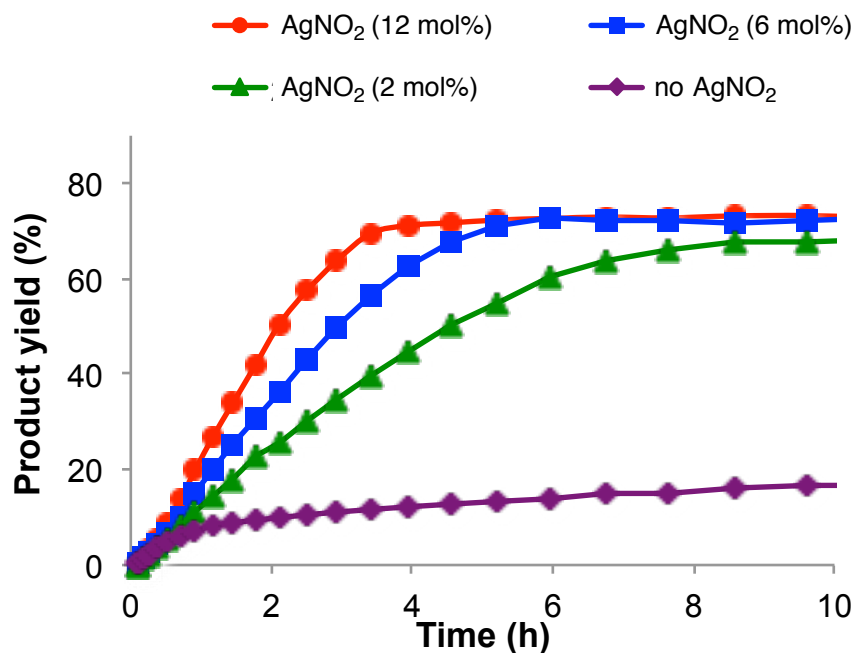
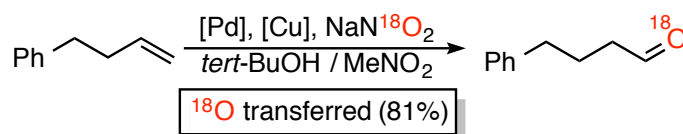


Figure 2.4 Reaction profiles with a range of nitrite catalyst loadings.

Given the unusual reactivity of the nitrite-modified Wacker oxidation and the complexity of the catalytic system comprised of several co-catalytic species, we conducted a series of experiments aiming to deconvolute the roles of the reaction components. As copper salts are commonly employed as redox-catalysts in Wacker-type oxidations,¹⁶ it was not surprising that removal of copper from the process provided only traces of products. Exposure of alkene to stoichiometric palladium and silver nitrite, however, also provided sluggish oxidation rates and poor selectivity. An analogous reaction was conducted with stoichiometric palladium in the absence of copper salts under Tsuji–Wacker conditions and, as expected, product was rapidly formed. These results clearly implicate copper as having a more intimate role than as a simple redox catalyst for palladium. To confirm the mechanistic necessity of the palladium salt for product formation, stoichiometric copper dichloride and silver nitrite (no palladium) were subjected to the alkene but provided no conversion. Thus, it appears that both palladium and copper are crucial metals for mechanistic steps prior to product formation.

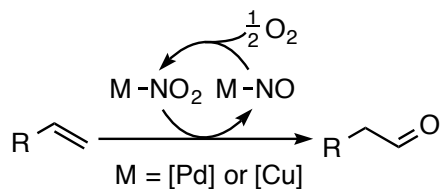
With the aim of providing key preliminary mechanistic insight into this transformation, we sought to elucidate the origin of the aldehydic oxygen atom in our system. To this end, we treated 4-phenyl-1-butene with stoichiometric ¹⁸O-labeled NaNO₂ (NaNO₂ provided comparable selectivity and efficiency to AgNO₂, see Figure 2.1) along with PdCl₂(PhCN)₂ and CuCl₂·2H₂O. We were delighted to find compelling evidence that the oxygen is derived from the nitrite salt, as the

^{18}O -label was effectively (81%) incorporated into the aldehyde (Scheme 2.4). Incomplete incorporation is likely due to exchange with adventitious water, however, a competing traditional Wacker-type nucleophilic attack cannot be ruled out.



Scheme 2.4 Stoichiometric ^{18}O -labeling experiment.

Under our catalytic reaction conditions, NO formed after oxygen transfer could be aerobically oxidized back to NO_2 , enabling the catalytic use of the nitrite salt (Scheme 2.5).⁴⁴ Prior to this work, contradictory reports have suggested that palladium nitrite complexes could oxidize alkenes via attack of either *tert*-BuOH or the nitrite ligand. Anti-Markovnikov attack by *tert*-BuOH has been substantiated with specific substrates,^{33,35,40,45} however, it is unlikely to occur under the present conditions, as the aldehydic oxygen atom should not be derived from nitrite after *tert*-BuOH attack. On the other hand, definitive attack by nitrite salts has been demonstrated only in systems that exhibit high Markovnikov selectivity.⁴⁶ The ^{18}O -labeling experiment presented herein thus constitutes the first conclusive experimental illustration that nitrite salts can indeed transfer an oxygen atom to the terminal position of alkenes.



Scheme 2.5 Plausible mode of oxygen atom transfer

The unusual anti-Markovnikov regioselectivity of the oxygen transfer from the nitrite salt combined with the propensity of such salts to generate NO₂ radical *in situ*,^{47,48} leads us to propose that a metal-mediated delivery of an NO₂ radical species across the alkene could be the key mechanistic feature of this reaction (Figure 2.5).

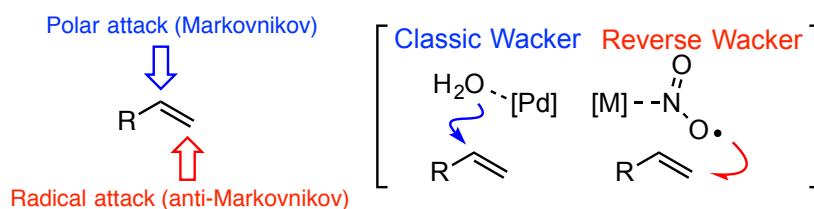


Figure 2.5 Radical model to explain anti-Markovnikov selectivity.

In traditional Wacker-type oxidations, attack by water upon the coordinated alkene is a polar addition and thus is controlled by Markovnikov's rule.⁴⁹ In contrast, radical-type addition to alkenes proceeds selectively at the terminal position due to the increased stability of the secondary radical intermediate.⁵⁰ Although vinylcyclopropane radical traps appeared to open under the reaction conditions, our attempts to probe radical intermediacy have been

stymied by difficulty to distinguish between one- or two-electron ring opening pathways.⁵¹ However, we expect that the significant insight provided by the ¹⁸O labeling experiment will continue to provide crucial guidance for further mechanistic study, aimed to determine the ultimate origin of anti-Markovnikov selectivity.

Conclusion

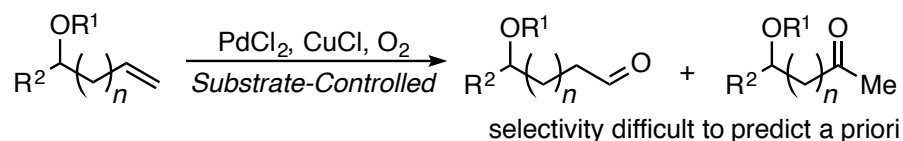
A Wacker-type oxidation of unbiased alkenes affording the anti-Markovnikov aldehyde products has been developed. The success of this system with challenging aliphatic substrates combined with the lack of substrate-derived interference by allylic and homoallylic functionality bodes well for further development of the reaction into an efficient synthetic tool. An informative ¹⁸O-labeling experiment suggests an unusual mechanistic manifold, potentially involving metal-catalyzed attack at the terminal position of the alkene by an NO₂ radical.

Nitrite-Modified Wacker Oxidation to Access Functionalized Aldehydes

Introduction

As discussed in Chapter 1, the innate Wacker regioselectivity is sensitive to both proximal coordinating groups.³¹ Thus, the ratio of aldehyde to ketone products formed from oxidation of functionalized substrates can be challenging to predict a

priori (Scheme 2.6).^{30,31}



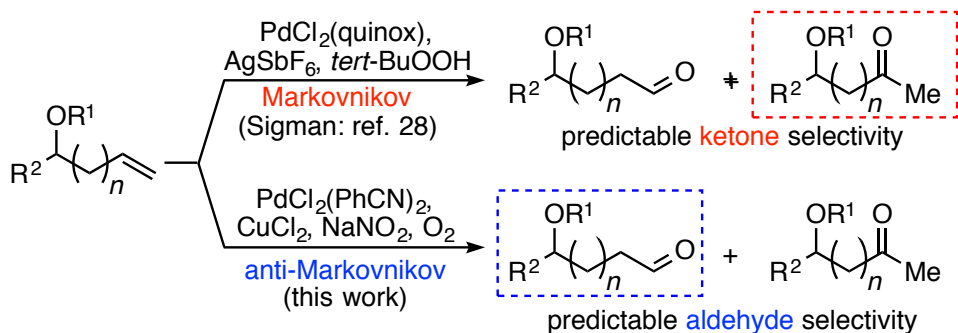
Scheme 2.6 Tsuj–Wacker conditions provide both aldehyde and ketone products.

Sigman and coworkers recently developed a Wacker-type oxidation system that delivered catalyst-controlled ketone selectivity.^{28,29} This system was employed in the oxidation of functionalized alkenes to overcome their poor innate selectivity and provide methyl ketone products in high yield (Scheme 2.7). Unfortunately, the development of a catalyst-controlled anti-Markovnikov Wacker oxidation has seen only preliminary success.^{31,39–41} Work in this area, including our own work discussed earlier in this chapter, has focused on aliphatic alkene model systems and no Wacker-type oxidation has provided reliable aldehyde selectivity across a wide range of allylic and homoallylic functional groups.

A general, anti-Markovnikov oxidation of readily accessible oxygen-containing alkenes would enable efficient access to synthetically versatile polyfunctional building blocks. Furthermore, enantioenriched allylic and homoallylic alcohol derivatives can be easily prepared via established synthetic routes.⁵² Due to the synthetic versatility of the aldehyde functional group,^{7,8,12} a reliable aldehyde-selective Wacker would enable diverse catalytic strategies to address the historical challenge¹⁰ of anti-Markovnikov alkene

functionalization.^{6,38,53–57}

As discussed in the introduction to this chapter, previous efforts to prepare functionalized aldehydes via Wacker oxidations have exploited specifically tailored directing groups to obtain substrate-controlled anti-Markovnikov selectivity.³¹ Unfortunately, this approach lacks flexibility and requires the synthetic route to be planned around the installation and removal of directing auxiliaries. Furthermore, reliance upon a narrow class of directing groups can result in inherent synthetic incompatibilities. For example, although allylic furfuryl esters provide high substrate-derived aldehyde selectivity, allylic stereocenters are racemized by a reversible palladium catalyzed rearrangement.³³ Moreover, functional groups in the homoallylic position are rarely effective at overcoming Markovnikov's rule.³¹ Thus, a catalyst-controlled method to oxidize diverse oxygen-containing alkenes to aldehydes remains an elusive but highly desirable tool for organic synthesis.⁴



Scheme 2.7 Catalyst-controlled solutions to Markovnikov and anti-Markovnikov regioselectivity in Wacker-type oxidations.

Results and Discussion

The first section of this chapter outlined the development of a nitrite-modified Wacker-type catalyst system capable of reversing the innate Markovnikov selectivity exhibited by aliphatic alkenes.⁵⁸ Additionally, we illustrated that a variety of phthalimide substrates undergo aldehyde-selective oxidation. Thus, we next set out to evaluate whether Lewis-basic oxygen functional groups would interfere with or enhance the aldehyde-selectivity of the reaction. In addition to its synthetic value, we anticipated that this line of inquiry would also provide key mechanistic insight into this newly developed nitrite-modified Wacker process.

A series of alkene-containing phenyl ether substrates of varying chain length were subjected to both nitrite-modified Wacker conditions and Tsuji–Wacker conditions to evaluate the influence of proximal oxygen-containing functional groups on the regioselectivity (Figure 2.6). The high anti-Markovnikov selectivity exhibited by an unbiased substrate (1-dodecene) under nitrite-modified Wacker conditions was markedly enhanced as the ether moiety approached the alkene. Exceptional aldehyde selectivity (>90%) was observed both with the allylic ($n=1$) and homoallylic phenyl ether ($n=2$), despite the significant difference in the innate regioselectivity of the two substrates under Tsuji–Wacker conditions. Moreover, substrates bearing a distal ether functional group ($n=3$) retained the high regioselectivity observed in the unfunctionalized systems. These encouraging results are consistent with a catalyst-controlled process in which the selectivity is further enhanced by proximal heteroatoms. Following this

preliminary success, we sought to optimize the reaction conditions. With oxygenated alkenes, NaNO_2 proved to be an effective and inexpensive source of nitrite. This result stands in contrast to the results observed with aliphatic substrates (*vide supra*), where it was found that AgNO_2 was necessary for acceptable reaction rate and aldehyde-selectivity.

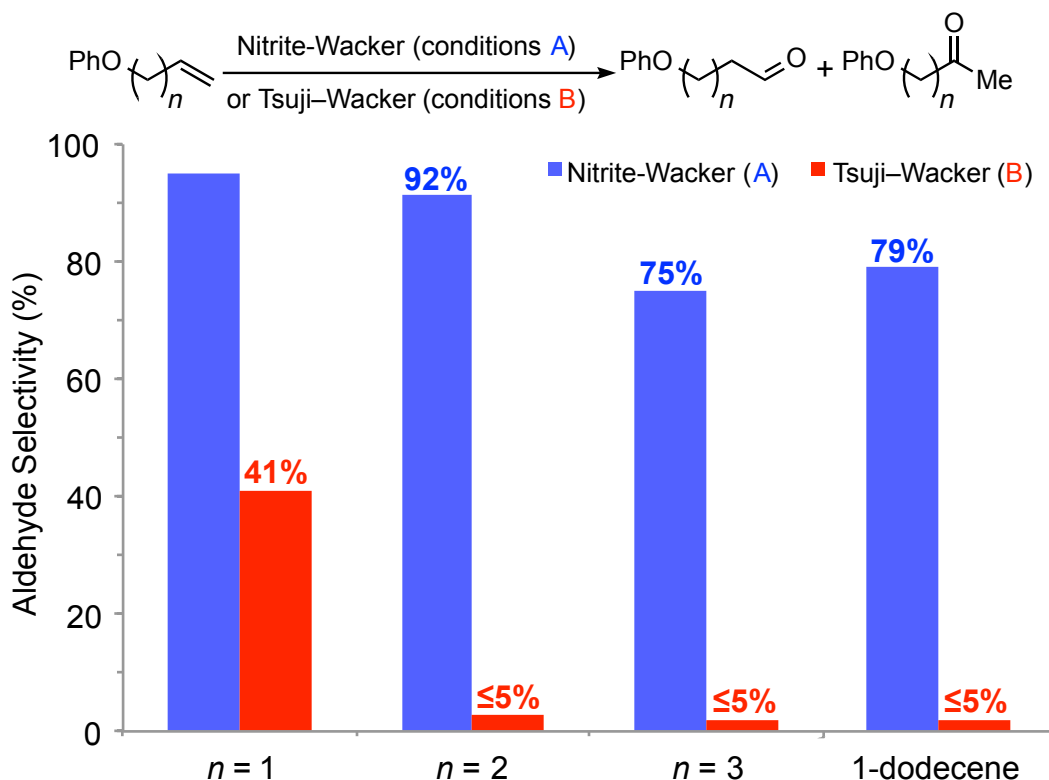


Figure 2.6. The influence of phenoxy group proximity on regioselectivity in Wacker-type oxidations. **A** (blue): see Table 2.1 for conditions. **B** (red): PdCl_2 (10%), CuCl (1 equiv), $\text{DMF}/\text{H}_2\text{O}$ (7:1), RT, O_2 (1 atm), 24 h.

To be a general catalyst-controlled methodology to access functionalized aldehydes, the high anti-Markovnikov selectivity must not be dependent on

specific directing groups. With this in mind, we examined a collection of substrates bearing different oxygen-containing functional groups in both the allylic or homoallylic position under the optimized conditions (Table 2.2). The oxidation of these substrates took place with high aldehyde selectivity (89–96%), allowing the aldehyde product to be isolated in preparatively useful yields (64–88%), irrespective of the nature of the oxygen-containing functional group. In particular, alkyl, aryl and silyl ethers, as well as acetyl esters, were all well tolerated. For comparison, each substrate was additionally subjected to Tsuji–Wacker conditions to determine its innate selectivity. In contrast to the high anti-Markovnikov selectivity observed across the series under nitrite-modified Wacker conditions, the innate selectivity varied greatly as a function of substrate. The excellent aldehyde-selectivity provided by the nitrite-modified Wacker oxidation of homoallylic substrates is particularly notable due to their high innate Markovnikov selectivity ($\geq 80\%$ ketone-selective). Notably, the selectivity was independent of the innate selectivity, clearly demonstrating catalyst-controlled regioselectivity.

The success of this reaction with challenging, innately ketone-selective homoallylic alcohol derivatives led to the exploration of how the steric properties of this class of substrates influences reactivity and selectivity (Table 2). Having demonstrated that such substrates perform similarly in the reaction irrespective of the substituent on oxygen, a benzyl group was selected as a representative protecting group. Variation at the α -position of the ether provided no significant effect on yield or selectivity (Table 2, entries 1 and 2). Bulkier substrates required

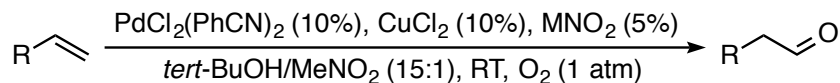
increased reaction time and replacement of NaNO₂ with the more active AgNO₂ to provide analogous yield and selectivity (entries 4 – 9).

Table 2.2 Influence of oxygen functional groups on Wacker oxidations^a

$$\text{R}-\text{CH}=\text{CH}_2 \xrightarrow[\text{tert-BuOH/MeNO}_2 (15:1), \text{RT}, \text{O}_2 (1 \text{ atm})]{\text{PdCl}_2(\text{PhCN})_2 (10\%), \text{CuCl}_2 (10\%), \text{NaNO}_2 (5\%)} \text{R}-\text{CH}_2-\text{CHO}$$

Entry	Substrate	Oxidation Yield (Aldehyde Yield) ^b	Selectivity ^c	Innate Selectivity (Tsuji-Wacker) ^d
1		76%	90:10	4:96
2		76%	90:10	20:80
3		71% ^e	92:8	9:91
4		88%	91:9	3:97
5		85%	94:6	7:93
6 ^f		75% ^e	94:6	64:46
7		82%	96:4	41:59
8		64% ^e	92:8	86:14

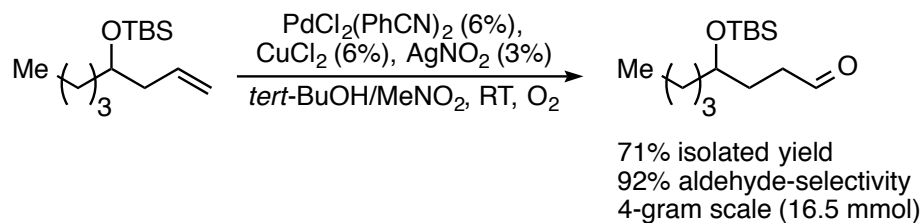
^a0.5 mmol alkene (0.0625M), 5 h. ^bYield of isolated aldehyde product. ^cSelectivity (aldehyde:ketone) obtained by ¹H NMR analysis of the unpurified reaction mixture. ^dReaction conditions: 0.1 mmol alkene, PdCl₂ (10 mol%), CuCl (1 equiv), DMF/H₂O (7:1, 0.125M), RT (20–25 °C), run to ≥95% conversion. ^eYield determined by ¹H NMR analysis of the unpurified reaction mixture. ^fAgNO₂ used in place of NaNO₂.

Table 2.3 Influence of steric profile on aldehyde-selective Wacker^a

Entry	Substrate	Nitrite Source	Aldehyde Yield ^b	Selectivity ^c	Innate Selectivity (Tsuji–Wacker) ^d
1		NaNO ₂	80%	93:7	7:93
2		NaNO ₂	74%	94:6	20:80
3		NaNO ₂	51% ^e	93:7	9:91
4		AgNO ₂	77% ^f	90:10	–
5		NaNO ₂	37% ^e	95:5	8:92
6 ^g		NaNO ₂	75% ^e	88:12	–
7 ^g		AgNO ₂	77%	95:5	–
8		NaNO ₂	38%	66:34	10:90
9 ^g		AgNO ₂	65%	75:25	–

^a0.5 mmol alkene (0.0625M), 5 h. ^bYield of isolated aldehyde product. ^cSelectivity (aldehyde:ketone) obtained by ¹H NMR analysis of the unpurified reaction mixture. ^d0.1 mmol alkene, PdCl₂ (10 mol%), CuCl (1 equiv), DMF/H₂O (7:1, 0.125M), RT (20–25 °C), run to ≥95% conversion (24 h). Selectivity determined by ¹H NMR analysis. ^eYield determined by ¹H NMR analysis. ^fIsolated as an inseparable mixture of aldehyde and ketone. ^g24 h reaction time

In order to assess the applicability of the process on a larger scale, the reaction was attempted on a 4-gram scale with reduced catalyst loading (Scheme 2.8). The reaction was 92% aldehyde-selective, delivering 71% of the aldehyde product. This result suggests that the reaction will be readily amenable to producing significant quantities of the desired aldehyde products.

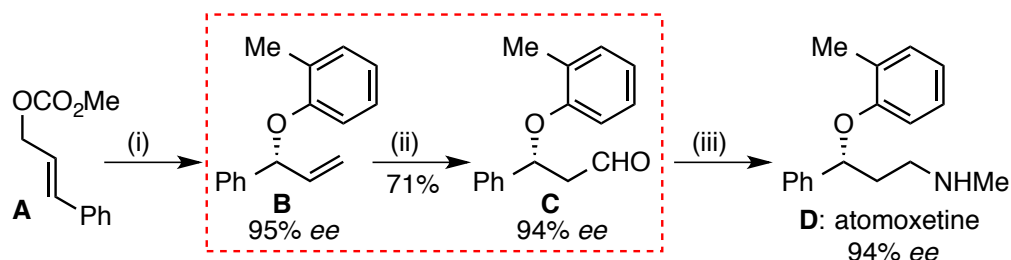


Scheme 2.8 Aldehyde-selective Wacker on 16.5 mmol scale

with reduced loading of catalysts.

A catalyst-controlled anti-Markovnikov Wacker oxidation combined with established enantioselective methodologies enables a powerful strategy to access versatile enantioenriched building blocks. To demonstrate the utility of this synthetic approach, we targeted atomoxetine, a norepinephrine reuptake inhibitor approved for the treatment of attention deficit disorder (Scheme 2).⁵⁹ At the outset, one potential concern with this approach was whether the stereocenter proximal to the alkene would racemize under the nitrite-modified reaction conditions. To test the viability of this route, cinnamyl alcohol derivative **A** was transformed into chiral allylic ether **B** via a highly enantioselective iridium-catalyzed allylic substitution reaction.⁶⁰ Upon treatment of **B** with the anti-Markovnikov Wacker conditions, the corresponding aldehyde, **C**, was produced in good yield. Subsequent derivatization via reductive amination demonstrated that the targeted drug, **D**, could be accessed without loss of enantiopurity over the course of the synthetic sequence. The success of this strategy, particularly the retention of stereochemical information at the allylic position, showcases that the nitrite-modified Wacker oxidation is compatible with well-established

asymmetric methods and provides access to valuable synthetic products in a modular, catalytic manner.



Scheme 2.9. Synthesis of atomoxetine. (i) $[\text{Ir}(\text{COD})\text{Cl}]_2$ (1 mol%), (*R,R,R*)-(3,5-Dioxa-4-phospha-cyclohepta[2,1-a;3,4-a']dinaphthalen-4-yl)bis(1-phenylethyl)amine (2 mol%), THF, 50 °C, 16 h; (ii) $\text{PdCl}_2(\text{PhCN})_2$ (10%), $\text{CuCl}_2 \cdot 2\text{H}_2\text{O}$ (10%), AgNO_2 (5%), *tert*-BuOH/MeNO₂ (15:1), O₂ (1 atm), RT, 5 h (iii) NaBH_3CN (2 equiv), MeNH₃Cl (excess), RT, 24 h.

To provide a foundation for further mechanistic study, we next probed the substrate-derived factors that enhance the catalyst-controlled aldehyde selectivity. To this end, the relative rates of functionalized and unfunctionalized substrates were obtained in a series of one-pot intermolecular competition experiments (Figure 2.7). Both functionalized substrates exhibited a substantial increase in the rate of aldehyde formation relative to the unfunctionalized 1-dodecene. We suspect that coordination of the Lewis basic oxygen atom to palladium increases the rate since inductive effects would be mitigated as the oxygen atom is moved further from the alkene.

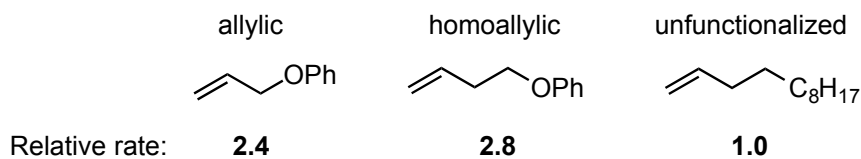
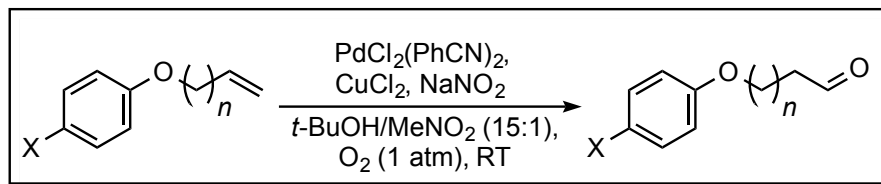


Figure 2.7 Relative rates of oxidation to aldehyde as a function of substrate under nitrite-modified Wacker conditions (see Table 1 for conditions).

To further probe the role of the oxygen atom, allylic and homoallylic aryl ethers of varied electronic profiles were prepared and evaluated under the reaction conditions. Inductive effects have recently been demonstrated to play a major role in determining regioselectivity in palladium-catalyzed processes,^{61,62} an observation that will be further discussed in Chapter 5. Interestingly, under the nitrite-modified Wacker conditions, the aldehyde-selectivity and rate are only subtly influenced by electronic variation (Figure 3). The minimal inductive influence is consistent with an apolar, radical-type addition.^{49,50,63} In the first section of this chapter, a radical mechanism to explain the anti-Markovnikov selectivity was suggested in light of ¹⁸O-labeling experiments. In addition to illustrating the minimal inductive influence on alkene oxidation, these experiments suggest that electronic modulation does little to enhance or mitigate the coordinating influence of the Lewis basic oxygen functional groups.



		X = NO ₂	X = H	X = OMe
<i>n</i> = 1 (allylic)	Selectivity	97:3	97:3	96:4
	Relative rate	1.2	1.0	1.2

<i>n</i> = 2 (homoallylic)	Selectivity	90:10	91:9	90:10
	Relative rate	1.3	1.0	1.1

Figure 2.8. Selectivity and relative rates of oxidation to aldehyde as a function of the substrate's electronic properties under nitrite-modified Wacker conditions (see Table 1 for conditions, 10 m reaction time).

Conclusion

In summary, this anti-Markovnikov, nitrite-modified Wacker oxidation provides a facile route for the preparation of functionalized aldehydes from a wide variety of oxygenated alkenes. The reliability and versatility of the methodology bodes well for its immediate application in target-oriented synthesis. The potential of the transformation was illustrated in the rapid, enantioselective synthesis of atomoxetine. Finally, key substrate-derived influences on the regioselectivity were explored, which provided important mechanistic information regarding the interplay between catalyst- and substrate-control, which will guide ongoing mechanistic evaluation of this important process.

Experimental Section

Materials and Methods

General Reagent Information: Preparation of non-commercial substrates: Unless stated otherwise, all reactions except for the Wacker oxidations were carried out in oven- and flame-dried glassware (200 °C) using standard Schlenk techniques and were run under argon atmosphere. Wacker oxidations were carried out without exclusion of air. The reaction progress was monitored by TLC. Starting materials and reagents were purchased from *Sigma Aldrich*, *Acros*, *Fluka*, *Fischer*, *TCI* or *Synquest Laboratories* and were used without further purification, unless stated otherwise. Solvents for the reactions were of quality puriss., p.a. of the companies *Fluka* or *J.T. Baker* or of comparable quality. Anhydrous solvents were purified by passage through solvent purification columns. For aqueous solutions, deionized water was used.

General Analytical Information: Nuclear Magnetic Resonance spectra were measured with a *Varian-Inova 500* spectrometer (500 MHz), a *Varian-Inova 400* spectrometer (400 MHz), or a *Varian-Mercury Plus 300* spectrometer (300 MHz). The solvent used for the measurements is indicated. All spectra were measured at room temperature (22–25 °C). Chemical shifts for the specific NMR spectra were reported relative to the residual solvent peak [CDCl_3 : $\delta_{\text{H}} = 7.26$; CDCl_3 : $\delta_{\text{C}} = 77.16$]. The multiplicities of the signals are denoted by *s* (singlet), *d* (doublet), *t*

(triplet), *q* (quartet), *p* (pentet) and *m* (multiplet). The coupling constants *J* are given in Hz. All ¹³C-NMR spectra are ¹H-broadband decoupled, unless stated otherwise. High-resolution mass spectrometric measurements were provided by the California Institute of Technology Mass Spectrometry Facility using a JEOL JMS-600H High Resolution Mass Spectrometer. The molecule-ion M⁺, [M + H]⁺, and [M-X]⁺, respectively, or the anion are given in *m/z*-units. Response factors relative to tridecane were collected for 1-dodecene, dodecanal and 2-dodecanone following literature procedures.⁶⁴

General Considerations: Thin Layer Chromatography analyses were performed on silica gel coated glass plates (0.25 mm) with fluorescence-indicator UV₂₅₄ (Merck, TLC silica gel 60 F₂₅₄). For detection of spots, UV light at 254 nm or 366 nm was used. Alternatively, oxidative staining using aqueous basic potassium permanganate solution (KMnO₄) was performed. Flash column chromatography was conducted with *Silicagel 60* (Fluka; particle size 40–63 μM) at 24 °C and 0–0.3 bar excess pressure (compressed air) using Et₂O/pentane unless state otherwise.

General procedures

Procedure (A) for larger-scale (0.5 mmol) oxidation of aliphatic alkenes (isolation): PdCl₂(PhCN)₂ (0.06 mmol, 0.023 g), CuCl₂*2H₂O (0.06 mmol, 0.0102 g) and AgNO₂ (0.03 mmol, 0.0046 g) were weighed into a 20 mL vial charged

with a stir bar. The vial was sparged for 2 min with oxygen (1 atm, balloon). Premixed and oxygen saturated t BuOH (7.5 mL) and MeNO₂ (0.5 mL) was added followed by the alkene (0.5 mmol) via syringe. The solution was saturated with oxygen by an additional 45 seconds of sparging. The reaction was then allowed to stir at room temperature for 6 hours. Next, the reaction was quenched by addition to water (*ca.* 50mL) and extracted three times with dichloromethane (*ca.* 25 mL). The combined organic layers were subsequently washed with a saturated solution of NaHCO₃ and dried over Na₂SO₄. The solvent was removed under reduced pressure and the desired aldehyde product was purified using flash chromatography (pentane/ether). Selectivity was determined from ¹H NMR analysis of the unpurified mixture.

Procedure (B) for smaller-scale (0.2 mmol) oxidation of 1-dodecene (GC analysis): PdCl₂(PhCN)₂ (0.024 mmol, 0.0092 g), CuCl₂·2H₂O (0.024 mmol, 0.0041 g) and AgNO₂ (0.012 mmol, 0.0018 g) were weighed into a 2 dram screw-cap vial charged with a stir bar. The vial was sparged for 45 seconds with oxygen (1 atm, balloon) and then subsequently tridecane (0.00246 mmol, 6 μL), t BuOH (3 mL), MeNO₂ (0.2 mL) and 1-dodecene (0.2 mmol, 44.4 μL) were added in that order via syringe. The solution was saturated with oxygen by an additional 45 seconds of sparging. The reaction was then allowed to stir at room temperature for 6 hours. Next, an aliquot (*ca.* 0.2 mL) was injected into a 2 mL vial containing an estimated 1 mL of premixed EtOAc/pyridine solution (3:1) to quench the

reaction. The resulting solution was subsequently subjected to GC analysis to determine yield and selectivity.

Procedure (C) for small-scale (0.2mmol) oxidation of alkenes (NMR analysis): PdCl₂(PhCN)₂ (0.024 mmol, 0.0092 g), CuCl₂·2H₂O (0.024 mmol, 0.0041 g) and AgNO₂ (0.012 mmol, 0.0018 g) were weighed into a 2 dram screw-cap vial charged with a stir bar. The vial was sparged for 45 seconds with oxygen (1 atm, balloon) then subsequently *t*-BuOH (3 mL), MeNO₂ (0.2 mL) and alkene (0.2 mmol) were added in that order via syringe. The solution was saturated with oxygen by an additional 45 seconds of sparging. The reaction was then allowed to stir at room temperature for 6 hours. Next, the reaction mixture was diluted with water (*ca.* 20 mL) and subsequently extracted three times with CDCl₃, dried with Na₂SO₄ and concentrated under reduced pressure for ¹H NMR analysis. Immediately prior to NMR analysis nitrobenzene was added as an internal standard. The resulting solution was subsequently subjected to ¹H NMR analysis to determine yield and selectivity.

Procedure (D) for preparative scale (0.5 mmol) oxidation of functionalized alkenes (isolation): PdCl₂(PhCN)₂ (0.05 mmol, 19.2 mg), CuCl₂·2H₂O (0.05 mmol, 8.5 mg) and NaNO₂ (0.025 mmol, 1.7 mg) were weighed into a 20 mL vial charged with a stir bar. The vial was sparged for 1 minute with oxygen (1 atm, balloon). Premixed and oxygen saturated *t*-BuOH (7.5 mL) and MeNO₂ (0.5 mL)

was added followed by the alkene (0.5 mmol). The solution was saturated with oxygen by an additional 30 seconds of sparging. The reaction was then allowed to stir at room temperature (20-25°C) for 4 h under 1 atm oxygen (balloon). Next, the reaction was quenched by addition to water (*ca.* 50mL) and extracted three times with dichloromethane (*ca.* 25 mL). The combined organic layers were subsequently washed with a saturated solution of NaHCO₃ and dried over Na₂SO₄. The solvent was removed under reduced pressure and the desired aldehyde product was purified using flash chromatography (pentane/ether). The selectivity was calculated by ¹H NMR analysis of the unpurified reaction mixture.

Procedure (E) for analytical scale (0.2 mmol) oxidation of alkenes (NMR analysis): PdCl₂(PhCN)₂ (0.02 mmol, 7.7 mg), CuCl₂·2H₂O (0.02 mmol, 3.6 mg) and NaNO₂ (0.01 mmol, 0.7 mg) were weighed into a 8 mL vial charged with a stir bar. The vial was sparged for 1 minute with oxygen (1 atm, balloon). Premixed and oxygen saturated *t*-BuOH (3 mL) and MeNO₂ (0.2 mL) was added followed by the alkene (0.2 mmol). The solution was saturated with oxygen by an additional 15 seconds of sparging and then sealed under an atmosphere of oxygen. The reaction was then allowed to stir at room temperature (20-25°C) for 4 h. Next, the reaction was quenched by addition to water (*ca.* 10mL) and extracted three times with dichloromethane (*ca.* 5 mL). The combined organic layers were subsequently washed with a saturated solution of NaHCO₃ and dried over Na₂SO₄. After volatiles were removed under reduced pressure,

nitrobenzene was added as an internal standard. The resulting solution was subsequently subjected to ^1H NMR analysis to determine yield and selectivity.

Procedure for Tsuji–Wacker oxidations: PdCl_2 (1.8 mg, 0.01 mmol) and CuCl (9.9 mg, 0.1 mmol) were weighed into a 8 mL vial. DMF (0.7 mL) and water (0.1 mL) were both added to the vial. The vial was sparged with oxygen (1 atm, balloon) for 3 minutes. The solution was stirred for another 1 h before alkene (0.1 mmol) was added. The reaction was stirred for at room temperature (20-25°C). After 24 h, the reaction mixture was quenched by addition of water (*ca.* 10 mL) and extracted three times with dichloromethane (*ca.* 5 mL). The combined organic layers were subsequently washed with a saturated solution of LiCl(aq) . After volatiles were removed under reduced pressure, nitrobenzene was added as an internal standard. The resulting solution was subsequently subjected to ^1H NMR analysis to determine yield and selectivity.

Collection of Reaction Profiles

Procedure B was followed. Time points were collected with a Freeslate (formly symyx) at the given times and quenched with a 3:1 mixture of EtOAc and pyridine, followed by GC analysis using tridecane as an internal standard. Reaction temperature was maintained at 20 °C throughout the course of the reaction. After GC analysis, the data was processed and graphed using Microsoft Excel.

Optimization of the Nitrite Additive

All entries in Table 2.1 produced following procedure B with the noted modifications.

entry	Nitrite source	Overall yield (aldehyde yield)	aldehyde/ketone (% selectivity)
1	Ref 35 (Grubbs)	9 (<1)	.16 (14)
2	Ref 39 (Feringa)	68 (12)	.22 (18)
3	<i>tert</i> -BuONO	76 (43)	1.3 (57)
4	<i>tert</i> -BuONO ^a	82 (38)	.85 (46)
5	<i>n</i> -BuONO	81 (51)	1.7 (63)
6	NOBF ₄	80 (54)	2.1 (68)
7	AgNO ₂	77 (61)	3.8 (79)
8	AgNO ₂ ^b	80 (63)	3.8 (79)
9	NaNO ₂ ^b	82 (62)	3 (75)
10	AgNO ₃	32(13)	.72 (42)
11	AgNO ₂ ^c	77 (49)	1.7 (63)
12	PdNO ₂ Cl(MeCN) ₂ ^d	70 (34)	.9 (48)

^a1 equiv *tert*-BuONO used instead of 12%. ^b6% nitrite used ^cMeNO₂ was omitted and reaction run at 30 °C. ^dNo PdCl₂(PhCN)₂

¹⁸O-Labeling Study

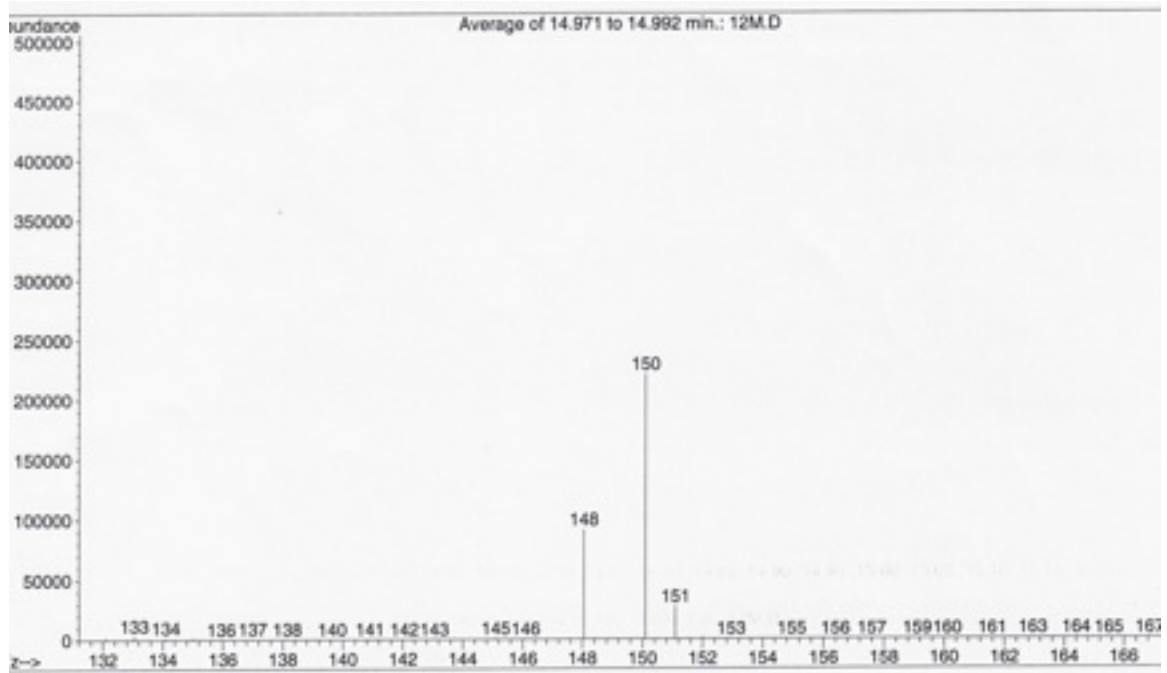
Labeling Experiment Procedure: In a drybox under a nitrogen atmosphere, 1 mg (0.013 mmol) Na¹⁵N¹⁸O₂ (90% ¹⁸O, 95% ¹⁵N specified by Sigma-Aldrich) was weighed into a 2 mL vial, followed by the addition of 5.2 mg PdCl₂(PhCN)₂ (0.013 mmol) and 1.8 mg anhydrous CuCl₂ (0.013 mmol). 200 μL of pre-mixed dry *t*-BuOH and MeNO₂ (15:1) was then added, followed by vigorously agitation for one minute. Following agitation, 2 μL (0.013 mmol) 4-phenyl-1-butene was added. The reaction mixture was stirred for 12 min at room temperature. An aliquot of

the mixture 100 μL was then rapidly taken out of the drybox and quenched by addition into 1 mL dry pyridine, immediately followed by freezing in liquid nitrogen. The sample was kept at $-178\text{ }^{\circ}\text{C}$ and was allowed to warm to room temperature directly before injection into the GC-MS.

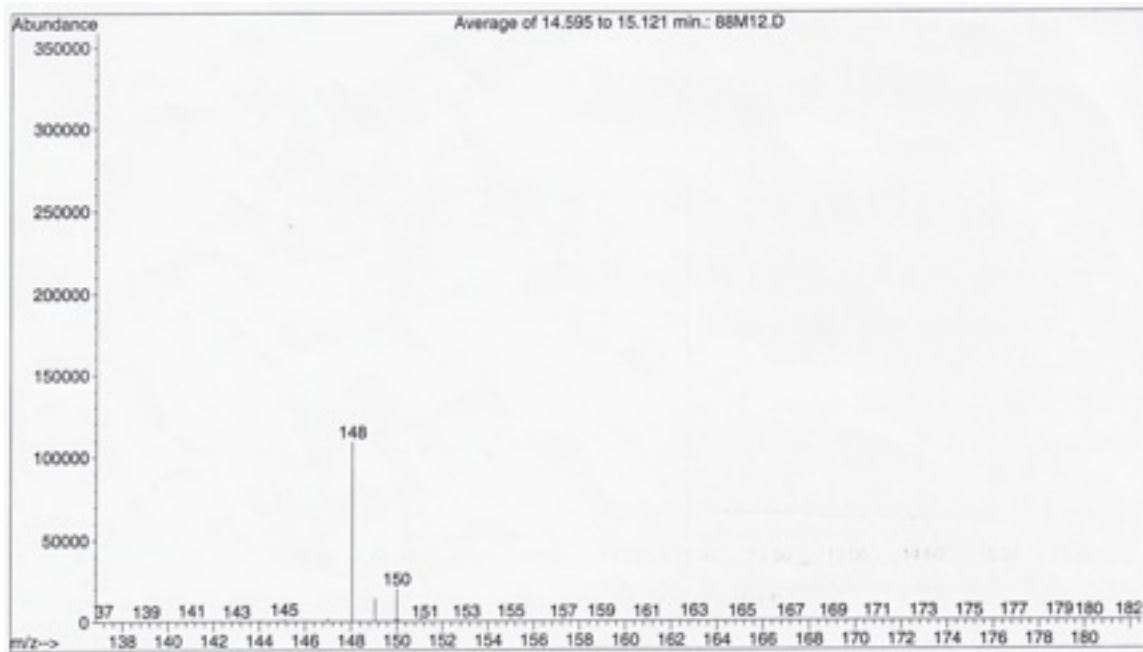
Labeling Experiment Analysis: The level of incorporation was determined by the counts of m/z 150, 151 divided by the total counts (of m/z 148, 149, 150, 151). This % incorporation (73%) was then subsequently adjusted by the initial purity of the ^{18}O -label (90%) to determine the percentage of ^{18}O transferred from the nitrite salt (81%).

Control experiment procedure: The product aldehyde (4-phenylbutanal) was subjected to the same reaction conditions and subsequent analysis as described above for the labeling experiment. The % ^{18}O transfer was thus determined to be 18%.

Mass spectrum of ^{18}O -enriched 4-phenylbutanal:



Mass spectrum of 4-phenylbutanal after being subjected to the ^{18}O -labeling conditions (control):



Detailed discussion of labeling experiment: The reaction was not allowed to reach completion because residual water can rapidly exchange with the aldehyde signal by formation of a transient hemiacetal. This exchange would be expected to dilute the isotopic label. Thus, we suspect the 19% dilution of isotopic label can be accounted for by exchange of the aldehydic oxygen atom. The reaction yield was estimated by ^1H NMR analysis (using benzonitrile as an internal standard) on an unlabeled sample prepared by the same protocol. Yield of aldehyde was estimated to be 35% from this analogous reaction. Labeling was also observed (to a lesser extent ~60%) in the ketone product. However, it has been previously shown with ^{18}O -labeled nitrite that palladium can transfer oxygen from nitrite in a ketone selective Wacker-type oxidation.⁴⁶ 4-Phenylbutene was selected as the substrate for its prominent molecular ion. The molecular ion for 1-dodecanal was challenging to obtain reproducibly.

Intermolecular Competition Experiments

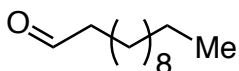
Competition experiment procedure: Each initial rate measurement was made in duplicate and the values averaged. The following procedure was used: $\text{PdCl}_2(\text{PhCN})_2$ (0.02 mmol, 7.7 mg), $\text{CuCl}_2 \cdot 2\text{H}_2\text{O}$ (0.02 mmol, 3.6 mg) and NaNO_2 (0.01 mmol, 0.7 mg) were weighed into a 8 mL vial charged with a stir bar. The vial was sparged for 1 minute with oxygen (1 atm, balloon). Premixed and oxygen saturated *t*-BuOH (3 mL) and MeNO_2 (0.2 mL) was added followed by the addition of pre-mixed alkenes (0.1 mmol of each alkene). The solution was

saturated with oxygen by an additional 10 seconds of sparging. The reaction was then allowed to stir at room temperature (20–25°C) for 10 minutes. Next, the reaction was quenched by addition of pyridine (5 μ L) and then water (10mL) and extracted three times with dichloromethane (*ca.* 5 mL). The combined organic layers were subsequently washed with a saturated solution of NaHCO₃ (*ca.* 5 mL) and dried over Na₂SO₄. The resulting solution was subjected to ¹H NMR analysis to determine relative rates. Benzonitrile signals were used as an internal standard to confirm that conversion was <15% in each case.

The selectivity of each substrate under the nitrite-modified Wacker was independently measured using procedure E.

Product Characterization

In all cases, the selectivity was calculated by ¹H NMR of the crude reaction mixture. The ratio of the aldehydic proton signal to the clearest signal from the methyl ketone was used. Long relaxation delays (d1=15) were applied due to the long t₁ of the aldehydic proton signal.

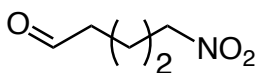


Dodecanal (Table 2.1, entry 1): 63% aldehyde yield obtained using procedure B.

Dodecanal (Table 2.1, entry 2): 56 mg (61% yield) obtained using procedure A.

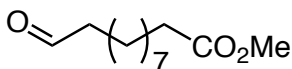
¹H NMR (500 MHz, CDCl₃) δ 9.76 (t, *J* = 1.9 Hz, 1H), 2.43 (td, *J* = 7.4, 1.9 Hz,

2H), 1.64 (tt, $J = 7.5, 7.5$ Hz, 2H), 1.49 – 1.18 (m, 16H), 0.97 – 0.77 (t, $J = 6.8, 3$ H). Spectral data were in accordance with a commercial sample.

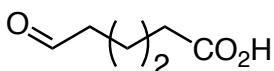


5-Nitropentanal (Table 2.1, entry 3): 46 mg (70%) obtained using procedure A.

$^1\text{H NMR}$ (400 MHz, CDCl_3) δ 9.78 (t, $J = 1.1$ Hz, 1H), 4.40 (t, $J = 6.8$ Hz, 2H), 2.54 (td, $J = 7.1, 1.1$ Hz, 2H), 2.09 – 2.00 (m, 2H), 1.77 – 1.68 (m, 2H). **$^{13}\text{C NMR}$** (101 MHz, CDCl_3) δ 200.84, 75.17, 42.78, 26.57, 18.74. **HRMS** (EI+) calcd for $\text{C}_5\text{H}_9\text{O}_2\text{N}$ (M - CHO) 102.0555, found 102.0560.

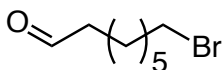


Methyl 11-oxoundecanoate (Table 2.1, entry 4): 63 mg (59% yield) obtained using procedure A. **$^1\text{H NMR}$** (500 MHz, CDCl_3) δ 9.74 (t, $J = 1.9$ Hz, 1H), 3.56 (s, 3H), 2.40 (td, $J = 7.4, 1.9$ Hz, 2H), 2.28 (t, $J = 7.6$ Hz, 2H), 1.73 – 1.48 (m, 4H), 1.34 – 1.20 (s, 10H). Spectral data were in accordance with the literature.⁶⁵

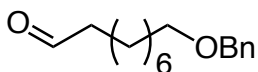


7-oxoheptanoic acid (Table 2.1, entry 5): 51% aldehyde yield obtained using procedure C with the following modifications: work up was conducted by initial

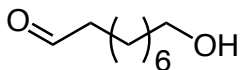
dilution with 0.5M HCl instead of water and mestylene was added as an internal standard instead of nitrobenzene.



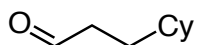
8-Bromooctanal (Table 2.1, entry 6): 67 mg (65% yield). $^1\text{H NMR}$ (300 MHz, CDCl_3) δ 9.76 (t, $J = 1.8$ Hz, 1H), 3.40 (t, $J = 6.8$ Hz, 2H), 2.42 (td, $J = 7.3, 1.8$ Hz, 2H), 1.83 (p, $J = 6.8$ Hz, 2H), 1.62 (m, 2H), 1.42 (m, 2H), 1.34 (m, $J = 5.1, 3.7$ Hz, 4H). Spectral data were in accordance with the literature.⁶⁶



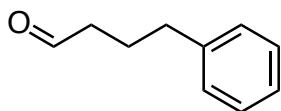
9-(Benzyloxy)nonanal (Table 2.1, entry 7): 73 mg (59% yield). $^1\text{H NMR}$ (300 MHz, CDCl_3) δ 9.76 (t, $J = 1.9$ Hz, 1H), 7.39 – 7.27 (m, 5H), 4.50 (s, 2H), 3.46 (t, $J = 6.6$ Hz, 2H), 2.53 – 2.31 (td, $J = 7.4, 1.9$ Hz, 2H), 1.70 – 1.53 (m, 4H), 1.42 – 1.22 (m, 8H). Spectral data were in accordance with the literature.⁶⁷



9-Hydroxynonanal (Table 2.1, entry 8): 36 mg (45% yield). $^1\text{H NMR}$ (500 MHz, CDCl_3) δ 9.76 (t, $J = 1.8$ Hz, 1H), 3.64 (t, $J = 5.6$ Hz, 2H), 2.43 (td, $J = 7.4, 1.9$ Hz, 2H), 1.69 - 1.24 (m, 12H). Spectral data were in accordance with the literature.⁶⁸

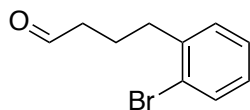


3-Cyclohexylpropanal (Table 2.1, entry 9): 60% aldehyde yield obtained using procedure C.

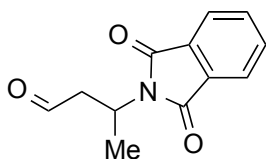


4-Phenylbutanal (Table 2.1, entry 10): 51 mg (69% yield). $^1\text{H NMR}$ (500 MHz, CDCl_3) δ 9.76 (t, $J = 1.6$ Hz, 1H), 7.32 – 7.27 (m, 2H), 7.24 – 7.15 (m, 3H), 2.67 (t, $J = 7.6$ Hz, 2H), 2.46 (td, $J = 7.3, 1.6$ Hz, 2H), 1.97 (p, $J = 7.4$ Hz, 2H).

Spectral data were in accordance with the literature.⁶⁹

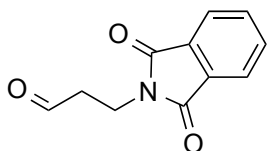


4-(2-bromophenyl)butanal (Table 2.1, entry 11): 64% aldehyde yield obtained using procedure C.

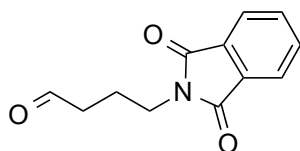


3-(1,3-dioxoisindolin-2-yl)butanal (Figure 2.2, entry 1): 86mg (79% yield) obtained using procedure A. $^1\text{H NMR}$ (500 MHz, CDCl_3) δ 9.75 (t, $J = 1.3$ Hz, 1H), 7.85 – 7.79 (m, 2H), 7.74 – 7.68 (m, 2H), 4.97 – 4.86 (m, 1H), 3.31 (ddd, $J =$

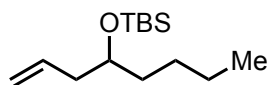
18.0, 8.2, 1.4 Hz, 1H), 3.01 (ddd, $J = 18.0, 6.2, 1.1$ Hz, 1H), 1.50 (d, $J = 7.0$ Hz, 3H). Spectra data were in accordance with the literature.¹⁰



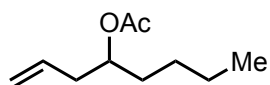
3-(1,3-dioxoisindolin-2-yl)propanal (Figure 2.2, entry 2): 76mg (75% yield) obtained using procedure A. ¹H NMR (500 MHz, CDCl₃) δ 9.82 (t, $J = 1.4$ Hz, 1H), 7.87 – 7.82 (m, 2H), 7.74 – 7.71 (m, 2H), 4.04 (t, $J = 7.0$ Hz, 2H), 2.88 (td, $J = 7.0, 1.4$ Hz, 2H). Spectra data were in accordance with the literature.⁷⁰



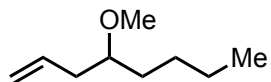
4-(1,3-dioxoisindolin-2-yl)butanal (Figure 2.2, entry 3): 84mg (77% yield) obtained using procedure A. ¹H NMR (500 MHz, CDCl₃) δ 9.77 (t, $J = 1.2$ Hz, 1H), 7.86 – 7.82 (m, 2H), 7.75 – 7.70 (m, 2H), 3.74 (t, $J = 6.8$ Hz, 2H), 2.54 (td, $J = 7.3, 1.2$ Hz, 2H), 2.02 (p, $J = 7.0$ Hz, 2H). Spectra data were in accordance with the literature.⁷⁰



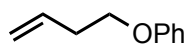
tert-Butyldimethyl(oct-1-en-4-yloxy)silane: Prepared according to the literature.⁷¹ **¹H NMR** (500 MHz, CDCl₃) δ 5.87 – 5.74 (m, 1H), 5.07 – 5.02 (m, 1H), 5.02 – 4.99 (m, 1H), 3.68 (p, *J* = 5.8 Hz, 1H), 2.29 – 2.14 (m, 2H), 1.50 – 1.21 (m, 6H). 0.89 (s, 9H), 0.88 (m, 3H), 0.05 (s, 6H). Spectral data were in accordance with the literature.⁷¹



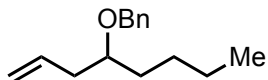
Oct-1-en-4-yl acetate: 4-Dimethylaminopyridine (122mg, 1 mmol) was weighed into a flask with a stir bar. Dichloromethane (10 mL), 1-octen-4-ol (1.54 mL, 10 mmol) and acetic anhydride (1.9 mL, 20 mmol) were added to the vial and stirred overnight (10 hours). The reaction mixture was diluted with water (*ca.* 125 mL) and extracted with dichloromethane (*ca.* 50 mL x3) and the combined organics were washed with brine and subsequently dried over MgSO₄. Purification by column chromatography gave the desired compound (1.52g, 89% yield) as a colorless oil. **¹H NMR** (500 MHz, CDCl₃) δ 5.73 (ddt, *J* = 17.2, 10.2, 7.1 Hz, 1H), 5.08 – 5.00 (m, 2H), 4.89 (ddd, *J* = 12.7, 6.6, 5.7 Hz, 1H), 2.34 – 2.22 (m, 2H), 2.01 (s, 3H), 1.59 – 1.47 (m, 2H), 1.45 – 1.17 (m, 4H), 0.96 – 0.81 (m, 3H). **¹³C NMR** (126 MHz, CDCl₃) δ 170.71, 133.78, 117.47, 73.27, 38.62, 33.24, 27.43, 22.49, 21.17, 13.93. **HRMS** (EI+) calc'd for C₇H₁₃O₂ (M-CH₂CHCH₂) 129.0916, found 129.0917.



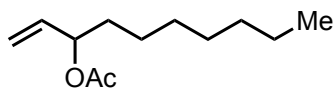
4-Methoxyoct-1-ene: NaH (60wt% dispersion in mineral oil, 600 mg, 15 mmol) was weighed into a flask with a stir bar. Tetrahydrofuran (10 mL) was added to the vial and the mixture was cooled to 0 °C. 1-Octen-4-ol (1.54 mL, 10 mmol) were added slowly to the suspension. MeI (0.75 mL, 12 mmol) was next added slowly to the reaction mixture. The reaction mixture was allowed to warm to room temperature and stirred overnight (*ca.* 10 h). The reaction mixture was diluted with water (*ca.* 125 mL) and extracted with diethyl ether (*ca.* 50 mL x3) and the combined organics were washed with brine and subsequently dried over MgSO₄. Purification by column chromatography gave the desired compound (1.01g, 71% yield) as a colorless oil. ¹H NMR (500 MHz, CDCl₃) δ 5.82 (ddt, *J* = 17.2, 10.2, 7.1 Hz, 1H), 5.06 (m, 2H), 3.34 (s, 3H), 3.20 (p, *J* = 5.9 Hz, 1H), 2.26 (m, 2H), 1.47 (m, 2H), 1.31 (m, 4H), 0.90 (m, 3H). Spectral data were in accordance with the literature.⁷²



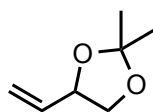
(but-3-en-1-yloxy)benzene: Prepared according to the literature.⁷³ ¹H NMR (500 MHz, CDCl₃) δ 7.31 – 7.26 (m, 2H), 6.97 – 6.92 (m, 1H), 6.92 – 6.90 (m, 2H), 5.95 (ddt, *J* = 17.1, 10.3, 6.7 Hz, 1H), 5.20 – 5.09 (m, 2H), 4.03 (t, *J* = 6.7 Hz, 2H), 2.60 – 2.51 (m, 2H). Spectral data were in accordance with the literature.⁷³



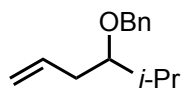
((oct-1-en-4-yloxy)methyl)benzene: NaH (60wt% dispersion in mineral oil, 600 mg, 15 mmol) was weighed into a flask with a stir bar. Tetrahydrofuran (10 mL) was added to the vial and the mixture was cooled to 0 °C. 1-Octen-4-ol (1.54 mL, 10 mmol) was added slowly to the suspension. Benzyl bromide (1.4 mL, 12 mmol) was next added slowly to the reaction mixture. The reaction mixture was allowed to warm to room temperature and stirred overnight (*ca.* 10 h). The reaction mixture was diluted with water (*ca.* 125 mL) and extracted with diethyl ether (*ca.* 50 mL x3) and the combined organics were washed with brine and subsequently dried over MgSO₄. Purification by column chromatography gave the desired compound (1.48g, 68% yield) as a colorless oil. **¹H NMR** (500 MHz, CDCl₃) δ 7.41 – 7.34 (m, 4H), 7.33 – 7.27 (m, 1H), 5.89 (ddt, *J* = 17.2, 10.2, 7.1 Hz, 1H), 5.21 – 5.06 (m, 2H), 4.60 (d, *J* = 15.0 Hz, 1H), 4.52 (d, *J* = 15.0 Hz, 1H), 3.47 (dq, *J* = 6.7, 5.6 Hz, 1H), 2.47 – 2.26 (m, 2H), 1.67 – 1.50 (m, 2H), 1.50 – 1.26 (m, 4H), 0.93 (t, *J* = 7.0 Hz, 1H). **¹³C NMR** (126 MHz, CDCl₃) δ 138.97, 135.12, 128.29, 127.72, 127.42, 116.79, 78.58, 70.89, 38.33, 33.52, 27.58, 22.81, 14.11. **HRMS** (EI+) calc'd for C₁₂H₁₇O (M - CH₂CHCH₂) 177.1279, found 177.1284.



Dec-1-en-3-yl acetate: the literature.⁷⁴ $^1\text{H NMR}$ (500 MHz, CDCl_3) δ 5.82 – 5.72 (m, 1H), 5.26 – 5.19 (m, 2H), 5.14 (dt, $J = 10.4, 1.2$ Hz, 1H), 2.05 (s, 3H), 1.72 – 1.52 (m, 2H), 1.36 – 1.23 (m, 10H), 0.90 (d, $J = 12.5$ Hz, 3H). Spectral data were in accordance with the literature.⁷⁴

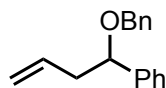


2,2-Dimethyl-4-vinyl-1,3-dioxolane: prepared according to the literature.⁷⁵ $^1\text{H NMR}$ (300 MHz, CDCl_3) δ 5.82 (m, 1H), 5.36 (m, 1H), 5.22 (ddd, $J = 10.3, 1.5, 0.8$ Hz, 1H), 4.50 (dtd, $J = 7.3, 6.7, 6.3, 0.9$ Hz, 1H), 4.11 (dd, $J = 8.1, 6.2$ Hz, 1H), 3.60 (t, $J = 7.9$ Hz, 1H), 1.41 (d, $J = 10.5$ Hz, 6H). Spectral data were in accordance with the literature.⁷⁵



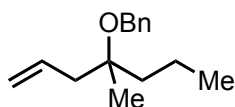
(((2-methylhex-5-en-3-yl)oxy)methyl)benzene: prepared according to literature.⁷⁶ $^1\text{H NMR}$ (500 MHz, CDCl_3) δ 7.38 – 7.31 (m, 4H), 7.30 – 7.24 (m, 1H), 5.89 (ddt, $J = 17.2, 10.2, 7.1$ Hz, 1H), 5.10 (ddt, $J = 17.1, 2.2, 1.5$ Hz, 1H), 5.05 (ddt, $J = 10.2, 2.2, 1.2$ Hz, 1H), 4.58 (d, $J = 10$ Hz, 1H), 4.50 (d, $J = 10$ Hz, 1H), 3.20 (dt, $J = 6.2, 5.5$ Hz, 1H), 2.31 (ddd, $J = 7.3, 5.8, 1.3$ Hz, 2H), 1.95 –

1.80 (m, 1H), 0.96 (d, $J = 6.8$ Hz, 3H), 0.93 (d, $J = 6.8$ Hz, 3H). Spectral data were in accordance with the literature.⁷⁶



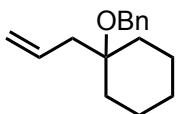
(1-(benzyloxy)but-3-en-1-yl)benzene: prepared according to literature.⁷⁷ ¹H

NMR (500 MHz, CDCl₃) δ 7.41 – 7.27 (m, 10H), 5.78 (ddt, $J = 17.1, 10.2, 6.9$ Hz, 1H), 5.07 – 5.00 (m, 2H), 4.47 (d, $J = 12.0$ Hz, 1H), 4.37 (dd, $J = 7.6, 5.8$ Hz, 1H), 4.27 (m, 1H), 2.65 (dddt, $J = 14.4, 7.7, 6.9, 1.3$ Hz, 1H), 2.44 (dddt, $J = 14.2, 7.1, 5.8, 1.3$ Hz, 1H). Spectral data were in accordance with the literature.⁷⁷

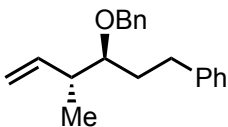


(((4-methylhept-1-en-4-yl)oxy)methyl)benzene: NaH (60wt% dispersion in mineral oil, 600 mg, 15 mmol) was weighed into a flask with a stir bar. Dimethylacetamide (10 mL) was added to the vial and the mixture was cooled to 0 °C. 4-Methylhept-1-en-4-ol (1.28 g, 10 mmol) was added slowly to the suspension. Benzyl bromide (1.4 mL, 12 mmol) was next added slowly to the reaction mixture. The reaction mixture was allowed to warm to room temperature and stirred overnight (*ca.* 10 h). The reaction mixture was diluted with water (*ca.* 125 mL) and extracted with diethyl ether (*ca.* 50 mL x3) and the combined organics were washed with brine and subsequently dried over MgSO₄. Purification by column chromatography gave the desired compound (1.29 g, 59%

yield) as a colorless oil. **¹H NMR** (400 MHz, CDCl₃) δ 7.38 – 7.22 (m, 5H), 5.97 – 5.83 (m, 1H), 5.14 – 5.06 (m, 2H), 4.44 (s, 2H), 2.43 – 2.29 (m, 2H), 1.62 – 1.49 (m, 2H), 1.48 – 1.36 (m, 2H), 1.22 (s, 3H), 0.94 (t, *J* = 7.2 Hz, 3H). **¹³C NMR** (101 MHz, CDCl₃) δ 139.75, 134.63, 128.22, 127.26, 127.04, 117.18, 76.86, 63.23, 42.95, 40.42, 23.26, 16.71, 14.65. **HRMS** (EI+) calc'd for C₁₂H₁₇O (M - CH₂CHCH₂) 177.1279, found 177.1283.

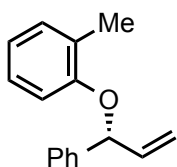


(((1-allylcyclohexyl)oxy)methyl)benzene: Prepared according to the literature.⁷⁷ **¹H NMR** (500 MHz, CDCl₃) δ 7.40 – 7.36 (m, 2H), 7.36 – 7.31 (m, 2H), 7.28 – 7.23 (m, 1H), 5.98 – 5.80 (m, 1H), 5.12 – 5.04 (m, 2H), 4.42 (s, 2H), 2.34 (dt, *J* = 7.2, 1.3 Hz, 2H), 1.87 – 1.81 (m, 2H), 1.69 – 1.56 (m, 3H), 1.50 – 1.43 (m, 2H), 1.42 – 1.32 (m, 2H), 1.32 – 1.20 (m, 1H). Spectral data were in accordance with the literature.⁷⁷



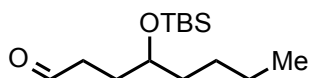
(*trans*-3-(benzyloxy)-4-methylhex-5-en-1-yl)benzene: NaH (60 wt% dispersion in mineral oil, 600 mg, 15 mmol) was weighed into a flask with a stir bar. Dimethylacetamide (10 mL) was added to the vial and the mixture was cooled to 0 °C. *trans*-4-methyl-1-phenylhex-5-en-3-ol (1.9 g, 10 mmol) was added slowly to

the suspension. Benzyl bromide (1.4 mL, 12 mmol) was next added slowly to the reaction mixture. The reaction mixture was allowed to warm to room temperature and stirred overnight (*ca.* 10 h). The reaction mixture was diluted with water (*ca.* 125 mL) and extracted with diethyl ether (*ca.* 50 mL x3) and the combined organics were washed with brine and subsequently dried over MgSO₄. Purification by column chromatography gave the desired compound (1.47 g, 52% yield) as a colorless oil. **¹H NMR** (400 MHz, CDCl₃) δ 7.44 – 7.13 (m, 10H), 5.88 – 5.76 (m, 1H), 5.12 – 5.01 (m, 2H), 4.62 (d, *J* = 10.1, 1H), 4.52 (d, *J* = 10.1 1H), 3.35 (dt, *J* = 8.4, 4.3 Hz, 1H), 2.84 – 2.76 (m, 1H), 2.60 (ddd, *J* = 13.9, 9.8, 6.7 Hz, 2H), 1.88–1.70 (m, 2H), 1.05 (d, *J* = 6.9 Hz, 3H). **¹³C NMR** (126 MHz, CDCl₃) δ 142.45, 140.79, 138.87, 128.42, 128.33, 128.31, 127.81, 127.50, 125.69, 114.64, 82.11, 71.73, 40.16, 32.46, 32.23, 14.50. **HRMS** (EI+) calc'd for C₂₀H₂₄O (M+) 280.1827, found 280.1818.

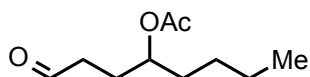


(*R*)-1-phenyl-1-(2-methylphenoxy)-2-propene: prepared according to the literature.⁷⁸ **¹H NMR** (500 MHz, CDCl₃) δ 7.44 – 7.41 (m, 2H), 7.40 – 7.34 (m, 2H), 7.31 – 7.27 (m, 1H), 7.16 – 7.13 (m, 1H), 7.05 (tdd, *J* = 8.0, 1.5, 0.9 Hz, 1H), 6.86 – 6.80 (m, 1H), 6.79 (d, *J* = 8.2 Hz, 1H), 6.10 (ddd, *J* = 17.1, 10.4, 5.8, Hz, 1H), 5.65 (d, *J* = 5.8 Hz, 1H), 5.38 (d, *J* = 17.3, Hz, 1H), 5.24 (dq, *J* = 10.4, 1.2 Hz,

1H), 2.33 (s, 3H). Spectral data were in accordance with the literature.⁷⁸ $[\alpha]_D = -7.6$ (c 0.94, CHCl₃), which is in accordance with literature values.⁸ HPLC analysis indicated an enantiomeric excess of 95% [Chiralcel® OJ-H column, eluting with 99.9:0.1 hexane/*i*-PrOH, 0.7 mL/min, 220 nm; (*S*) enantiomer t_R , 16.2, (*R*) enantiomer t_R 16.7 min].

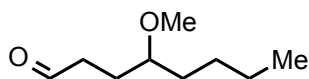


4-((*tert*-butyldimethylsilyloxy)octanal (Table 2.2, entry 1): 98.6 mg (76% yield) obtained using procedure D. ¹H NMR (500 MHz, CDCl₃) δ 9.79 (t, $J = 1.7$ Hz, 1H), 3.71 (tt, $J = 6.2, 4.5$ Hz, 1H), 2.49 (td, $J = 7.5, 1.7$ Hz, 2H), 1.89 – 1.80 (m, 1H), 1.71 (dt, $J = 13.7, 6.9$ Hz, 1H), 1.51 – 1.34 (m, 2H), 1.35 – 1.20 (m, 4H), 0.88, (m, 3H), 0.87 (s, 9H), 0.04 (d, $J = 4.1$ Hz, 6H). Spectral data were in accordance with the literature.⁷¹

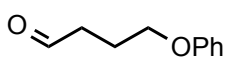


1-oxooctan-4-yl acetate (Table 2.2, entry 2): 70.8 mg (76% yield) obtained using procedure D. ¹H NMR (500 MHz, CDCl₃) δ 9.76 (t, $J = 1.4$ Hz, 1H), 4.89 (dddd, $J = 8.2, 7.3, 5.4, 4.0$ Hz, 1H), 2.48 (ddt, $J = 8.2, 6.7, 1.3$ Hz, 2H), 2.04 (s, 3H), 1.99 – 1.90 (m, 1H), 1.88 – 1.79 (m, 1H), 1.63 – 1.46 (m, 2H), 1.36 – 1.23 (m, 4H), 0.89 (t, $J = 7.0$ Hz, 3H). ¹³C NMR (126 MHz, CDCl₃) δ 201.47, 170.82,

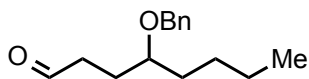
73.33, 39.96, 33.83, 27.40, 26.36, 22.50, 21.15, 13.94. **HRMS** (EI+) calc'd for $C_8H_{15}O_2$ (M - CH_3CO) 143.1072, found 143.1109.



4-methoxyoctanal (Table 2.2, entry 3): 71% obtained using procedure E.

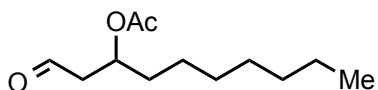


4-phenoxybutanal (Table 2.2, entry 4): 72.0 mg (88% yield) obtained using procedure D. 1H NMR (500 MHz, $CDCl_3$) δ 9.85 (t, $J = 1.4$ Hz, 1H), 7.32 – 7.24 (m, 2H), 6.95 (tt, $J = 7.4, 1.1$ Hz, 1H), 6.88 (dt, $J = 7.8, 1.0$ Hz, 2H), 4.01 (t, $J = 6.0$ Hz, 2H), 2.68 (td, $J = 7.1, 1.3$ Hz, 2H), 2.13 (tt, $J = 7.0, 6.0$ Hz, 2H). Spectral data were in accordance with the literature.ⁱ

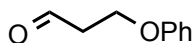


4-(benzyloxy)octanal (Table 2.2, entry 5): 99.9 mg (85% yield) obtained using procedure D. 1H NMR (500 MHz, $CDCl_3$) δ 9.76 (t, $J = 1.7$ Hz, 1H), 7.40 – 7.26 (m, 5H), 4.54 – 4.50 (m, 1H), 4.45 – 4.41 (m, 1H), 3.41 (dtd, $J = 7.3, 6.0, 4.1$ Hz, 1H), 2.52 (ddt, $J = 7.4, 6.9, 1.6$ Hz, 2H), 1.92 (dddd, $J = 14.5, 7.6, 6.9, 4.1$ Hz, 1H), 1.85 – 1.76 (m, 1H), 1.62 (dtd, $J = 13.6, 5.8, 4.7$ Hz, 1H), 1.52 – 1.42 (m, 1H), 1.33 (ttt, $J = 6.0, 4.2, 3.2, 2.0$ Hz, 4H), 0.91 (t, $J = 7.1$ Hz, 3H). ^{13}C NMR (126 MHz, $CDCl_3$) δ 202.55, 138.57, 128.36, 127.83, 127.57, 77.91, 70.87,

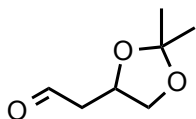
40.00, 33.34, 27.42, 26.28, 22.84, 14.06. **HRMS** (EI+) calc'd for C₁₅H₂₂O₂ (M+) 234.1620, found 234.1632.



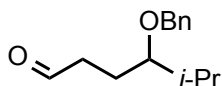
1-oxodecan-3-yl acetate (Table 2.2, entry 6): 75% obtained using procedure E.



3-phenoxypropanal (Table 2.2, entry 7): 61.3 mg (82% yield) obtained using procedure D. ¹H NMR (500 MHz, CDCl₃) δ 9.76 (t, *J* = 1.7 Hz, 1H), 7.32 – 7.27 (m, 2H), 7.00 – 6.95 (m, 1H), 6.93 – 6.90 (m, 2H), 4.32 (t, *J* = 6.1 Hz, 2H), 2.91 (td, *J* = 6.1, 1.6 Hz, 2H). Spectral data were in accordance with the literature.⁷⁹

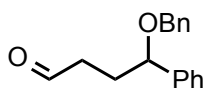


2-(2,2-dimethyl-1,3-dioxolan-4-yl)acetaldehyde (Table 2.2, entry 8): 64% yield obtained using procedure E.

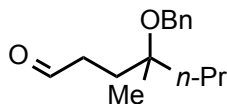


4-(benzyloxy)-5-methylhexanal (Table 2.3, entry 1): 88.1 mg (80% yield) obtained using procedure D. ¹H NMR (500 MHz, CDCl₃) δ 9.66 (t, *J* = 1.7 Hz, 1H), 7.30 – 7.17 (m, 5H), 4.46 (d, *J* = 12.5, 1H), 4.34 (d, *J* = 12.5 1H), 3.11 (ddd,

$J = 8.6, 5.4, 3.4$ Hz, 1H), 2.43 (m, 2H), 1.90 (dtd, $J = 13.7, 6.9, 5.4$ Hz, 1H), 1.78 (m, 1H), 1.70 (m, 1H), 0.89 (d, $J = 6.9$ Hz, 3H), 0.85 (d, $J = 6.9$ Hz, 3H). ^{13}C NMR (126 MHz, CDCl_3) δ 202.68, 138.60, 128.35, 127.85, 127.57, 83.14, 71.64, 40.39, 30.27, 22.49, 18.72, 17.30. **HRMS** (EI+) calc'd for $\text{C}_{14}\text{H}_{20}\text{O}_2$ (M+) 220.1463, found 220.1466.

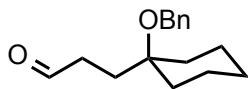


4-(benzyloxy)-4-phenylbutanal (Table 2.3, entry 2): 94.1 mg (74% yield) obtained using procedure D. ^1H NMR (500 MHz, CDCl_3) δ 9.74 (t, $J = 1.6$ Hz, 1H), 7.35 (m, 10H), 4.47 (d, $J = 11.7$ Hz, 1H), 4.37 (dd, $J = 8.3, 4.8$ Hz, 1H), 4.25 (d, $J = 11.7$ Hz, 1H), 2.54 (m, 2H), 2.14 (dtd, $J = 14.2, 8.4, 7.1$ Hz, 1H), 2.04 (m, 1H). ^{13}C NMR (126 MHz, CDCl_3) δ 202.21, 141.55, 138.18, 128.60, 128.38, 127.87, 127.81, 127.62, 126.63, 80.20, 70.52, 40.46, 30.91. **HRMS** (EI+) calc'd for $\text{C}_{11}\text{H}_{13}\text{O}_2$ (M - C_6H_5) 177.0916, found 177.0956.

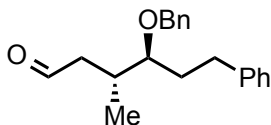


4-(benzyloxy)-4-methylheptanal (Table 2.3): 90.2 mg (77% yield) obtained using procedure D except NaNO_2 is replaced with AgNO_2 and the reaction is allowed to proceed for 24 h. Isolated as an inseparable mixture of aldehyde and ketone (9:1). Spectral data reported for aldehyde product (major). ^1H NMR (500

MHz, CDCl₃) δ 9.79 (t, *J* = 1.6 Hz, 1H), 7.35 – 7.31 (m, 4H), 7.28 – 7.24 (m, 1H), 4.37 (s, 2H), 2.55 (ddt, *J* = 8.4, 6.7, 1.6 Hz, 2H), 1.99 – 1.92 (m, 1H), 1.89 – 1.80 (m, 1H), 1.60 – 1.50 (m, 2H), 1.43 – 1.35 (m, 2H), 1.23 (s, 3H), 0.95 (t, *J* = 7.3 Hz, 3H). ¹³C NMR (126 MHz, CDCl₃) δ 202.66, 139.36, 128.30, 127.23, 127.19, 76.23, 63.25, 40.66, 38.73, 30.32, 23.02, 17.04, 14.69. HRMS (EI+) calc'd for C₁₃H₁₉O (M - CH₂CHO) 191.1436, found 191.1444.

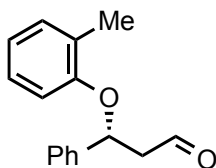


3-(1-(benzyloxy)cyclohexyl)propanal (Table 2.3): 94.8 mg (77% yield) obtained using procedure D except NaNO₂ is replaced with AgNO₂ and the reaction is allowed to proceed for 24 h. ¹H NMR (500 MHz, CDCl₃) δ 9.81 (t, *J* = 1.4 Hz, 1H), 7.38 – 7.32 (m, 4H), 7.29 – 7.24 (m, 1H), 4.35 – 4.29 (s, 2H), 2.54 (ddd, *J* = 9.1, 6.5, 1.5 Hz, 2H), 1.87 (m, 4H), 1.63 (m, 3H), 1.48 (m, 2H), 1.32 (m, 3H). ¹³C NMR (101 MHz, CDCl₃) δ 202.58, 139.30, 128.31, 127.23, 127.18, 74.77, 62.24, 37.90, 34.45, 28.51, 25.85, 21.92. HRMS (EI+) calc'd for C₁₆H₂₂O₂ (M+) 246.1620, found 246.1618.



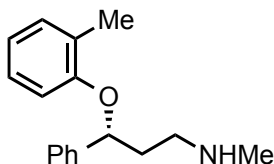
trans-4-(benzyloxy)-3-methyl-6-phenylhexanal (Table 2.3): 96.3 mg (65% yield) obtained using procedure D except NaNO₂ is replaced with AgNO₂ and the

reaction is allowed to proceed for 24 h. **¹H NMR** (500 MHz, CDCl₃) δ 9.72 (t, *J* = 2.1 Hz, 1H), 7.38 – 7.14 (m, 10H), 4.55 – 4.48 (m, 2H), 3.26 (td, *J* = 6.1, 4.3 Hz, 1H), 2.77 (ddd, *J* = 13.7, 9.9, 6.0 Hz, 1H), 2.66 (ddd, *J* = 13.8, 10.0, 6.7 Hz, 1H), 2.50 – 2.43 (m, 2H), 2.34 – 2.26 (m, 1H), 1.90 – 1.81 (m, 2H), 1.00 (d, *J* = 6.7 Hz, 3H). **¹³C NMR** (126 MHz, CDCl₃) δ 202.07, 142.18, 138.39, 128.43, 128.39, 128.34, 127.92, 127.66, 125.86, 82.08, 71.66, 47.86, 32.27, 31.27, 31.06, 16.36. **HRMS** (EI+) calc'd for C₂₀H₂₄O₂ (M+) 296.1776, found 296.1778.



(*R*)-3-phenyl-3-(2-methylphenoxy)propanal: 85.3 mg (71% yield) obtained using procedure D except NaNO₂ is replaced with AgNO₂. **¹H NMR** (500 MHz, CDCl₃) δ 9.88 (dd, *J* = 2.5, 1.6 Hz, 1H), 7.41 – 7.33 (m, 4H), 7.32 – 7.27 (m, 1H), 7.13 (ddd, *J* = 7.4, 1.7, 0.9 Hz, 1H), 6.98 (td, *J* = 8.1, 1.7 Hz, 1H), 6.82 (td, *J* = 7.4, 1.1 Hz, 1H), 6.65 (dd, *J* = 8.1, 1.2 Hz, 1H), 5.72 (dd, *J* = 8.6, 4.2 Hz, 1H), 3.15 (ddd, *J* = 16.6, 8.6, 2.6 Hz, 1H), 2.88 (ddd, *J* = 16.6, 4.2, 1.6 Hz, 1H), 2.28 (s, 3H). **¹³C NMR** (126 MHz, CDCl₃) δ 199.83, 155.38, 140.36, 130.77, 128.91, 128.06, 127.16, 126.58, 125.67, 120.88, 112.88, 74.88, 51.91, 16.42. **HRMS** (EI+) calc'd for C₁₆H₁₆O₂ (M+) 240.1150, found 240.1155. [α]_D = -10.1 (c 0.48,

CHCl₃). Enantiomeric excess checked by derivatization to atomoxetine (*vide infra*).



(*R*)-3-phenyl-3-(2-methylphenoxy)propanal was derivatized to atomoxetine by treatment of the aldehyde with excess NaBH₃CN (*ca.* 3 equiv) and methylamine hydrochloride (*ca.* 50 equiv) to provided a crude mixture (37% yield of atomoxetine according to ¹H NMR analysis), which was purified by preparatory thin layer chromatography for characterization and determination of enantiomeric excess. ¹H NMR (500 MHz, CDCl₃) δ 7.37 – 7.29 (m, 4H), 7.27 – 7.22 (m, 1H), 7.12 (ddd, *J* = 7.3, 1.7, 0.9 Hz, 1H), 6.98 – 6.92 (m, 1H), 6.78 (td, *J* = 7.4, 1.1 Hz, 1H), 6.62 – 6.58 (m, 1H), 5.28 (dd, *J* = 8.3, 4.4 Hz, 1H), 2.90 – 2.80 (m, 2H), 2.47 (s, 3H), 2.32 (s, 3H), 2.30 – 2.19 (m, 1H), 2.11 (dtd, *J* = 14.2, 7.3, 4.5 Hz, 1H). Spectral data were in accordance with the literature.⁸⁰ [α]_D = -31.6 (c 0.10, CHCl₃), which is in accordance with literature values.⁸⁰ SFC analysis indicated an enantiomeric excess of 94% [Chiralcel® OD-H column, eluting with 20% MeOH, 2.5 mL/min, 220 nm; (*S*) enantiomer *t*_R, 3.95, (*R*) enantiomer *t*_R 5.4 min].

References

- (1) Weissermel, K.; Arpe, H. J. *Industrial Organic Chemistry*, 4 ed.; Wiley-VCH, New York, **2003**

- (2) Trost, B. M. *Acc. Chem. Res.* **2002**, *35*, 695.
- (3) Gooch, E. E. *J. Chem. Educ.* **2001**, *78*, 1358.
- (4) Mahatthananchai, J.; Dumas, A. M.; Bode, J. W. *Angew. Chem. Int. Ed.* **2012**, *51*, 10954.
- (5) Haggin, J. *Chem. Eng. News* **1993**, *71*, 23.
- (6) Beller, M.; Seayad, J.; Tillack, A.; Jiao, H. *Angew. Chem. Int. Ed.* **2004**, *43*, 3368.
- (7) Smith, M. B.; March, J. *March's Advanced Organic Chemistry*, 5 ed.; Wiley, New York, **2001**.
- (8) Wang, C.; Pettman, A.; Basca, J.; Xiao, J. *Angew. Chem. Int. Ed.* **2010**, *49*, 7548.
- (9) Conley, B. L.; Pennington-Boggio, M. K.; Boz, E.; Williams, T. J. *Chem. Rev.* **2010**, *110*, 2294.
- (10) Weiner, B.; Baeza, A.; Jerphagnon, T.; Feringa, B. *J. Am. Chem. Soc.* **2009**, *131*, 9473.
- (11) Carreira, E. M.; Kvaerno, L. *Classics in Stereoselective Synthesis*, 1st ed.; Wiley-VCH, **2009**.
- (12) Eilbracht, P.; Bäracker, L.; Buss, C.; Hollmann, C.; Kitsos-Rzychon, B. E.; Kranemann, C. L.; Rische, T.; Roggenbuck, R.; Schmidt, A. *Chem. Rev.* **1999**, *99*, 3329.
- (13) Seayad, A.; Ahmed, M.; Klein, H.; Jackstell, R.; Gross, T.; Beller, M. *Science* **2002**, *297*, 1676.

- (14) Sheldon, R. A.; Cornils, B.; Herrmann, W. A. *Applied Homogeneous Catalysis with Organometallic Compounds*, 2nd ed.; Wiley-VCH, Weinheim, **2002**.
- (15) Smidt, J.; Hafner, W.; Sedlmeier, J.; Jira, R.; Rüttinger, R. *Angew. Chem.* **1959**, *71*, 176–182.
- (16) Tsuji, J. *Synthesis* **1984**, 369–384.
- (17) Takacs, J. M.; Xt, J. *Curr. Org. Chem.* **2003**, *7*, 369–396
- (18) Tsuji, J. *Palladium Reagents and Catalysts: New Perspectives for the 21st Century*; 2nd ed. Wiley, **2004**
- (19) Jira, R. *Angew. Chem. Int. Ed.* **2009**, *48*, 9034–9037.
- (20) Mitsudome, T.; Mizumoto, K.; Mizugaki, T.; Jitsukawa, K.; Kaneda, K. *Angew. Chem. Int. Ed.* **2010**, *49*, 1238-1240.
- (21) DeLuca, R. J.; Edwards, J. L.; Steffens, L. D.; Michel, B. W.; Qiao, X.; Zhu, C.; Cook, S. P.; Sigman, M.S. *J. Org. Chem.* **2013**, *78*, 1682–1686.
- (22) Mitsudome, T.; Yoshida, S.; Mizugaki, T.; Jitsukawa, K.; Kaneda, K. *Angew. Chem. Int. Ed.* **2013**, *52*, 5961-5964.
- (23) Mitsudome, T.; Yoshida, S.; Tsubomoto, Y.; Mizugaki, T.; Jitsukawa, K.; Kaneda, K. *Tetrahedron Lett.* **2013**, *54*, 1596.
- (24) Mitsudome, T.; Umetani, T.; Nosaka, N.; Mori, K.; Mizugaki, T.; Ebitani, K.; Kaneda, K. *Angew. Chem. Int. Ed.* **2006**, *45*, 481–485.
- (25) Cornell, C. N.; Sigman, M.S. *Inorg. Chem.* **2007**, *46*, 1903–1909.
- (26) Gligorich, K. M.; Sigman, M. S. *Chem. Commun.* **2009**, 3854–3867.

- (27) Campbell, A. N.; Stahl, S. S. *Acc. Chem. Res.* **2012**, *45*, 851–863.
- (28) Michel, B. W.; Camelio, A. M.; Cornell, C. N.; Sigman, M. S. *J. Am. Chem. Soc.* **2009**, *131*, 6076–6077.
- (29) Michel, B. W.; McCombs, J. R.; Winkler, A.; Sigman, M. S. *Angew. Chem. Int. Ed.* **2010**, *49*, 7312–7315.
- (30) Sigman, M. S.; Werner, E. W. *Acc. Chem. Res.* **2012**, *45*, 874–884.
- (31) Muzart, J. *Tetrahedron* 2007, *63*, 7505–7521.
- (32) Weiner, B.; Baeza, A.; Jerphagnon, T.; Feringa, B. L. *J. Am. Chem. Soc.* **2009**, *131*, 9473–9474.
- (33) Dong, J. J.; Fañanás-Mastral, M.; Alsters, P. L.; Browne, W. R.; Feringa, B. L. *Angew. Chem. Int. Ed.* **2013**, *52*, 5561–5565.
- (34) Wright, J. A.; Gaunt, M. J.; Spencer, J. B. *Chem. Eur. J.* **2006**, *12*, 949–955.
- (35) Teo, P.; Wickens, Z. K.; Dong, G.; Grubbs, R. H. *Org. Lett.* **2012**, *14*, 3237–3239.
- (36) Yamamoto, M.; Nakaoka, S.; Ura, Y.; Kataoka, Y. *Chem. Commun.* **2012**, *48*, 1165–1167
- (37) Tsuji, J.; Nagashima, H.; Nemoto, H. *Org. Synth.* **1984**, *62*, 9.
- (38) L. Hintermann, *Top. Organomet. Chem.* **2010**, 123–155
- (39) Feringa, B. L. *Chem. Commun.* **1986**, 909.
- (40) Wenzel, T. T. *Chem. Commun.* **1993**, 862–864.
- (41) Ogura, T.; Kamimura, R. Shiga, A.; Hosokawa, T. *Bull. Chem. Soc. Jpn.*

- 2005**, 78, 1555–1557.
- (42) Y. Lu, D.-H. Wang, K. M. Engle, J.-Q. Yu, *J. Am. Chem. Soc.* **2010**, 132, 5916–5921.
- (43) For example: if *tert*-BuOH is replaced by MeNO₂, no conversion is observed.
- (44) Wenzel, T. *J. Chem. Soc., Chem. Commun.* **1989**, 932–933.
- (45) G. Dong, G.; Teo, P.; Wickens, Z. K.; Grubbs, R. H. *Science* **2011**, 333, 1609–1612.
- (46) Andrews, M. A.; Kelly, K. P. *J. Am. Chem. Soc.* **1981**, 103, 2894–2896.
- (47) M. Thiemann, M.; Scheibler, E.; Wiegand, K. W. *Nitric Acid, Nitrous Acid, and Nitrogen Oxides. Ullmann's Encyclopedia of Industrial Chemistry.*
- (48) If the reaction is run in an unsealed vessel (exposed to air), significantly lower yield and selectivity is observed relative to the reaction sealed under air. This is consistent with the formation of NO₂.
- (49) Keith, J. A.; Henry, P. M. *Angew. Chem. Int. Ed.* **2009**, 48, 9038–9049.
- (50) Zard, S. Z. *Radical Reactions in Organic Synthesis*; Oxford University Press Inc., New York, **2003**.
- (51) Fischetti, W.; Heck, R. F. *J. Organomet. Chem.* **1985**, 293, 391–405.
- (52) For a general reference regarding the synthesis of enantioenriched building blocks: Carreira, E. M.; Kvaerno, L. *Classics in Stereoselective Synthesis*; 1st ed. Wiley-VCH, **2009**.
- (53) Utsunomiya, M.; Kuwano, R.; Kawatsura, M.; Hartwig, J. F. *J. Am. Chem.*

- Soc.* **2003**, *125*, 5608–5609.
- (54) Utsunomiya, M.; Hartwig, J. F. *J. Am. Chem. Soc.* **2004**, *126*, 2702–2703.
- (55) Hamilton, D. S.; Nicewicz, D. A. *J. Am. Chem. Soc.* **2012**, *134*, 18577–18580.
- (56) Nguyen, T. M.; Nicewicz, D. A. *J. Am. Chem. Soc.* **2013**, *135*, 9588–9591.
- (57) Zhu, S.; Niljianskul, N.; Buchwald, S. L. *J. Am. Chem. Soc.* **2013**, *135*, 15746–15749.
- (58) Wickens, Z. K.; Morandi, B.; Grubbs, R. H. *Angew. Chem. Int. Ed.* **2013**, *52*, 11257–11260.
- (59) Heiligenstein, J. H.; Tollefson, G. D. US5658590 A, **1997**.
- (60) López, F.; Ohmura, T.; Hartwig, J. F. *J. Am. Chem. Soc.* **2003**, *125*, 3426–3427.
- (61) Morandi, B.; Wickens, Z. K.; Grubbs, R. H. *Angew. Chem. Int. Ed.* **2013**, *52*, 9751–9754.
- (62) Mei, T.-S.; Werner, E. W.; Burckle, A. J.; Sigman, M. S. *J. Am. Chem. Soc.* **2013**, *135*, 6830–6833.
- (63) As will be discussed in chapter 5, as well as in reference 61, we found that alkenes bearing electron deficient benzoate derivatives in the allylic position were oxidized significantly more slowly than electron rich benzoate derivatives. In that case, significant cationic character in the transition state was suggested.
- (64) Ritter, T.; Hejl, A.; Wenzel, A. G.; Funk, T. W.; Grubbs, R. H.

Organometallics **2006**, *25*, 5740–5745.

- (65) Gorczynski, M. J.; Smitherman, P. K.; Akiyama, T. E.; Wood, H. B.; Berger, J. P.; King, S. B.; Morrow, C. S. *J. Med. Chem.* **2009**, *52*, 4631–4639.
- (66) Clyne, D.; Weiler, L. *Tetrahedron* **1999**, *55*, 13659–13682.
- (67) Raghavan, S.; Krishnaiah, V. *J. Org. Chem.* **2010**, *75*, 748–761.
- (68) Nagano, Y.; Orita, A.; Otera, J. *Tetrahedron* **2002**, *58*, 8211–8217.
- (69) Ghosh, A. K.; Nicponski, D. R. *Org. Lett.* **2011**, *13*, 4328–4331.
- (70) C. Chaoxian, Y. Shichao, C. Bonan, Z. Xumu *Chem. Eur. J.* **2012**, *32*, 9992 – 9998
- (71) Hayashi, K.; Tanimoto, H.; Zhang, H.; Morimoto, T.; Nishiyama, Y.; Kakiuchi, K. *Org. Lett.* **2012**, *14*, 5728–5731
- (72) Ceccarelli, S.; Piarulli, U; Gennari, C. *J. Org. Chem.* **2000**, *65*, 6254–6256
- (73) Lipshutz, B.; Ghorai, S.; Leong, W. W. Y. *J. Org. Chem.* **2009**, *74*, 2854–2857
- (74) Frémont, P.; Marion, N.; Nolan, S. *J. Organomet. Chem.* **2009**, *694*, 551–560
- (75) Izquierdo, I.; Plaza, M. T.; Robles, R.; Rodríguez, C. *Tetrahedron: Asymmetry* **1996**, *7*, 3593.
- (76) Murugan, K.; Srimurugan, S.; Chen, C. *Tetrahedron* **2011**, *67*, 5621–5629.
- (77) Schneider, U.; Dao, H. T.; Kobayashi, S. *Org. Lett.* **2010**, *12*, 2488–2491.
- (78) López, F.; Ohmura, T.; Hartwig, J. *J. Am. Chem. Soc.* **2003**, *125*, 3426–

3427

- (79) Roda, G.; Riva, S.; Danieli, B. *Tetrahedron: Asymmetry* **1999**, *10*, 3939
- (80) Rej, R. K.; Das, T.; Hazra, S.; Nanda, S. *Tetrahedron: Asymmetry* **2013**, *24*, 913 - 918

CHAPTER 3

AEROBIC PALLADIUM-CATALYZED ALKENE DIOXYGENATION ENABLED BY CO-CATALYTIC NITRITE

The text in this chapter was reproduced in part with permission from:

Wickens, Z. K.; Guzmán, P. E.; Grubbs, R. H. *Angew. Chem. Int. Ed.* **2015**, *54*, 236–240.

Copyright 2015 John Wiley and Sons

Abstract

Catalytic nitrite was found to enable carbon-oxygen bond-forming reductive elimination from unstable alkyl palladium intermediates, providing dioxygenated products from alkenes. A variety of functional groups are tolerated and high yields (up to 94%) are observed with many substrates, including a multi-gram scale reaction. Nitrogen dioxide, which could form from nitrite under the reaction conditions, was shown to be kinetically competent in the dioxygenation of alkenes. Furthermore, the reductive elimination event was probed with ^{18}O -labeling experiments, which demonstrated that both oxygen atoms in the difunctionalized products are derived from one molecule of acetic acid.

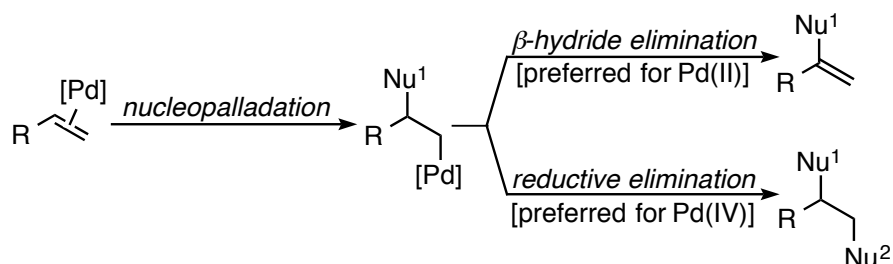
Introduction

The development of selective, catalytic oxidations of hydrocarbons has enabled the preparation of functionalized molecules from simple and readily accessible starting materials. Palladium catalysis has enabled a wide variety of practical and broadly adopted oxidative transformations of hydrocarbons.^{1,2} In the past decade, researchers have taken advantage of the facile reductive elimination from high-valent palladium centers (Pd(IV) and Pd(III)) to enable reactivity complementary to Pd(II/0) oxidative transformations.³⁻¹⁰ This high-valent mechanistic manifold has enabled attractive complexity-building transformations such as C–H oxidations^{5,7} and alkene difunctionalizations, such as dioxygenation,¹¹⁻¹⁵ aminooxygenation,¹⁶⁻²⁰ and diamination.²¹⁻²⁵ Unfortunately, wasteful, high-energy

stoichiometric oxidants, such as $\text{PhI}(\text{OAc})_2$, are typically required to access high-valent palladium centers. Despite the apparent advantages of replacing these stoichiometric oxidants with abundant and environmentally benign O_2 , the use of O_2 to access high-valent palladium intermediates remains a tremendous challenge due to the high kinetic barriers of aerobic oxidation of organopalladium(II) intermediates.^{8,26-29} Thus, there is a pressing need to develop strategies to facilitate reductive elimination using O_2 as the terminal oxidant.

In contrast to oxidation of Pd(II) to Pd(IV), strategies to oxidize Pd(0) to Pd(II) using O_2 as the terminal oxidant are well established. Pd(II/0) transformations were rendered aerobic over half a century ago by employing copper salts as electron transfer mediators (ETMs) to circumvent the kinetic barriers that limited direct aerobic oxidation of palladium catalysts.³⁰⁻³⁴ This development precipitated the widespread industrial adoption of the Wacker process for the bulk preparation of acetaldehyde from ethylene using O_2 as the terminal oxidant.³⁵ If a suitably oxidizing and kinetically reactive ETM could be identified, this strategy would enable use of O_2 as a terminal oxidant in high-valent palladium catalysis. Recently, NO_x species have been shown to be capable of mediating the aerobic oxidation of stable alkyl-Pd(II) palladacycles to their high-valent congeners.³⁶⁻³⁸ However, many Pd(IV/II) processes require rapid oxidation of a kinetically unstable organopalladium species to circumvent intramolecular decomposition pathways.^{39,40} For example, palladium-catalyzed

alkene difunctionalization reactions rely upon immediate oxidation of alkyl–Pd(II) intermediates to avoid the facile β -hydride elimination that produces Wacker-type byproducts (Scheme 3.1). An ETM strategy capable of providing aerobic access to these products would not only be a valuable alternative to conventional synthetic methodologies but would also demonstrate the potential of an ETM strategy to enable facile reductive elimination in a kinetically challenging context.



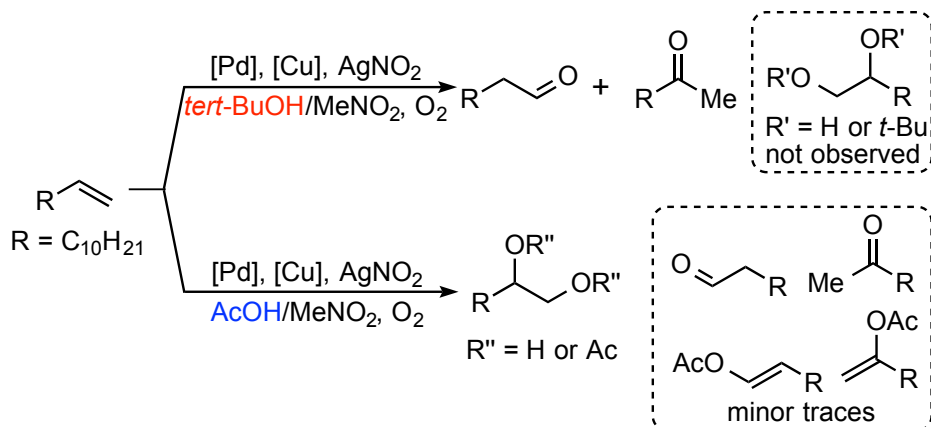
Scheme 3.1 Mechanistic manifolds for alkene oxidation proceeding nucleopalladation. (top) β -hydride elimination. (bottom) reductive elimination.

In Chapter 2, the development of an unusual nitrite-modified Wacker-type oxidation system was outlined. In that reaction, nitrogen dioxide was suspected to be formed as a reactive intermediate. Under acidic conditions, O_2 possesses an oxidation potential comparable to $\text{PhI}(\text{OAc})_2$.³⁸ Thus, acidification of our catalytic system could enable catalytic NO_x to oxidize an alkyl–Pd(II) intermediate and facilitate C–O bond forming reductive elimination to provide difunctionalized products. The efficient aerobic oxidation of NO makes these species ideal electron transfer mediators.^{41,42} To lend further support to this hypothesis,

palladium nitrite complexes have been demonstrated to produce mixtures of hydroxyacetate and Wacker-type products (roughly 1:1) with modest (mostly <10) turnovers under acidic conditions.⁴³ As a preliminary arena in which to evaluate this strategy of achieving facile reductive elimination from alkylpalladium intermediates, we investigated the dioxygenation of alkenes. An aerobic, palladium-catalyzed dioxygenation would provide an attractive alternative to toxic OsO₄, which is classically employed in alkene dihydroxylation.^{44,45}

Results and Discussion

Replacement of the alcohol solvent in our previously reported nitrite-modified Wacker oxidation conditions with acetic acid suppressed Wacker-type oxidation (characteristic of Pd(II)) and promoted alkene difunctionalization (characteristic of Pd(IV) or Pd(III)) (Scheme 3.2).



Scheme 3.2 Divergent reactivity with nitrite co-catalysts as a function of solvent.

[Pd] = PdCl₂(PhCN)₂ and [Cu] = CuCl₂•2H₂O.

Initial optimization revealed that increasing the amount of the nitromethane co-solvent and raising the temperature slightly to 35 °C improved the reproducibility of the reaction. Additionally, it is common practice to shield reactions involving silver salts from light and this proved necessary to maintain reproducible kinetic profiles.

Intriguingly, each catalytic component of the nitrite-modified Wacker oxidation system (see Chapter 2) was necessary to facilitate mild alkene difunctionalization (Table 3.1, entries 2–4). No oxidation products were observed in the absence of either palladium (entry 2) or nitrite (entry 3). In addition to simply omitting the palladium salt, catalytic Brønsted acids such as TfOH and HBF₄ were used in place of palladium salts but produced no dioxygenated products. Omission of the copper salt resulted in poor selectivity for the dioxygenated reductive elimination products relative to β-hydride elimination products. Furthermore, copper was found to be necessary to achieve efficient catalytic turnover (entry 4). However, although copper is commonly employed as an oxidant for Pd(0), another classical oxidant to mediate Pd(II/0) catalytic cycles, benzoquinone, proved an unsuitable substitute, providing poor yield and selectivity (entry 5). The origin of the empirical observations regarding copper is unclear at this time. It is possible that a heterobimetallic complex is formed.⁴⁶ Alternatively, it is possible that copper is necessary to oxidize Pd(0) species, despite the lack of competency of benzoquinone in its place. Replacement of AgNO₂ with NaNO₂ resulted in dioxygenated products in low yield, demonstrating

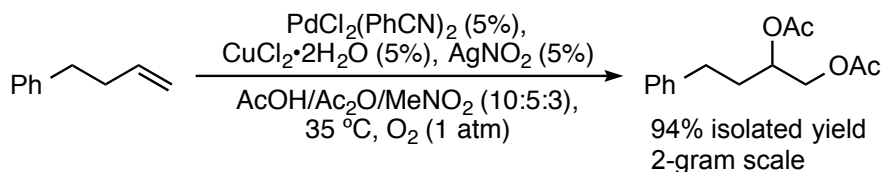
that nitrite alone is sufficient to facilitate the key product-forming reductive elimination and that the Ag(I) counterion is critical for efficient oxidation (entry 6).^{47,48} Silver nitrate similarly catalyzed product formation, albeit with reduced yield (entry 7). In the presence of nitrite and nitrate salts, no significant Wacker-type byproducts were observed by ¹H NMR. Despite the significant excess of acetic acid, palladium and copper acetate salts were not competent catalysts under these conditions (entry 8).

Table 3.1 Effect of divergence from optimal conditions.

Entry	Variation	Yield (%) ^a	Selectivity ^b
1	none	≥95	≥20:1
2	no PdCl ₂ (PhCN) ₂	0	–
3	no AgNO ₂	0	–
4	no CuCl ₂ ·2H ₂ O	6	3:2
5	BQ replaces CuCl ₂ ·H ₂ O	8	1:1.3
6	NaNO ₂ replaces AgNO ₂	7	≥20:1
7	AgNO ₃ replaces AgNO ₂	44	≥20:1
8	no Ac ₂ O	≥95 ^c	≥20:1
9	Pd(OAc) ₂ and Cu(OAc) ₂	0	–

^aDetermined by ¹H NMR analysis of the unpurified reaction mixture. ^bThe ratio of dioxygenated products to Wacker-type ketone and vinyl acetate products was determined using ¹H NMR analysis of the unpurified reaction mixture. ^cObserved as a 1:1.5 mixture of monoacetates (see supporting information for details).

To fully realize the environmental and economic benefits offered by employing molecular oxygen as the stoichiometric oxidant, the process must be scalable. To evaluate the reaction efficacy on preparative scale, a 2-gram scale reaction was performed (Scheme 3.3). The high efficiency that was observed on small scale was mirrored upon scale-up.

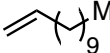
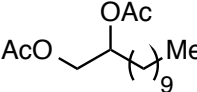
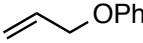
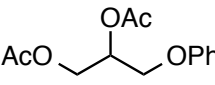
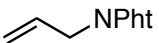
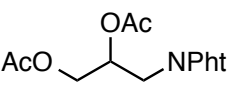
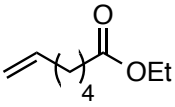
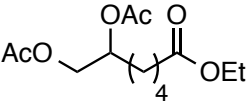
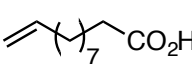
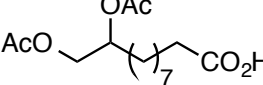
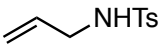
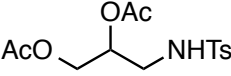
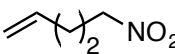
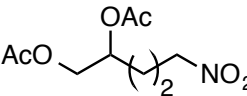
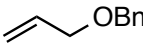
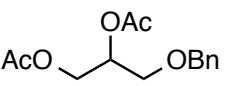
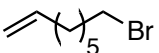
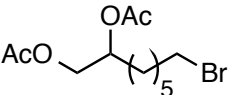
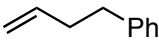
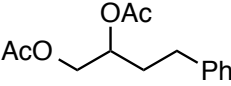


Scheme 3.3 Aldehyde-selective Wacker on 2-gram scale

Given the potential synthetic utility of this aerobic, palladium-catalyzed dioxygenation reaction, the functional group tolerance of the transformation was next examined by subjecting alkenes bearing a variety of functional groups to the reaction conditions (Table 3.1). Primary alkyl bromides, esters, alkyl and aryl ethers, phthalimides, sulfonamides, carboxylic acids and nitro groups were all well tolerated under the reaction conditions. This broad functional group compatibility bodes well not only for the adoption of this aerobic dioxygenation reaction in synthesis but also for the potential application of a nitrite-based ETM strategy for other aerobic, palladium-catalyzed alkene difunctionalization reactions, such as aminooxygenation and diamination.

Table 3.2 Evaluation of functional group tolerance^a

$$\text{R}-\text{CH}=\text{CH}_2 \xrightarrow[\text{AcOH}/\text{Ac}_2\text{O}/\text{MeNO}_2 (10:5:3), 35^\circ\text{C}, \text{O}_2 (1 \text{ atm})]{\text{PdCl}_2(\text{PhCN})_2 (5\%), \text{CuCl}_2 \cdot 2\text{H}_2\text{O} (5\%), \text{AgNO}_2 (5\%)} \text{R}-\text{CH}(\text{OAc})-\text{CH}_2-\text{OAc}$$

Entry	Starting Material	Product	Yield ^b
1			83%
2			81%
3			73%
4			91%
5 ^c			74%
6			53%
7			83%
8 ^d			63%
9			84%
10			90%

^aAlkene (0.5 mmol) treated with $\text{PdCl}_2(\text{MeCN})_2$ (5%), $\text{CuCl}_2 \cdot 2\text{H}_2\text{O}$ (5%), AgNO_2 (5%) in $\text{AcOH}/\text{Ac}_2\text{O}/\text{MeNO}_2$ (10:5:3, 8 mL) under an O_2 atmosphere (1 atm) at 35 °C. Each reaction was shielded from light with aluminum foil. ^bYield of isolated product. ^cYield determined by ^1H NMR analysis of the unpurified reaction mixture. ^dThe crude reaction mixture was treated with $\text{DMAP}/\text{Ac}_2\text{O}$ to complete conversion from monoacetate to diacetate prior to isolation.

Having demonstrated the synthetic utility of the process, we sought to elucidate the role of the key nitrite co-catalyst in the reaction. We suspected that the AgNO_2 salt produces an NO_x species, such as nitrogen dioxide, *in situ*, which would be sufficiently oxidizing and kinetically reactive to oxidize unstable palladium(II)–alkyl intermediates to Pd(III) or Pd(IV) analogs faster than β -hydride elimination. To probe this hypothesis, reaction profiles of the stoichiometric oxidation of 1-dodecene employing nitrite and nitrogen dioxide were compared (Figure 3.1). Both nitrite and nitrogen dioxide mediated conversion of the alkene to the diacetate product, conclusively demonstrating that nitrogen dioxide is a kinetically competent reactive intermediate. The competency of nitrogen dioxide in place of silver nitrite combined with the non-zero dioxygenation yields observed with catalytic NaNO_2 (Table 3.1) leads us to suspect that the Ag(I) cation does not play a central mechanistic role. We speculate that the superiority of the silver salt is due to rapid salt metathesis rates with the metal chloride salts but it may alternatively encourage catalytic turnover. Importantly, if neither oxidant is added, stoichiometric palladium and copper are insufficient to provide dioxygenated products, illustrating that the NO_x catalyst is necessary to reach the product-forming step of the transformation. These experiments are consistent with a mechanistic picture in which the NO_x species mediates the C–O bond-forming reductive elimination step. Given the high oxidation potential of NO_x species such as NO_2 , an NO_x species derived from nitrite may oxidize the Pd(II)–alkyl species to a high-valent palladium-alkyl intermediate to circumvent b-

hydride elimination and accelerate reductive elimination. However, the intriguing possibility of a rapid ligand mediated C–O bond-forming reductive elimination from Pd(II) cannot be ruled out.

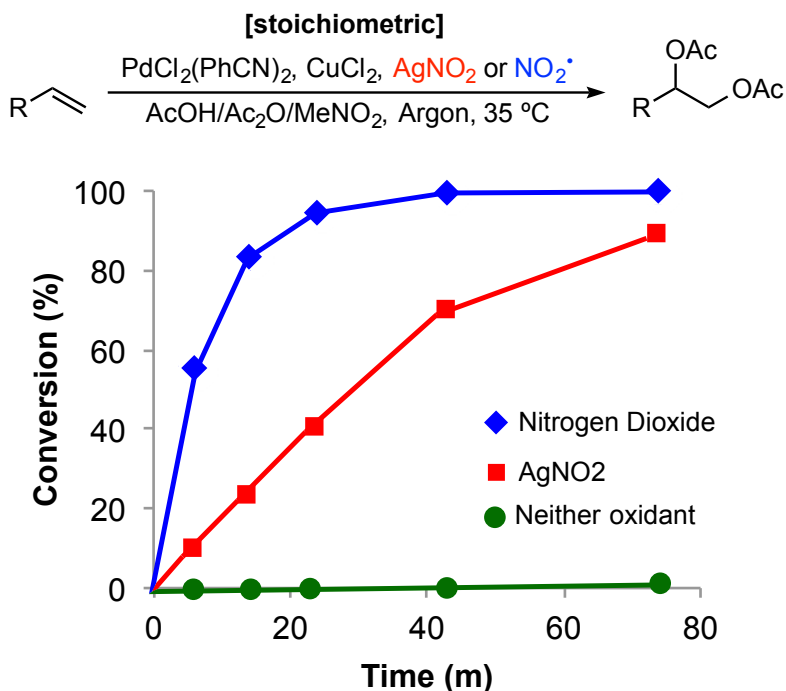


Figure 3.1 Stoichiometric reaction profiles to evaluate the nitrite additive.

To gain further insight into the C–O bond-forming reductive elimination event, the source of the oxygen atoms in the dioxygenated product was elucidated. The oxygen atoms could conceivably be derived from molecular oxygen, nitrite, acetic acid, or adventitious water. To discriminate between these possibilities, the reaction was conducted with ^{18}O -labeled AcOH (Table 3.3). Upon ester hydrolysis, this experiment provided conclusive evidence that both

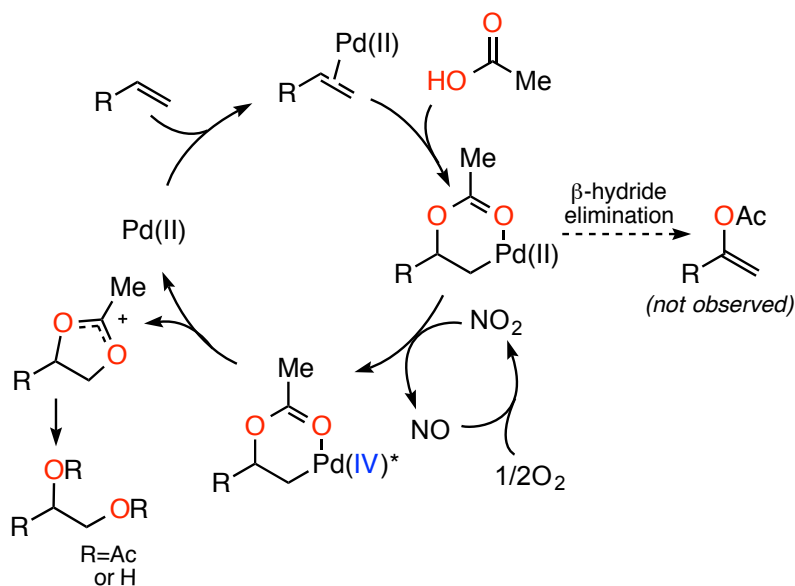
oxygen atoms in the difunctionalized product were derived from the solvent, AcOH. To determine whether the two oxygen atoms were derived from a single molecule of acetic acid, we devised a modified ^{18}O labeling experiment in which the reaction was conducted in a 1:1 mixture of ^{18}O -AcOH and ^{16}O -AcOH. Only $^{18}\text{O}/^{18}\text{O}$ - and $^{16}\text{O}/^{16}\text{O}$ -diol products (**A** and **C**, respectively) were observed, illustrating that both oxygen atoms are derived from a single molecule of acetic acid. Prior to ester hydrolysis the hydroxyacetate product was determined to be doubly labeled, indicating that the carbonyl oxygen atom is not derived from acetic acid. For further discussion of the labeling experiment, see the experimental section.

Table 3.3 ^{18}O labeling experiments^a

Acetic acid source	$^{18}\text{O} / ^{18}\text{O}$ (A)	$^{18}\text{O} / ^{16}\text{O}$ (B'+B'')	$^{16}\text{O} / ^{16}\text{O}$ (C)
	91%	<5%	<5%
 (1 : 1)	51%	<5%	48%

^a4-phenylbutene (0.1 mmol) treated with $\text{PdCl}_2(\text{PhCN})_2$ (10 mol%), $\text{CuCl}_2 \cdot 2\text{H}_2\text{O}$ (10 mol%), AgNO_2 (10 mol%) in $\text{AcOH}/\text{MeNO}_2$ (4:1, 0.5 mL) under an O_2 atmosphere (1 atm) at 35 °C. See experimental section for details.

Taken together, these experiments suggest a reaction manifold in which initial alkene nucleopalladation with acetic acid is followed by oxidation to a high-valent palladium intermediate (Pd(IV) or Pd(III)) by an NO_x species (potentially NO₂). This high-valent palladium intermediate next undergoes intramolecular reductive elimination to liberate an acetoxonium ion that is subsequently hydrolyzed. This mechanism is analogous to the mechanism suggested by Dong and coworkers for the PhI(OAc)₂ mediated dioxygenation of alkenes.^[26] However, subsequent work cast doubt on the involvement of Pd(IV) intermediates their catalytic system as strong acid combined with PhI(OAc)₂ was sufficient to dioxygenated similar substrates.⁴⁹



Scheme 3.4 Preliminary mechanistic proposal. Pd(IV)* indicates a high-valent palladium species (monomeric Pd(IV) and Pd(III)⁵⁰ as well as dimeric Pd(III) are equally consistent with the current mechanistic evidence).

Conclusion

In summary, we have demonstrated that challenging C–O bond-forming reductive eliminations from unstable palladium-alkyl species capable of β -hydride elimination can be affected by addition of a nitrite co-catalyst and molecular oxygen. This ETM strategy was demonstrated in the efficient dioxygenation of alkenes, providing a non-toxic and environmentally benign alternative to traditional alkene dioxygenation conditions. In addition to the synthetic value of this transformation, important mechanistic evidence regarding the role of the nitrite co-catalyst and the reductive elimination step was provided. We anticipate that this work will stimulate further exploration of strategies to replace high-energy stoichiometric oxidants with molecular oxygen.

Experimental Section

Materials and methods

General Reagent Information: Preparation of non-commercial substrates: Unless stated otherwise, all reactions except for the Wacker oxidations were carried out in oven- and flame-dried glassware (200 °C) using standard Schlenk techniques and were run under argon atmosphere. Wacker oxidations were carried out without exclusion of air. The reaction progress was monitored by TLC. Starting materials and reagents were purchased from *Sigma Aldrich*, *Acros*, *Fluka*, *Fischer*, *TCI* or *Synquest Laboratories* and were used without further

purification, unless stated otherwise. Solvents for the reactions were of quality puriss., p.a. of the companies *Fluka* or *J.T. Baker* or of comparable quality. Anhydrous solvents were purified by passage through solvent purification columns. For aqueous solutions, deionized water was used.

General Analytical Information: Nuclear Magnetic Resonance spectra were measured with a *Varian-Inova 500* spectrometer (500 MHz), a *Varian-Inova 400* spectrometer (400 MHz), or a *Varian-Mercury Plus 300* spectrometer (300 MHz). The solvent used for the measurements is indicated. All spectra were measured at room temperature (22–25 °C). Chemical shifts for the specific NMR spectra were reported relative to the residual solvent peak [CDCl₃: δ_{H} = 7.26; CDCl₃: δ_{C} = 77.16]. The multiplicities of the signals are denoted by *s* (singlet), *d* (doublet), *t* (triplet), *q* (quartet), *p* (pentet) and *m* (multiplet). The coupling constants *J* are given in Hz. All ¹³C-NMR spectra are ¹H-broadband decoupled, unless stated otherwise. High-resolution mass spectrometric measurements were provided by the California Institute of Technology Mass Spectrometry Facility using a JEOL JMS-600H High Resolution Mass Spectrometer. The molecule-ion M⁺, [M + H]⁺, and [M–X]⁺, respectively, or the anion are given in *m/z*-units. Response factors were collected for 1-dodecene and dodecane-1,2-diyl diacetate following literature procedures.^a

^a *Organometallics* **2006**, *25*, 5740.

General Considerations: Thin Layer Chromatography analyses were performed on silica gel coated glass plates (0.25 mm) with fluorescence-indicator UV₂₅₄ (*Merck*, TLC silica gel 60 F₂₅₄). For detection of spots, UV light at 254 nm or 366 nm was used. Alternatively, oxidative staining using aqueous basic potassium permanganate solution (KMnO₄) or ceric ammonium nitrate (CAN) was performed. Flash column chromatography was conducted with *Silicagel 60* (*Fluka*; particle size 40–63 μM) at 24 °C and 0–0.3 bar excess pressure (compressed air) using Et₂O/pentane unless state otherwise.

General Procedures

Procedure (A) for larger scale (0.5 mmol) oxidation of alkene substrates:

PdCl₂(MeCN)₂ (0.025 mmol, 6.5 mg), CuCl₂·2H₂O (0.025 mmol, 4.5 mg) and AgNO₂ (0.02 mmol, 3.8 mg) were weighed into a 20 mL vial charged with a stir bar. The vial was sparged for 1 minute with oxygen (1 atm, balloon). AcOH, Ac₂O and MeNO₂ were premixed in a 10:5:3 ratio and sparged with oxygen for 2 minutes. The oxygenated solvent mixture was then added to the vial (8 mL), followed by the alkene substrate (0.5 mmol) via syringe. After an additional 15 seconds of sparging with oxygen, the reaction vessel was shielded with light using aluminum foil. The reaction was then allowed to stir at 35 °C for 16 h under an atmosphere of oxygen (balloon). The reaction mixture was subsequently filtered and the solvent was removed under reduced vacuum. Dichloromethane was added and the resulting mixture was washed three times with saturated

NaHCO₃. After drying the organics with Na₂SO₄, the solvent was removed under reduced pressure and the crude mixture was purified by silica gel chromatography.

Procedure (B) for analytical scale oxidation of 1-dodecene (NMR analysis):

PdCl₂(PhCN)₂ (0.01 mmol, 3.8 mg), CuCl₂·2H₂O (0.01 mmol, 1.8 mg) and AgNO₂ (0.01 mmol, 1.5 mg) were weighed into a 8 mL vial charged with a stir bar. The vial was sparged for 1 minute with oxygen (1 atm, balloon). AcOH, Ac₂O and MeNO₂ were premixed in a 10:5:3 ratio and sparged with oxygen for 2 minutes. The oxygenated solvent mixture was then added to the vial (3.2 mL), followed by the 1-dodecene (0.2 mmol) via syringe. After an additional 15 seconds of sparging with oxygen, the reaction vessel was shielded with light using aluminum foil. The reaction was then allowed to stir at 35 °C for 16 h under an atmosphere of oxygen (balloon). The reaction mixture was subsequently filtered and the solvent was removed under reduced vacuum. Dichloromethane was added and the resulting mixture was washed three times with saturated NaHCO₃. After drying the organics with Na₂SO₄, the solvent was removed under reduced pressure, nitrobenzene (10 μL) was added as an internal standard and the mixture was dissolved in CDCl₃ and subjected to NMR analysis (15 s relaxation delay was account for the t1 of nitrobenzene).

Stoichiometric reaction profiles

Stoichiometric reaction with AgNO₂: PdCl₂(PhCN)₂ (0.02 mmol, 7.7 mg), CuCl₂·2H₂O (0.02 mmol, 3.4 mg) and AgNO₂ (0.02 mmol, 3.1 mg) were weighed into a 8 mL vial charged with a stir bar. The vial was sparged for 1 minute with argon (1 atm, balloon). AcOH, Ac₂O and MeNO₂ were premixed in a 10:5:3 ratio and degassed with argon for 2 minutes. The solvent mixture was then added to the vial (3.2 mL), followed by the 1-dodecene (0.02 mmol) via syringe. After an additional 15 seconds of sparging with argon, the reaction vessel was shielded with light using aluminum foil. The reaction was stirred under an inert atmosphere (balloon). Aliquots (ca. 100 μL) were removed and subjected to GC analysis using tridecane as an internal standard.

Stoichiometric reaction with nitrogen dioxide: First, nitrogen dioxide was condensed into a round bottom flask at -15 °C. PdCl₂(PhCN)₂ (0.02 mmol, 7.7 mg), CuCl₂·2H₂O (0.02 mmol, 3.4 mg) were weighed into a 8 mL vial charged with a stir bar. The vial was sparged for 1 minute with argon (1 atm, balloon). AcOH, Ac₂O and MeNO₂ were premixed in a 10:5:3 ratio and degassed with argon for 2 minutes. The solvent mixture was then added to the vial (3.2 mL). A stock solution of NO₂ was prepared by placing 2 mL of the degassed solvent mixture in a septum-capped 2 mL vial and adding condensed NO₂ (12.7 μL, 0.4 mmol) using a chilled gas tight microsyringe. Immediately after preparation, 100 μL of this solution (0.02 mmol NO₂) was added to the vial containing palladium

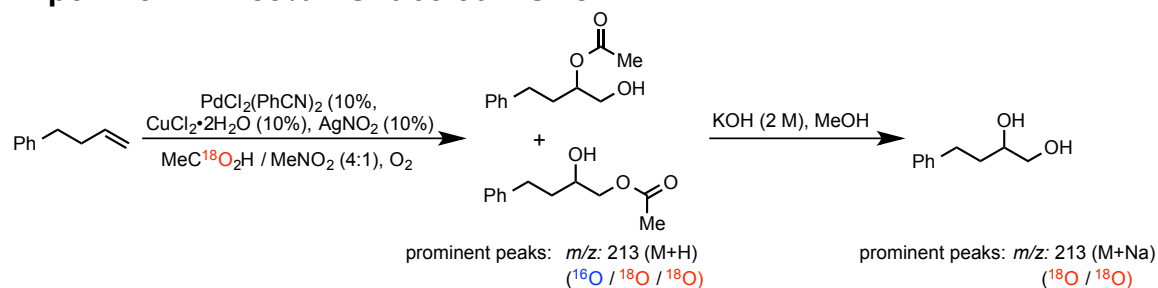
and copper followed by the 1-dodecene (0.02 mmol) via syringe. The reaction vessel was shielded with light using aluminum foil. The reaction was stirred under an inert atmosphere (balloon). Aliquots (ca. 100 μ L) were removed and subjected to GC analysis using tridecane as an internal standard.

¹⁸O-Labeling Experiments

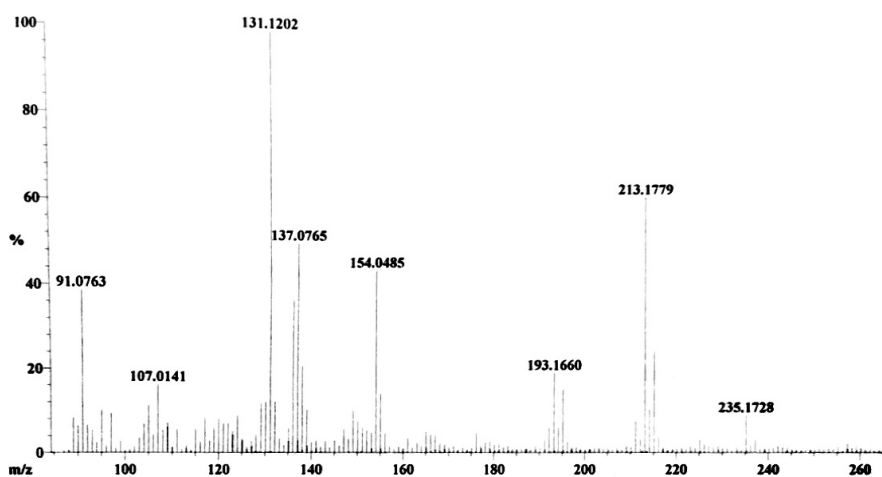
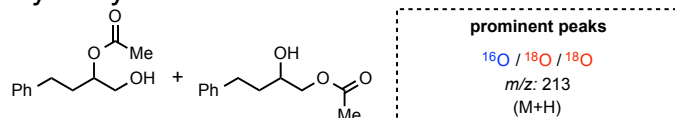
The procedure was modified as follows to accommodate the high cost of the ¹⁸O-labeled AcOH: PdCl₂(PhCN)₂ (0.01 mmol, 3.8 mg), CuCl₂·2H₂O (0.01 mmol, 1.8 mg) and AgNO₂ (0.01 mmol, 1.5 mg) were weighed into a 2 mL vial charged with a stir bar. The vial was sparged for 1 minute with oxygen (1 atm, balloon). ¹⁸O-labeled AcOH (400 μ L, 95% ¹⁸O specified by Sigma-Aldrich) and MeNO₂ (100 μ L) were added and sparged with oxygen for 15 seconds. The 1-dodecene (0.1 mmol) was next added via syringe. After an additional 10 seconds of sparging with oxygen, the reaction vessel was shielded with light using aluminum foil. The reaction was then allowed to stir at 35 °C for 5 h under an atmosphere of oxygen (balloon). The reaction mixture was subsequently filtered and the solvent was removed under reduced vacuum. At this stage, a small amount of residue was set aside for mass spec analysis (FAB+). The remaining material was dissolved in 2M KOH in MeOH and was heated to 50 °C for 8h. The mixture was diluted in dichloromethane and HCl (2 M) was added. The aqueous layer was washed three times with dichloromethane. The combined organics were dried over MgSO₄ and subsequently the volatiles were removed under

reduced pressure. The residue was subjected to mass spec (FAB+) and the percentage of ^{18}O -labeling was approximated by relative abundance of the molecular ions (+ sodium).

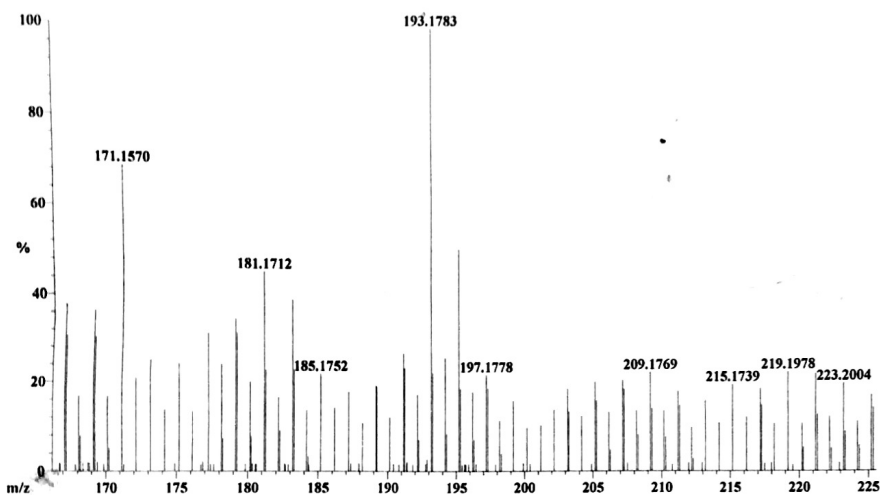
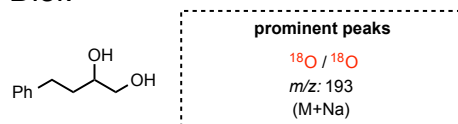
Experiment 1: 100% ¹⁸O-labeled HOAc



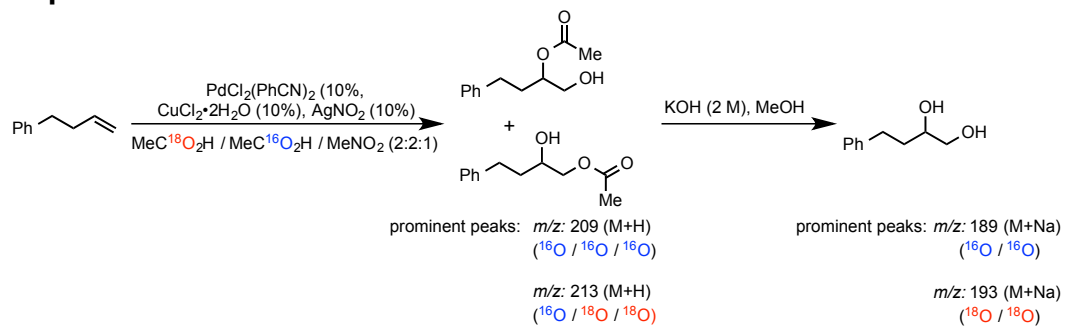
Hydroxymonoacetate:



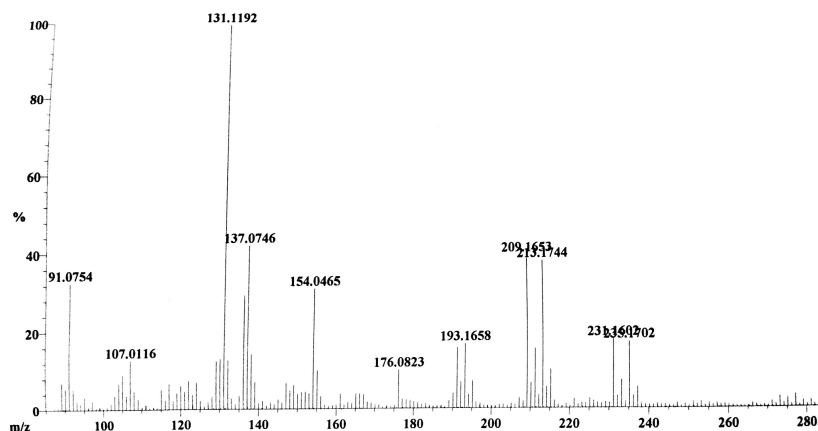
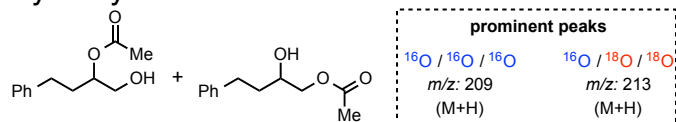
Diol:



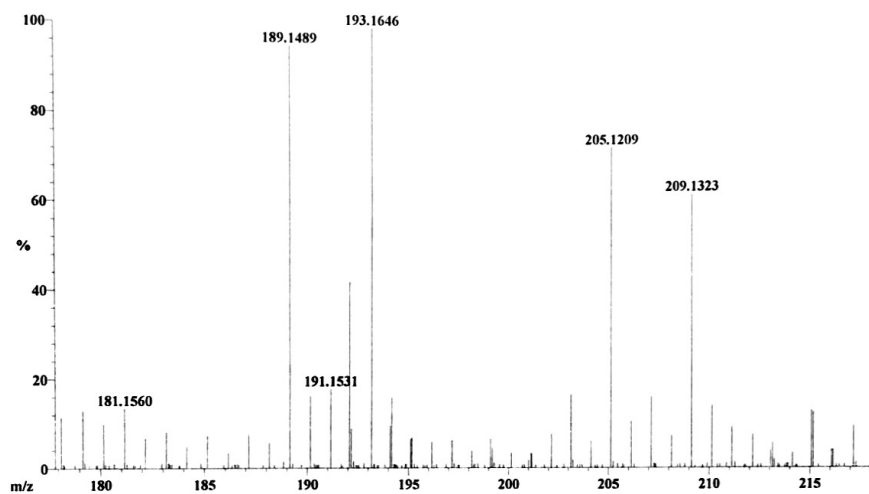
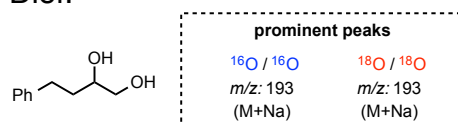
Experiment 2: 50% ¹⁸O-labeled HOAc and 50% unlabeled HOAc



Hydroxymonoacetate:

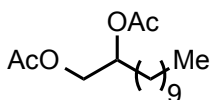


Diol:



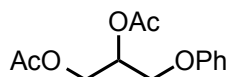
Detailed discussion of labeling experiment: The diol (rather than the mono- or diacetate) products were of particular interest due to the clarity of the position of the ^{18}O label. However, given that the diol oxygen atoms were the labeled positions, the masses observed in the monoacetate provide important evidence that the majority of the carbonyl oxygen atoms are *not* derived from the HOAc solvent. The likely source of ^{16}O in the carbonyl oxygen is from H_2O , upon hydrolysis of the acetoxonium ion. Relative abundance by FAB+ is not expected to provide quantitatively precise labeling percentages; however, the qualitative conclusions of the experiments are clearly supported by this analysis.

Product characterization

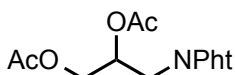


dodecane-1,2-diyl diacetate (Table 3.2 , entry 1): 119 mg (83% yield) obtained using procedure A. $^1\text{H NMR}$ (500 MHz, CDCl_3) δ 5.07 (dddd, $J = 7.5, 6.6, 5.8, 3.3$ Hz, 1H), 4.22 (dd, $J = 11.9, 3.3$ Hz, 1H), 4.03 (dd, $J = 11.9, 6.6$ Hz, 1H), 2.07 (s, 3H), 2.06 (s, 3H), 1.64 – 1.48 (m, 2H), 1.33 – 1.22 (m, 16H), 0.88 (t, $J = 6.9$ Hz, 3H). Spectral data were in accordance with the literature.^b

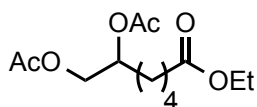
^b *Tetrahedron* **2004**, *60*, 703–710



3-phenoxypropane-1,2-diyl diacetate (Table 3.2 , entry 2): 102 mg (81% yield) obtained using procedure A. $^1\text{H NMR}$ (400 MHz, CDCl_3) δ 7.33 – 7.25 (m, 2H), 7.01 – 6.94 (m, 1H), 6.92 – 6.87 (m, 2H), 5.40 – 5.34 (m, 1H), 4.48 – 4.39 (m, 1H), 4.30 (dd, $J = 12.0, 6.0$ Hz, 1H), 4.12 (d, $J = 5.1$ Hz, 2H), 2.10 (s, 3H), 2.07 (s, 3H). Spectral data were in accordance with the literature.^c



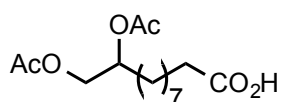
3-(1,3-dioxoisindolin-2-yl)propane-1,2-diyl diacetate (Table 3.2 , entry 3): 111mg (73% yield) obtained using procedure A. $^1\text{H NMR}$ (400 MHz, CDCl_3) δ 7.89 – 7.84 (m, 2H), 7.76 – 7.71 (m, 2H), 5.40 – 5.26 (m, 1H), 4.30 (dd, $J = 12.1, 4.1$ Hz, 1H), 4.20 – 4.12 (m, 1H), 3.96 (d, $J = 5.2$ Hz, 2H), 2.08 (s, 3H), 2.03 (s, 3H). $^{13}\text{C NMR}$ (101 MHz, CDCl_3) δ 170.47, 170.32, 168.00, 134.15, 131.84, 123.46, 69.32, 63.08, 38.17, 20.85, 20.68. **HRMS** (EI+) calc'd for $\text{C}_{15}\text{H}_{16}\text{NO}_6$ 306.0978, found 306.0979.



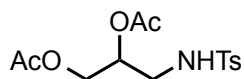
7-ethoxy-7-oxoheptane-1,2-diyl diacetate (Table 3.2 , entry 4): 125mg (91% yield) obtained using procedure A. $^1\text{H NMR}$ (400 MHz, CDCl_3) δ 5.05 (dt, $J = 9.9,$

^c *J. Am. Chem. Soc.* **2009**, *131*, 3846–3847

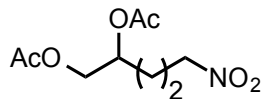
6.4 Hz, 1H), 4.21 (dd, $J = 11.9, 3.3$ Hz, 1H), 4.11 (q, $J = 7.1$ Hz, 2H), 4.02 (dd, $J = 11.9, 6.5$ Hz, 1H), 2.28 (t, $J = 7.4$ Hz, 2H), 2.05 (s, 3H), 2.05 (s, 3H), 1.70 – 1.52 (m, 4H), 1.47 – 1.28 (m, 2H), 1.24 (t, $J = 7.2$ Hz, 3H). ^{13}C NMR (101 MHz, CDCl_3) δ 173.33, 170.70, 170.51, 71.26, 64.95, 60.25, 34.03, 30.38, 24.65, 21.01, 20.73, 14.21. **HRMS** (EI+) calc'd for $\text{C}_{13}\text{H}_{23}\text{O}_6$ 275.1495, found 275.1484.



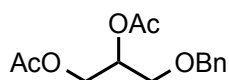
10,11-diacetoxyundecanoic acid (Table 3.2 , entry 5): 74% yield was obtained using procedure B on a 0.5 mmol scale (alkene).



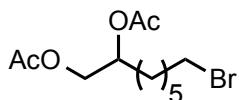
3-((4-methylphenyl)sulfonamido)propane-1,2-diyl diacetate (Table 3.2 , entry 6): 87 mg (53% yield) obtained using procedure A. ^1H NMR (500 MHz; CDCl_3) δ 7.74 (d, 2H, $J = 8$ Hz), 7.32 (d, $J = 8$ Hz, 2H), 5.10 (bs, 1H), 5.01 (p, $J = 5$ Hz, 1H), 4.22 (dd, $J = 4.5, 12$ Hz, 1H), 4.11 (dd, $J = 5.5, 12$ Hz, 1H), 3.22-3.13 (m, 2H), 2.43 (s, 3H), 2.04 (s, 3H), 2.02 (s, 3H); ^{13}C NMR (126 MHz, CDCl_3) δ 170.5, 170.2, 143.7, 136.7, 129.8, 127, 69.8, 62.4, 43, 21.5, 20.8, 20.6; **HRMS** (FAB+) calc'd for $\text{C}_{14}\text{H}_{20}\text{O}_6\text{NS}$ 330.1011, found 330.1017.



5-nitropentane-1,2-diyl diacetate (Table 3.2 , entry 7): 96 mg (83% yield) obtained using procedure A. $^1\text{H NMR}$ (500 MHz; CDCl_3) δ 5.11-5.06 (m, 1H), 4.41 (td, $J = 1.0, 7.0, 13.5$ Hz, 2H), 4.22 (dd, $J = 3.5, 12.0$ Hz, 1H), 4.05 (dd, $J = 6.0, 12.0$ Hz, 1H), 2.11-2.00 (m, 8H), 1.73-1.68 (m, 2H); $^{13}\text{C NMR}$ (126 MHz, CDCl_3) δ 170.6, 170.4, 74.8, 70.3, 64.5, 27.5, 23, 20.9, 20.7; **HRMS** (FAB+) calc'd for $\text{C}_9\text{H}_{15}\text{O}_6\text{N}$ 233.0899, found 233.0900.

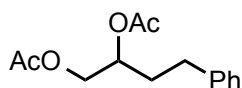


3-(benzyloxy)propane-1,2-diyl diacetate (Table 3.2 , entry 8): 84 mg (63% yield) obtained using procedure A. $^1\text{H NMR}$ (500 MHz; CDCl_3) δ 7.36-7.27 (m, 5H), 5.24-5.20 (m, 1H), 4.54 (app q, $J = 12$ Hz, 2H), 4.33 (dd, $J = 4.0, 12.0$ Hz, 1H), 4.19 (dd, $J = 6.0, 11.5$ Hz, 1H), 3.59 (dd, $J = 1.0, 5.5$ Hz, 2H), 2.08 (s, 3H), 2.03 (s, 3H); $^{13}\text{C NMR}$ (126 MHz, CDCl_3) δ 170.6, 170.3, 128.4, 127.8, 127.6, 73.2, 70.2, 68, 62.8, 21, 20.7; **HRMS** (FAB+) calc'd for $\text{C}_{14}\text{H}_{19}\text{O}_5$ 267.1232, found 267.1224.



8-bromooctane-1,2-diyl diacetate (Table 3.2 , entry 9): 130mg (84% yield) obtained using procedure A. $^1\text{H NMR}$ (500 MHz, CDCl_3) δ 5.07 (dddd, $J = 7.7,$

6.6, 5.7, 3.3 Hz, 1H), 4.22 (dd, $J = 11.9, 3.3$ Hz, 1H), 4.03 (dd, $J = 11.9, 6.6$ Hz, 1H), 3.40 (t, $J = 6.8$ Hz, 2H), 2.07 (s, 3H), 2.07 (s, 3H), 1.91 – 1.80 (m, 2H), 1.69 – 1.52 (m, 2H), 1.50 – 1.40 (m, 2H), 1.40 – 1.28 (m, 4H). ^{13}C NMR (126 MHz, CDCl_3) δ 170.77, 170.58, 71.41, 65.06, 33.80, 32.58, 30.57, 28.47, 27.92, 24.93, 21.08, 20.79. HRMS (EI+) calc'd for $\text{C}_{12}\text{H}_{22}\text{O}_4\text{Br}$ 309.0701, found 309.0714.



4-phenylbutane-1,2-diyl diacetate (Table 3.2 , entry 10): 113 mg (90% yield) obtained using procedure A. 3.56g (94% yield) was obtained upon increasing the reaction scale to 15.1 mmol. ^1H NMR (400 MHz, CDCl_3) δ 7.33 – 7.25 (m, 2H), 7.23 – 7.13 (m, 3H), 5.18 – 5.04 (m, 1H), 4.25 (dd, $J = 11.9, 3.4$ Hz, 1H), 4.07 (dd, $J = 12.0, 6.3$ Hz, 1H), 2.76 – 2.57 (m, 2H), 2.06 (s, 3H), 2.05 (s, 3H), 2.01 – 1.83 (m, 2H). ^{13}C NMR (101 MHz, CDCl_3) δ 170.71, 170.52, 140.89, 128.48, 128.27, 126.12, 71.12, 64.95, 32.38, 31.52, 21.01, 20.75. HRMS (EI+) calc'd for $\text{C}_{14}\text{H}_{19}\text{O}_4$ 251.1283, found 251.1284.

References

- (1) Tsuji, J. *Palladium Reagents and Catalysts: New Perspectives for the 21st Century*, 2nd ed.; Wiley, **2004**.
- (2) Backvall, J. E. *Modern Oxidation Methods*; Wiley-VCH, **2004**.
- (3) Muñiz, K. *Angew. Chem. Int. Ed.* **2009**, *48*, 9412.
- (4) Xu, L.-M.; Li, B.-J.; Yang, Z.; Shi, Z.-J. *Chem. Soc. Rev.* **2010**, *39*, 712.

- (5) Engle, K. M.; Mei, T.-S.; Wang, X.; Yu, J.-Q. *Angew. Chem. Int. Ed.* **2011**, *50*, 1478.
- (6) Sehnal, P.; Taylor, R. J. K.; Fairlamb, I. J. S. *Chem. Rev.* **2010**, *110*, 824.
- (7) Hickman, A. J.; Sanford, M. S. *Nature* **2012**, *484*, 177.
- (8) Vedernikov, A. N. *Acc. Chem. Res.* **2012**, *45*, 803.
- (9) Powers, D. C.; Ritter, T. **2012**, *45*, 840.
- (10) Powers, D. C.; Ritter, T. *Top. Organomet. Chem.* **2011**, *503*, 129.
- (11) Li, Y.; Song, D.; Dong, V. M. *J. Am. Chem. Soc.* **2008**, *130*, 2962.
- (12) Neufeldt, S. R.; Sanford, M. S. *Org. Lett.* **2013**, *15*, 46.
- (13) Wang, A.; Jiang, H.; Chen, H. *J. Am. Chem. Soc.* **2009**, *131*, 3846.
- (14) Wang, W.; Wang, F.; Shi, M. *Organometallics* **2010**, *29*, 928.
- (15) Park, C. P.; Lee, J. H.; Yoo, K. S.; Jung, K. W. *Org. Lett.* **2010**, *12*, 2450.
- (16) Alexanian, E. J.; Lee, C.; Sorensen, E. J. *J. Am. Chem. Soc.* **2005**, *127*, 7690.
- (17) Liu, G.; Stahl, S. S. *J. Am. Chem. Soc.* **2006**, *128*, 7179.
- (18) Desai, L. V.; Sanford, M. S. *Angew. Chem. Int. Ed.* **2007**, *46*, 5737.
- (19) Liskin, D. V.; Sibbald, P. A.; Rosewall, C. F.; Michael, F. E. *J. Org. Chem.* **2010**, *75*, 6294.
- (20) Zhu, H.; Chen, P.; Liu, G. *J. Am. Chem. Soc.* **2014**, *136*, 1766.
- (21) Streuff, J.; Hövelmann, C. H.; Nieger, M.; Muñoz, K. *J. Am. Chem. Soc.* **2005**, *127*, 14586.
- (22) Muñoz, K. *J. Am. Chem. Soc.* **2007**, *129*, 14542.

- (23) Muñiz, K.; Hövelmann, C. H.; Streuff, J. *J. Am. Chem. Soc.* **2008**, *130*, 763.
- (24) Sibbald, P. A.; Michael, F. E. *Org. Lett.* **2009**, *11*, 1147.
- (25) Iglesias, Á.; Pérez, E. G.; Muñiz, K. *Angew. Chem. Int. Ed.* **2010**, *49*, 8109.
- (26) Zhang, J.; Khaskin, E.; Anderson, N. P.; Zavalij, P. Y.; Vedernikov, A. N. *Chem. Commun.* **2008**, 3625.
- (27) Tang, F.; Zhang, Y.; Rath, N. P.; Mirica, L. M. *Organometallics* **2012**, *31*, 6690.
- (28) Khusnutdinova, J. R.; Rath, N. P.; Mirica, L. M. *J. Am. Chem. Soc.* **2012**, *134*, 2414.
- (29) Zhang, Y.-H.; Yu, J.-Q. *J. Am. Chem. Soc.* **2009**, *131*, 14654.
- (30) Smidt, J.; Hafner, W.; Sedlmeier, J.; Jira, R.; Rüttinger, R. *Angew. Chem.* **1959**, *71*, 176.
- (31) Gligorich, K. M.; Sigman, M. S. *Chem. Commun.* **2009**, 3854.
- (32) Campbell, A. N.; Stahl, S. S. *Acc. Chem. Res.* **2012**, *45*, 851.
- (33) Piera, J.; Bäckvall, J.-E. *Angew. Chem. Int. Ed.* **2008**, *47*, 3506.
- (34) Wu, W.; Jiang, H. *Acc. Chem. Res.* **2012**, *45*, 1736.
- (35) Jira, R. *Angew. Chem. Int. Ed.* **2009**, *48*, 9034.
- (36) Cámpora, J.; Palma, P.; del Río, D.; Carmona, E.; Graiff, C.; Tiripicchio, A. *Organometallics* **2003**, *22*, 3345.
- (37) Majhi, B.; Kundu, D.; Ahammed, S.; Ranu, B. C. *Chem. Eur. J.* **2014**, *20*,

9862.

- (38) Stowers, K. J.; Kubota, A.; Sanford, M. S. *Chem. Sci.* **2012**, *3*, 3192.
- (39) Rajabi, J.; Lorion, M. M.; Ly, V. L.; Liron, F.; Oble, J.; Prestat, G.; Poli, G. *Chem. Eur. J.* **2014**, *20*, 1539.
- (40) Sigman, M. S.; Jensen, K. H. *Org. Biomol. Chem.* **2008**, *6*, 4083.
- (41) Andrews, M. A.; Kelly, K. P. *J. Am. Chem. Soc.* **1981**, *103*, 2894.
- (42) Ford, P. C.; Lorkovic, I. M. *Chem. Rev.* **2002**, *102*, 993
- (43) Mares, F.; Diamond, S. E.; Regina, F. J. *J. Am. Chem. Soc.* **1985**, *107*, 3545.
- (44) Schroeder, M. *Chem. Rev.* **1980**, *80*, 187
- (45) Kolb, H. C.; VanNieuwenhze, M. S.; Sharpless, K. B. *Chem. Rev.* **1994**.
- (46) Hosokawa, T.; Nomura, T.; Murahashi, S. I. *J. Organomet. Chem.* **1998**, *551*, 387.
- (47) Lu, Y.; Wang, D.-H.; Engle, K. M.; Yu, J.-Q. *J. Am. Chem. Soc.* **2010**, *132*, 5916.
- (48) Anand, M.; Sunoj, R. B.; Schaefer, H. F., III. *J. Am. Chem. Soc.* **2014**, *136*, 5535.
- (49) Kang, Y.-B.; Gade, L. H. *J. Am. Chem. Soc.* **2011**, *133*, 3658.
- (50) Maestri, G.; Malcria, M.; Derat, E. *Chem. Commun.* **2013**, *49*, 10424.

CHAPTER 4

GENERAL AND PRACTICAL WACKER-TYPE OXIDATION OF INTERNAL ALKENES

The text in this chapter was reproduced in part with permission from:

Morandi, B.; Wickens, Z. K.; Grubbs, R. H. *Angew. Chem. Int. Ed.* **2013**, *52*, 2944–2948.

Copyright 2013 John Wiley and Sons

Morandi, B.; Wickens, Z. K.; Grubbs, R. H. *Angew. Chem. Int. Ed.* **2013**, *52*, 9751–9754.

Copyright 2013 John Wiley and Sons

Abstract

Herein, we report a simple and practical catalytic method for the preparation of ketones from a broad range of internal olefins that proceeds under ambient conditions and requires a common palladium complex, oxidant and dilute acid. The process exhibits wide functional group tolerance (alcohol, acid, aldehyde, ester, phenol, amide, alkyl, aryl, cyclic) and can be coupled to oxygen (1 atm, balloon) as a terminal oxidant using a biomimetic triple catalytic system and is thus amenable to larger scale applications. In the second section of this chapter, we identify a wide range of directing groups enabling a regioselective Wacker oxidation of unsymmetrically substituted internal alkenes, which occurs predictably at the distal position. This reactivity, when combined with cross metathesis, affords a powerful new tool for the synthesis of versatile functionalized ketones from simple terminal alkene building blocks.

Highly Active Wacker System for the Oxidation of Internal Alkenes

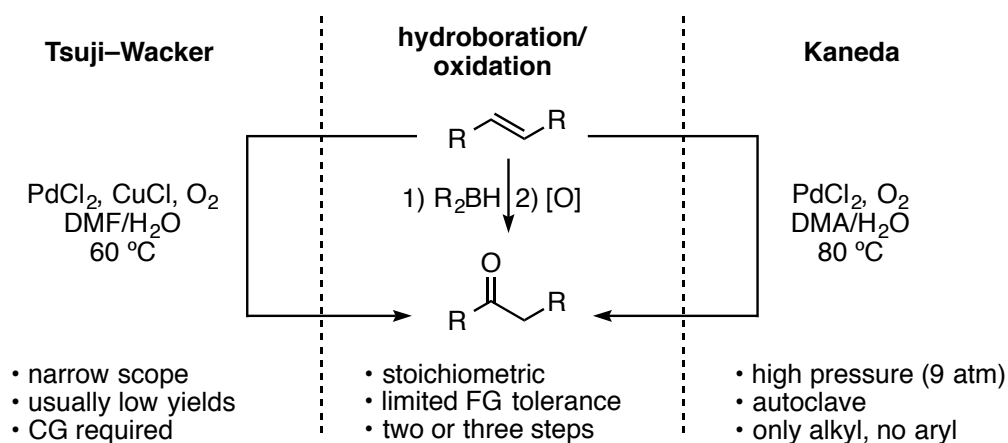
Introduction

Ketones are ubiquitous chemical entities across the molecular sciences.¹ They serve as versatile intermediates in target-oriented synthesis, are present in a wide range of natural products and drugs, are valuable industrial products and mediate important biochemical pathways. On the other hand, simple internal olefins are easily accessible from petroleum and renewable resources such as seed oils. Well-established synthetic routes exist to access more functionalized

internal alkenes, such as carbonyl olefination² and olefin metathesis.³ A simple catalytic oxidation of internal alkenes under ambient conditions would therefore represent a powerful synthetic tool to access valuable ketones; however, such a reaction has remained elusive. Due the lack of an efficient catalytic transformation, the hydroboration/oxidation sequence is still commonly used to access ketones from internal olefins, particularly in total synthesis and medicinal chemistry synthesis (Scheme 4.1).⁴⁻⁸ A major drawback of this procedure is the low functional group (FG) compatibility of highly reactive borane reagents, as well as the inherent stoichiometric and multistep nature of the process. A direct, catalytic methodology to perform this transformation would be highly desirable.

The Tsuji-Wacker reaction, as discussed in previous chapters of this thesis, is a well studied-catalytic transformation used to access methyl ketones from terminal alkenes.⁹⁻¹⁰ However, it is unreactive towards internal olefins unless suitable coordinating groups (CG) are present to facilitate the process.⁹ In the latter case, the success of the transformation is highly substrate-dependent, as shown by the variable yields obtained in the literature (examples of both successful¹¹⁻¹³ and unsuccessful¹⁴⁻¹⁶ results have been reported). These aspects considerably limit the scope of the transformation. More recently, Kaneda disclosed an elegant oxygen-coupled, copper-free Wacker oxidation of internal olefins.¹⁷ This protocol shows improved substrate scope, but requires the use of high oxygen pressures (9 atm prestir followed by 3 atm) and special equipment (autoclave). The high pressure of this reaction limits its application in laboratory-

scale research.¹⁸ Moreover, it has recently been emphasized that the ease of use of a synthetic methodology is of paramount importance to its broad adoption across the molecular sciences.^{19–23} Therefore, the development of a general and user-friendly palladium-catalyzed oxidation of internal olefins to access ketones is still an unmet challenge in catalysis.



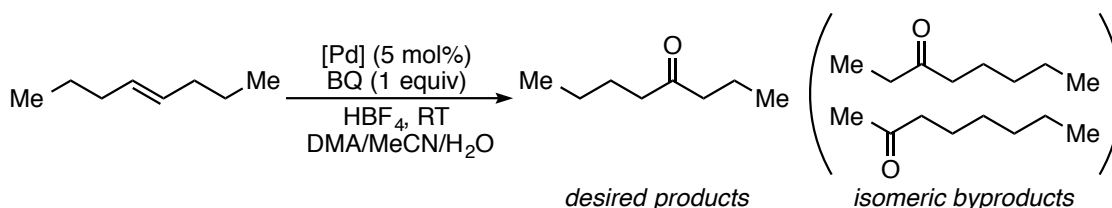
Scheme 4.1 Selected approaches to produce ketones from terminal alkenes.

Results and Discussion

At the outset of our investigations, we intended to devise a protocol including the following features to ensure broad synthetic utility: room temperature, ambient pressure, simple setup and broad functional group tolerance. We initially started with the following reaction conditions: CH₃CN/H₂O as the solvent, *trans*-4-octene as model substrate, palladium acetate as catalyst and benzoquinone (BQ) as an easy to handle, inexpensive oxidant (Table 4.1, entry 1). Initial experiments afforded no conversion to the desired product, 4-octanone. We hypothesized that

a biscationic palladium complex could show improved electrophilicity and facilitate the reaction of the inherently less reactive internal olefin. Gratifyingly, the use of $\text{Pd}(\text{MeCN})_2(\text{BF}_4)_2$ afforded nearly full conversion of the starting material to a mixture of octanone isomers (entry 2).

Table 4.1 Optimization Studies.^a



Entry	[Pd]	HBF_4 (M)	DMA/MeCN/ H_2O	Yield ^b
1	$\text{Pd}(\text{OAc})_2$	0	0/7/1	0 (0)
2	$\text{Pd}(\text{MeCN})_4(\text{BF}_4)_2$	0	0/7/1	37 (41)
3	$\text{Pd}(\text{MeCN})_4(\text{BF}_4)_2$	0	3.5/3.5/1	26 (1)
4	$\text{Pd}(\text{MeCN})_4(\text{BF}_4)_2$	0.27	3.5/3.5/1	81 (3)
5	$\text{Pd}(\text{OAc})_2$	0.27	3.5/3.5/1	87 (2)
6	$\text{Pd}(\text{OAc})_2$	0.27	7/0/1	32 (6)
7	$\text{Pd}(\text{OAc})_2$	0.27	0/7/1	89 (8)
8	$\text{Pd}(\text{OAc})_2$	0.13	3.5/3.5/1	69 (2)
9	$\text{Pd}(\text{OAc})_2$	0.4	3.5/3.5/1	84 (3)

^a0.2 mmol substrate, 16 h. ^bYield of 4-octanone in % obtained by GC using tridecane as a standard, yields in parentheses represent the combined yield of the isomeric byproducts.

The low yield of 4-octanone is due to rapid competing isomerization of the double bond under these conditions, resulting in extensive formation of 3- and 2-octanone. The addition of DMA as a co-solvent almost completely suppressed isomerization,^{17,24} but only low conversion of starting material was observed

(entry 3). In order to increase the reactivity of this system, a wide range of additives, including non-coordinating acids, were evaluated. Strong acid has been suggested to prevent formation of Pd-black and accelerate the oxidation of Pd(0) by benzoquinone in other palladium-catalyzed oxidations.²⁵⁻²⁸ In our case, addition of HBF₄ afforded full conversion to the desired product, 4-octanone, with only traces of the two other isomers (entry 4). The use of Pd(OAc)₂ as catalyst resulted in an even improved yield under the same conditions (entry 5). It is likely that a similar biscationic complex is generated *in situ* in the presence of HBF₄ via protonation of the acetate ligands. Control reactions showed that the use of a binary DMA/H₂O solvent mixture afforded a lower conversion and, surprisingly, increased formation of the isomers (entry 6). The MeCN/H₂O solvent system resulted in high conversion with increased isomerization (entry 7). Deviation from the ideal 1:1 ratio of DMA/MeCN proved ineffective. More DMA did not further improve the selectivity for oxidation over isomerization, whereas more MeCN accelerated the reaction at the cost of selectivity. An unprecedented synergistic solvent effect thus appears to be a key aspect of this reaction. Lowering the amount of acid had a deleterious effect on conversion, while increasing it did not afford any further improvement (entries 8-9). Use of weaker acids such as acetic acid afforded no product formation.

We then studied the scope of the transformation. Simple olefins, both acyclic and cyclic, were oxidized in an efficient manner (Table 4.2, entries 1-4). Styrene derivatives also afforded the product in high yields. High regioselectivity

for the Markovnikov product could be obtained for the methoxy-derivative (entry 5). The electron-neutral aromatic substrate afforded a nearly 1:1 mixture of isomers, with a slight difference in regioselectivity for the *trans* and the *cis*-alkene (entries 6-7). Cinnamyl acetate, in contrast, afforded full regioselectivity for the Markovnikov product, suggesting a strong directing effect of the acetate group (entry 8). Importantly, no benzaldehydes were obtained as side-products with styrenes (entries 5-8), which is in contrast to the reactions using high pressure of oxygen.^{29,30} O-functionalized homoallylic compounds afforded good regioselectivity (4:1) for oxidation of the more distal position (entries 9-10). The synthetic implications of this regioselectivity are studied in the second section of this chapter and the origin of this selectivity is explored in Chapter 5.

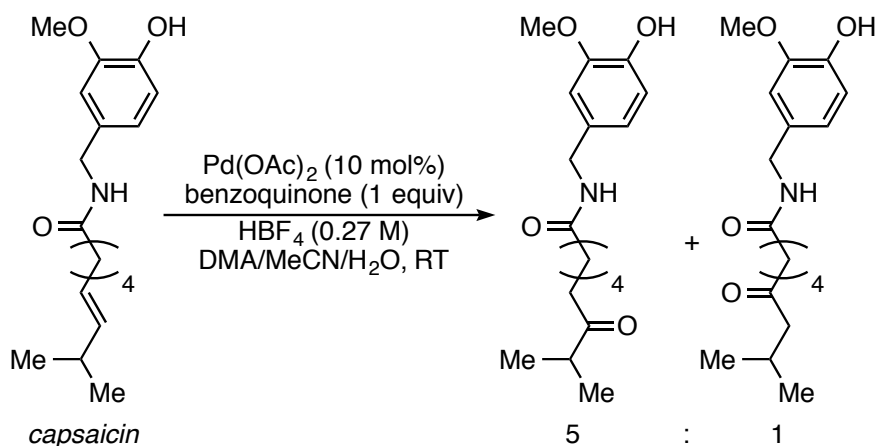
With continuing interest in testing the synthetic potential of our transformation, we probed its application on a polyfunctionalized natural product. Capsaicin is an important compound with applications in cancer^{31,32} and pain relief³³ research. The internal alkene group was smoothly oxidized in the presence of the other functional groups, affording high yield of the desired product. This result bodes well for the application of our methodology to more complex targets. The notable regioselectivity (5:1) was rationalized by steric repulsion in the hydroxypalladation step between the palladium center and the *iso*-propyl group.

Table 4.2 Substrate scope.^a

$$R^1-CH=CH-R^2 \xrightarrow[\text{DMA/MeCN/H}_2\text{O, RT}]{\text{Pd(OAc)}_2 \text{ (5 mol\%)} \\ \text{benzoquinone (1 equiv)} \\ \text{HBF}_4 \text{ (0.27 M)}} R^1-CH_2-CH(R^2)-C(=O)Me$$

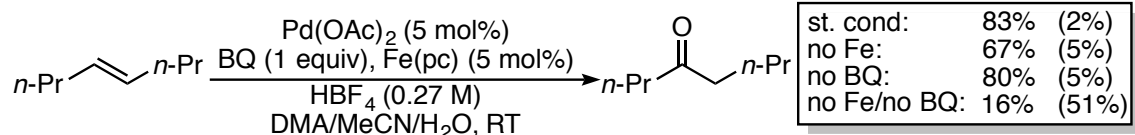
Entry	Starting Material	Product	Yield (%) ^b
1			78 87 ^c
2			70 ^c
3			87 ^c (2.5:1) ^d
4			75 ^c
5			84
6 ^e			91 (1:1) ^f
7 ^e			91 (1.4:1) ^f
8 ^{e,g}			80
9			75 ^h
10			91 (4:1) ^d
11 ^g			53

[a] 1 mmol alkene, DMA/MeCN/H₂O (3.5:3.5:1), 16 h. [b] Isolated yields in %. [c] GC-yield using tridecane as a standard. [d] Product ratio. [e] MeCN/H₂O (7:1). [f] Product ratio, isomers could be separated by CC. [g] 10 mol% Pd. [h] 19 % of the minor isomer was present and not isolated.

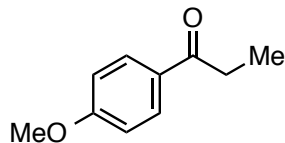


Scheme 4.2 Oxidation of a bioactive natural product.

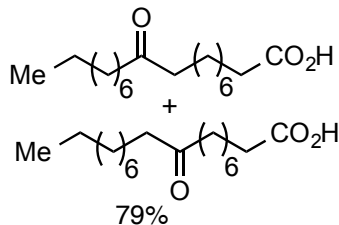
Recognizing the inherent limitation of the use of stoichiometric benzoquinone for larger-scale applications, we undertook preliminary investigations to use oxygen as terminal oxidant. Bäckvall has extensively studied a biomimetic triple catalytic system to facilitate palladium-catalyzed oxidation reactions under atmospheric pressure of oxygen using catalytic benzoquinone.^{34–36} Gratifyingly, initial results using only 10 mol% benzoquinone and 5 mol% Fe(pc) (pc = phthalocyanine) mirrored the outcome of the stoichiometric process (Scheme 4.3). Control experiments showed that the reaction using both the iron catalyst and benzoquinone afforded the highest yield and best prevented isomerization. Unexpectedly, catalyst turnover was also observed in the absence of redox catalysts. Indeed, the reaction went nearly to completion in all three control reactions performed. Under the directly oxygen-coupled system, full conversion to a mixture of octanone isomers (16 %, 20 %, 31 %) was obtained.



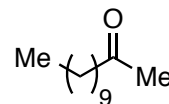
other substrates:



72%
[2-gram scale]



79%



76%

Scheme 4.3 Catalytic system for aerobic oxidation. Yields in parentheses

represent the combined yield of isomeric ketone byproducts.

This outcome might be the result of a synergistic solvent effect, as DMA was previously shown to facilitate direct coupling to oxygen in palladium-catalysis.^{17,24} The low selectivity for 4-octanone was a result of rapid competing isomerization under these conditions. It is conceivable that the iron catalyst and benzoquinone suppress isomerization via the trapping of a putative palladium-hydride species.³⁷ Alternatively, the redox catalysts could accelerate the rate of oxidation relative to that of isomerization. Benzoquinone can serve as a non-innocent oxidant in palladium-catalysis.³⁸⁻⁴⁰ Despite the mixture of isomers obtained, this result holds great promise for the potential development of a direct oxygen-coupled oxidation of internal olefins under ambient conditions.^{18,19,41,42} We then applied the triple catalytic system to the oxidation of several representative substrates and were delighted to find the reaction provided good yields of each product. The results obtained with this system bode well for larger-scale application, a feature further

confirmed by the comparable yield obtained for the oxidation of *trans*-anethole on a 2-gram scale.

Due to the scarcity of reports involving oxidation of internal olefins and the corresponding lack of mechanistic information, we became interested in following the progress of the reaction with stoichiometric benzoquinone and both *trans*-4-octene (A) and *cis*-4-octene (B) (figure 4.1). Oxidation of the *cis*-isomer was significantly faster and proceeded with slightly more isomerization than the *trans*-isomer, which suggests an increased rate of both isomerization and oxidation with the *cis*-alkene. It is worth noting that other *cis*-alkenes studied in this work did not show detectable isomerization by analysis of the crude NMR-spectrum. However, it is possible that the amount of isomers was too small for the detection limit of NMR-spectroscopy.

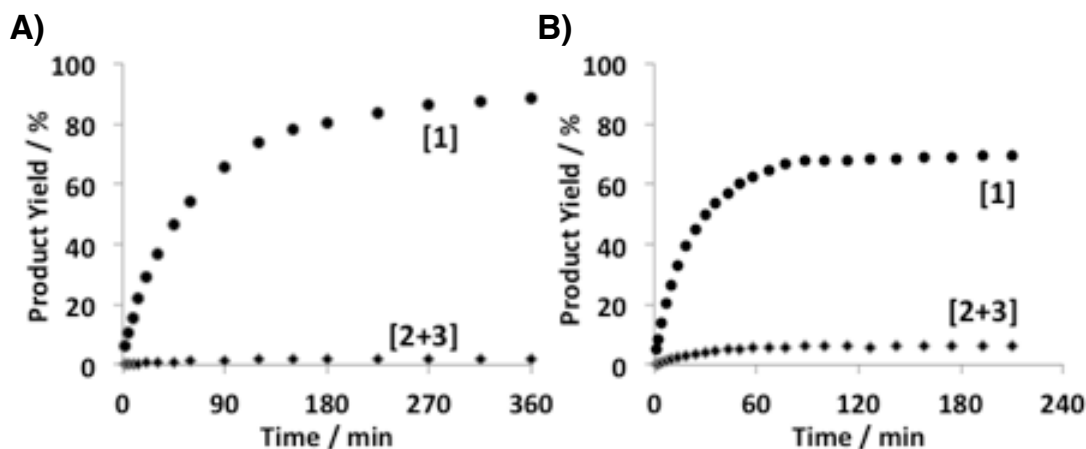


Figure 4.1 Reaction Progress. **A)** *trans*-4-octene as substrate. **B)** *cis*-4-octene as substrate. **1** = 4-octanone, **2** = 3-octanone, **3** = 2-octanone.

Conclusion

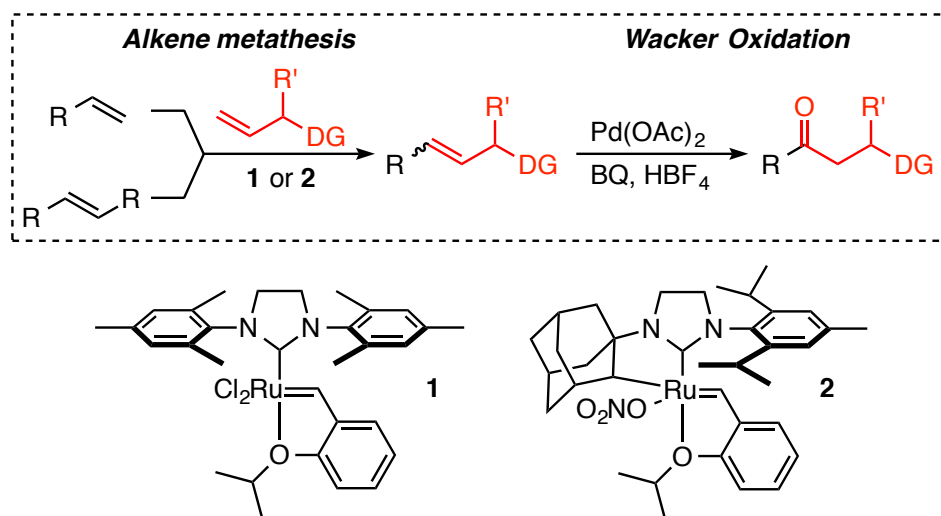
In this section, we have developed a general and practical palladium-catalyzed oxidation to access ketones from a wide variety of internal olefins. The novel transformation showed a wide substrate scope (alcohol, acid, aldehyde, ester, phenol, amide, alkyl, aryl, cyclic) under experimentally simple reaction conditions. Applications of this procedure to the oxidation of a natural product and unprotected seed-oil derivatives have been reported, as well as mechanistically intriguing features (synergistic solvent effect, acid dependence and increased reactivity of *cis*-alkenes). Importantly, an oxygen-coupled procedure was developed for larger scale applications. We anticipate that this reaction could find broad use across the chemical sciences due to its simplicity and generality.

Rapid Access to Functionalized Ketones from Internal Alkenes

Introduction

Functionalized ketones are key synthetic intermediates in target-oriented synthesis.¹ Important C-C bond forming processes such as the Aldol or Mannich reactions have enabled the preparation of hydroxyketones and aminoketones.⁴³ These products are highly sought-after intermediates in the preparation of natural products and drugs, and thus represent key synthetic targets. Novel complementary approaches to their synthesis are therefore in high demand.

Although alkene metathesis is a privileged carbon-carbon forming reaction, it has found only limited use in the preparation of ketones.³ This is due to the lack of an efficient methodology to catalyze the oxidation of internal alkenes to carbonyls with regiocontrol. The ubiquitously adopted palladium-catalyzed Tsuji-Wacker reaction would be a logical tool to achieve this transformation. However, the classical Tsuji-Wacker oxidation exhibits limited reactivity towards internal alkenes.⁹ We reasoned that the allylic heteroatom placed in close proximity to the alkene could provide an efficient handle to induce the desired regioselectivity. Previous examples of directed Wacker oxidations of internal alkenes have been limited in scope and frequently have proceeded in low yield, required peroxide oxidants or high oxygen pressure.^{11-16,43} Strikingly, a recent report from Feringa demonstrated the inability of neutral Pd(II)-complexes to oxidize internal alkenes bearing allylic ester moieties.⁴⁴ Instead, the internal allylic esters rearranged to the corresponding terminal alkenes prior to oxidation. The results described in the first section of this chapter suggest that the synthetic power of the Tsuji-Wacker oxidation could be translated to internal alkenes using a dicationic palladium catalyst (*vide supra*). This catalytic oxidation would enable rapid access to functionalized ketones when coupled to the carbon-carbon forming power of cross-metathesis (scheme 4.4).



Scheme 4.4 Cross metathesis/regioselective Wacker oxidation sequence for the preparation of ketones. BQ = benzoquinone; DG = directing group

Results and Discussion

Initial experiments using an optimized solvent system (DMA/MeCN/H₂O) led to long reaction times with incomplete conversion. Use of a binary solvent system (MeCN/H₂O) and acid^{25–28} led to a much more active system and full conversion was obtained. In contrast to the oxidation of unfunctionalized alkenes, DMA is not necessary to prevent isomerization in the presence of coordinating groups. Having an efficient protocol in hand, we tested a selection of simple mono-functionalized alkene substrates to efficiently probe the influence of diverse groups on the regioselectivity (Table 4.3). Allylic alcohol derivatives demonstrated that good regioselectivity could be obtained using common protecting groups, such as benzyl (9:1). Introduction of a benzoate group increased the regioselectivity to an excellent 20:1. This result is particularly

interesting in light of potential known side-reactions of allylic esters, such as the well-established palladium-catalyzed allylic substitution and rearrangement.¹¹ For example, a recent report from Feringa showed a strong preference for allylic rearrangement over oxidation of internal alkenes.⁴⁴ A branched allylic benzoate afforded a similar excellent result and thus bodes well for the use of more elaborated substrates (Entry 3). We then explored the ability of homoallylic functionalities to direct the oxidation reaction, since the corresponding oxidation products are not readily accessible via traditional carbon-carbon forming processes. Synthetically viable regiocontrol for the distal oxidation product was obtained with up to >20:1 selectivity (Entries 4-6). Interestingly, this approach is not limited to protected alcohols, as an β,γ -unsaturated methyl ester afforded the distal oxidation product (Entry 6). An allylic toluenesulfonamide gave the corresponding aminoketone derivative in high regioselectivity, expanding the reaction scope to nitrogen-derived directing groups (Entry 7).

With a regioselective Wacker oxidation of internal alkenes in hand, we sought to illustrate the power of a combined cross-metathesis/regioselective Wacker sequence in the preparation of hydroxyketones and aminoketones. Moreover, the coupling with cross-metathesis presented an opportunity to further probe the predictability of the regiocontrol using other directing groups (Scheme 4.5). An allylic carbonate and two allylic phthalimides were readily accessed using the Grubbs-Hoveyda second generation catalyst, **1**. The linear substrates afforded high regiocontrol for the distal oxidation product in the subsequent

Wacker oxidation. This is critical, as the terminal unbranched allyl phthalimide offers dramatically reduced regioselectivity compared to the branched allyl phthalimide in the Tsuji-Wacker oxidation (6:4).⁴⁵

Table 4.3 Initial Scope of directing groups.^a

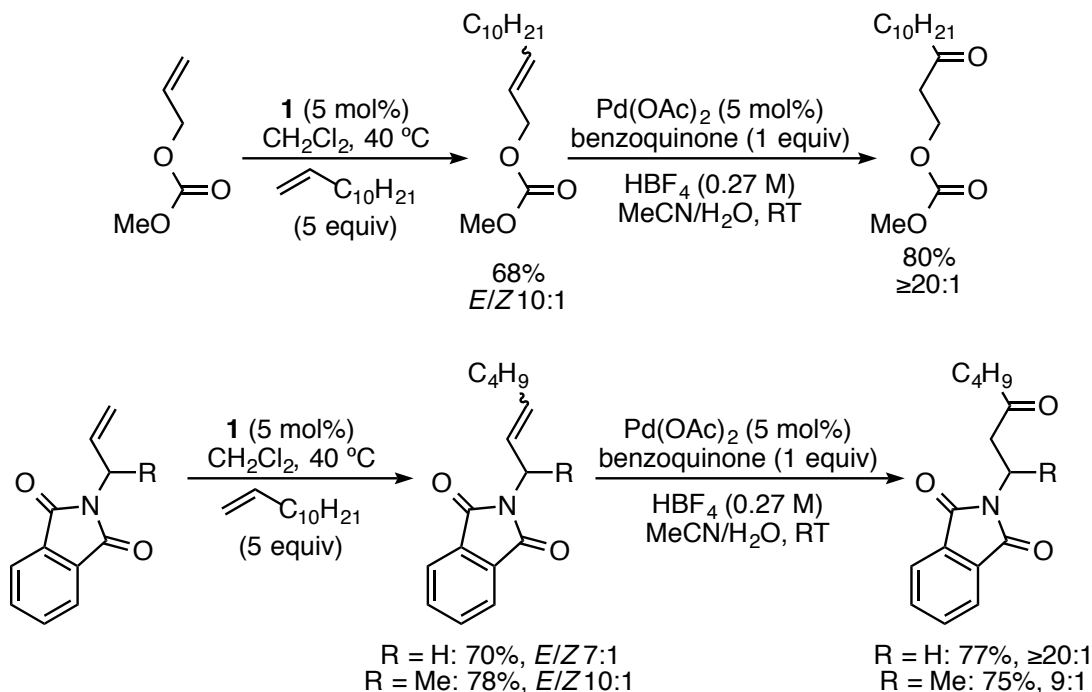
$$\text{R}-\text{CH}=\text{CH}-\text{CH}_2-\text{DG} \xrightarrow[\text{MeCN/H}_2\text{O (7:1)}]{\text{Pd(OAc)}_2 (7.5 \text{ mol\%}), \text{BQ (1 equiv)}, \text{HBF}_4 (0.27\text{M}), \text{RT}} \text{R}-\text{C}(=\text{O})-\text{CH}_2-\text{CH}_2-\text{DG}$$

Entry	Starting Material	Product	Yield (%) ^b	Selectivity ^b
1			71	9:1
2			80	20:1
3			80	≥20:1
4			80	6.5
5			83	10:1
6 ^e			70	≥20:1
7 ^e			72	≥20:1

^a1 mmol alkene, MeCN/H₂O (7:1), 16 h. ^bIsolated by silica gel in %. ^cSelectivity = ratio of distal oxidation to proximal oxidation based on ¹H-NMR analysis of the crude reaction mixture.

The branched allylic phthalimide similarly afforded the product with high regioselectivity and thus provides access to secondary aminoketones. Overall,

both common branched and linear protected amine and alcohol substrates enable a regioselective Wacker oxidation to be performed.

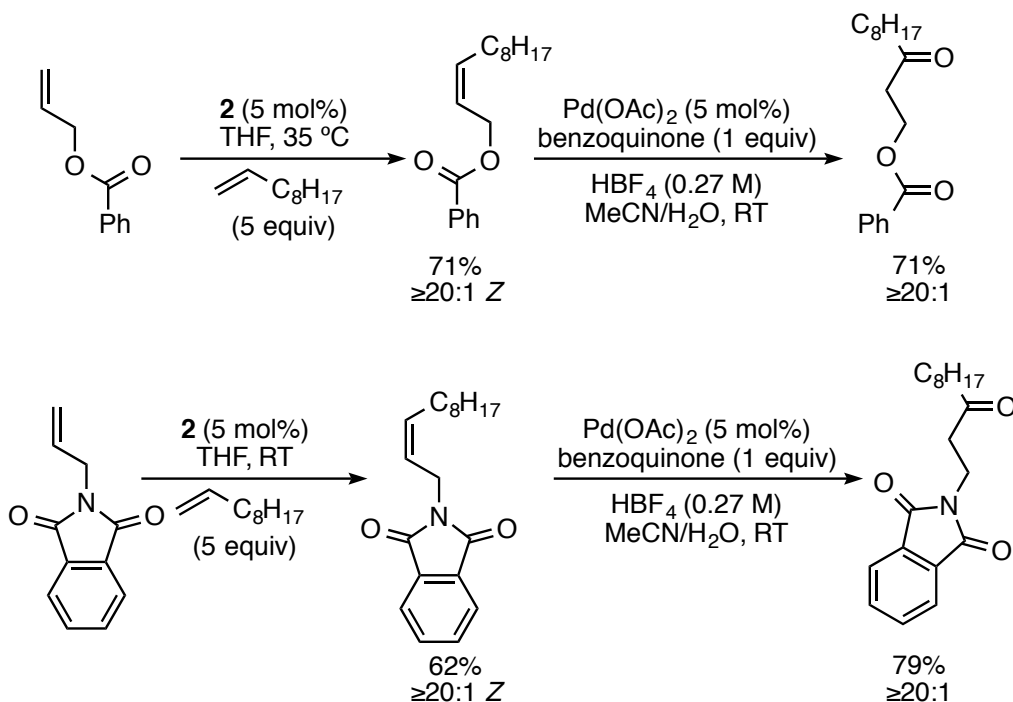


Scheme 4.5 Alkene preparation and further evaluation of directing groups enabled by cross-metathesis.

Despite recent progress in the oxidation of internal alkenes, *Z*-alkenes have proven either inert⁴⁶ or prone to positional isomerisation⁴⁷ in Wacker-type oxidations. Since many olefination reactions produce *Z*-alkenes or mixture of both *Z* and *E*-isomers, we sought to probe the effect of alkene geometry upon the oxidation.² To this end, it was critical to access the desired starting materials as stereochemically pure *Z*-isomers to clearly understand the underlying isomeric

dependence on the reaction outcome. We thus exploited a new class of chelated ruthenium alkene-metathesis catalysts that exhibit exquisite kinetic control to access the corresponding *Z*-substrates (Scheme 3).⁴⁸

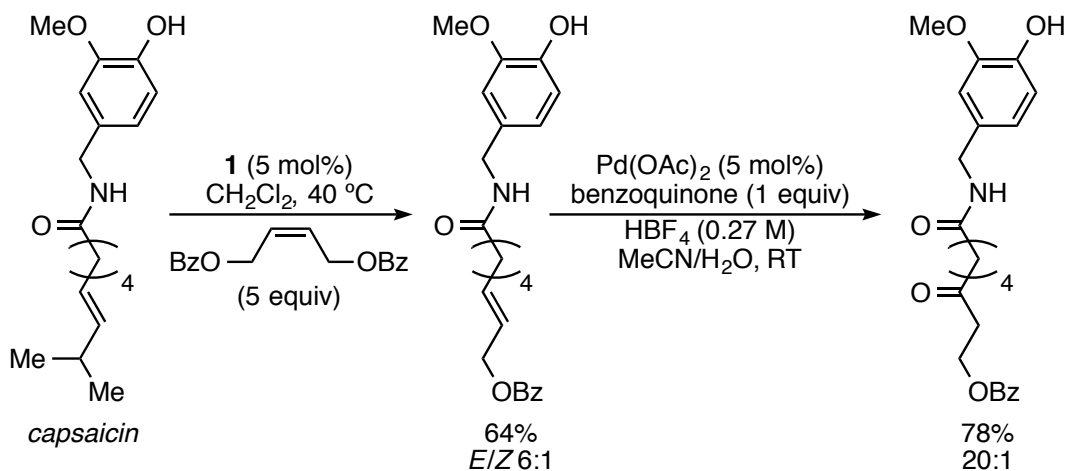
We were pleased to find that the chelated catalyst could cleanly prepare the desired *Z*-substrates from allyl benzoate and allyl phthalimide in good yields and >95% *Z* selectivity. These two products were then smoothly transformed into the corresponding ketones in high regioselectivity and yield, comparable to the results obtained for the *E*-isomers. These results thus establish that the efficiency of our oxidation protocol towards *E*-alkenes also applies to *Z*-alkenes.



Scheme 4.6 *Z*-Alkene preparation by cross-metathesis and evaluation of the influence of alkene geometry on Wacker oxidation regioselectivity and efficiency.

With the interest of further probing the synthetic utility of the metathesis/regioselective Wacker sequence, we probed this strategy in the context of a bioactive, polyfunctionalized alkene starting material, capsaicin.^{31–33}

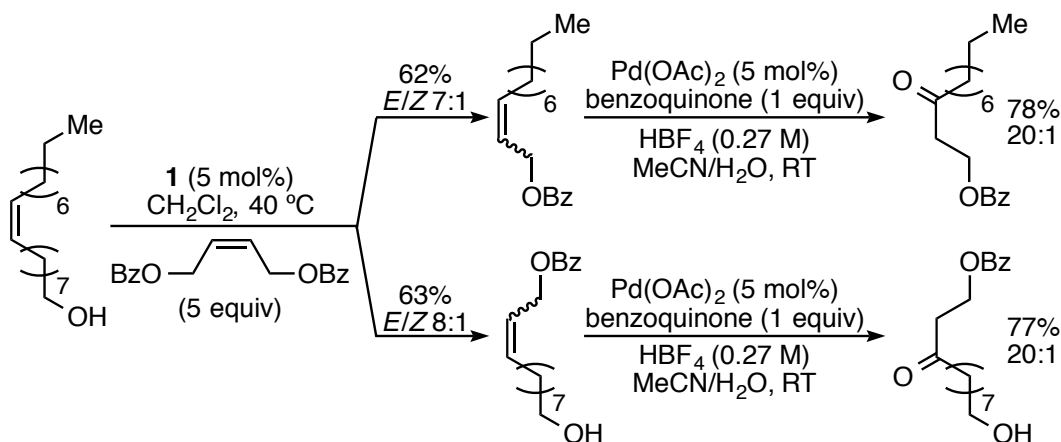
We were delighted to see that both steps worked in good yields, and the regioselectivity of the Wacker step proved as high as in the more simple examples. No interference with the directing ability of the benzoate moiety was observed, validating the potential of this strategy for complex molecule functionalization.



Scheme 4.7 Application of the synthetic sequence to a polyfunctionalized target.

We envisioned this methodology could also enable rapid generation of functionalized molecules from inexpensive and renewable seed-oil derivatives.^{49,50} Oleyl alcohol could be selectively transformed into two substituted allylic benzoate substrates using catalyst **1**. The two intermediates

could further be oxidized in high selectivity to the corresponding ketones under our standard oxidation conditions.



Scheme 4.8 Application of the synthetic sequence to selectively transform a seed-oil derivative into ketone building blocks

Conclusion

In this section, a new synthetic strategy to regioselectively access complex ketone products from simple starting materials was described. A wide range of functionalized alkenes were established as efficient substrates for a regioselective Wacker oxidation of internal alkenes, producing valuable synthetic intermediates (hydroxyketones, aminoketones, ketoesters). Efficiency of our regioselective Wacker oxidation protocol was demonstrated using both *E*- and *Z*-isomers prepared via cross-metathesis. Application to the functionalization of a bioactive natural product and seed-oil derivatives showcased the potential of this cross-metathesis/regioselective Wacker strategy in target-oriented synthesis. Overall, the high functional group tolerance of both the cross-metathesis step and

the Wacker oxidation, combined with the predictable regioselectivity of the oxidation step, holds great promise in the wide adoption of this strategy in organic synthesis.

Experimental Section

Materials and methods

General Reagent Information: Preparation of non-commercial substrates: Unless stated otherwise, all reactions except for the Wacker oxidations were carried out in oven- and flame-dried glassware (200 °C) using standard Schlenk techniques and were run under argon atmosphere. Wacker oxidations were carried out without exclusion of air. The reaction progress was monitored by TLC. Starting materials and reagents were purchased from *Sigma Aldrich*, *Acros*, *Fluka*, *Fischer*, *TCI* or *Synquest Laboratories* and were used without further purification, unless stated otherwise. Solvents for the reactions were of quality puriss., p.a. of the companies *Fluka* or *J.T. Baker* or of comparable quality. Anhydrous solvents were purified by passage through solvent purification columns. For aqueous solutions, deionized water was used.

General Analytical Information: Nuclear Magnetic Resonance spectra were measured with a *Varian-Inova 500* spectrometer (500 MHz), a *Varian-Inova 400* spectrometer (400 MHz), or a *Varian-Mercury Plus 300* spectrometer (300 MHz).

The solvent used for the measurements is indicated. All spectra were measured at room temperature (22–25 °C). Chemical shifts for the specific NMR spectra were reported relative to the residual solvent peak [CDCl_3 : $\delta_{\text{H}} = 7.26$; CDCl_3 : $\delta_{\text{C}} = 77.16$]. The multiplicities of the signals are denoted by *s* (singlet), *d* (doublet), *t* (triplet), *q* (quartet), *p* (pentet) and *m* (multiplet). The coupling constants *J* are given in Hz. All ^{13}C -NMR spectra are ^1H -broadband decoupled, unless stated otherwise. High-resolution mass spectrometric measurements were provided by the California Institute of Technology Mass Spectrometry Facility using a JEOL JMS-600H High Resolution Mass Spectrometer. The molecule-ion M^+ , $[\text{M} + \text{H}]^+$ and $[\text{M}-\text{X}]^+$ respectively or the anion are given in *m/z*-units. Response factors were collected for 4-octanone, 3-octanone, 2-octanone, cyclohexanone, dodecene, 2-dodecanone and lauric aldehyde following literature procedures.^a

General Considerations: Thin Layer Chromatography analyses were performed on silica gel coated glass plates (0.25 mm) with fluorescence-indicator UV_{254} (*Merck*, TLC silica gel 60 F_{254}). For detection of spots, UV light at 254 nm or 366 nm was used. Alternatively, oxidative staining using aqueous basic potassium permanganate solution (KMnO_4) or ceric ammonium nitrate (CAN) was performed. Flash column chromatography was conducted with *Silicagel 60* (*Fluka*; particle size 40–63 μM) at 24 °C and 0–0.3 bar excess pressure (compressed air) using Et_2O /pentane unless stated otherwise.

^a Ritter, T.; Hejl, A.; Wenzel, A. G.; Funk, T. W.; Grubbs, R. H. *Organometallics* **2006**, *25*, 5740.

General procedures

Procedure (1) for smaller-scale (0.2 mmol) oxidation of *trans*-4-octene (GC analysis): The corresponding palladium complex (0.01 mmol, 5 mol%) and benzoquinone (21.6 mg, 0.2 mmol, 1 equiv) were charged in a resealable 4-mL vial under air. The corresponding solvent mixture was then added, followed by the addition of aqueous HBF₄. After the addition of *trans*-4-octene (22.4 mg, 0.2 mmol), the homogenous reaction mixture was stirred for 16 h at room temperature. The crude reaction mixture was then partitioned using a mixture of ether and water (10 mL each), tridecane was added as a standard, and an aliquot of the organic phase was submitted to GC-analysis to determine the yield of 4-octanone, 3-octanone, 2-octanone.

Procedure (2) for larger-scale (1 mmol) oxidation of alkenes (isolation): Palladium acetate (11.5 mg, 0.05 mmol, 5 mol%) and benzoquinone (108 mg, 1.00 mmol) were charged in a resealable 20-mL vial under air. A mixture of DMA (2.2 mL), MeCN (2.2 mL) and water (0.63 mL) was added, followed by the addition of aqueous HBF₄ (0.18 mL, 48% in water, 1.38 mmol). After the addition of the corresponding substrate (1.00 mmol), the homogenous reaction mixture was stirred for 16 h at room temperature. The crude reaction mixture was then diluted with brine (30 mL) and ether (30 mL), the phases were separated and the aqueous phase was further extracted (2x) with ether. The combined organic phases were then dried over Na₂SO₄, filtered, and evaporated *in vacuo*. In some

cases, NMR-analysis of the crude mixture was performed to determine the regioselectivity of the process. The crude product was then further purified by column chromatography on silica gel using pentane/ether as eluent.

General Procedure (3) for larger-scale (1 mmol) oxidation of alkenes using O₂ as the terminal oxidant (isolation): Palladium acetate (11.5 mg, 0.05 mmol, 5 mol%), benzoquinone (10.8 mg, 0.10 mmol, 10 mol%) and Fe(phtalocyanin) (28.4 mg, 0.05 mmol, 5 mol%) were charged in a resealable 20-mL vial under air. A mixture of DMA (2.2 mL), MeCN (2.2 mL) and water (0.63 mL) was added, followed by the addition of aqueous HBF₄ (0.18 mL, 48% in water, 1.38 mmol). The mixture was then purged during 2 min using an oxygen balloon. After the addition of the corresponding substrate (1 mmol), the homogenous reaction mixture was stirred for 16 h at room temperature under an atmospheric pressure of oxygen (balloon). The crude reaction mixture was then diluted with brine (30 mL) and ether (30 mL), the phases were separated and the aqueous phase was further extracted (2x) with ether. The combined organic phases were then dried over Na₂SO₄, filtered, and evaporated *in vacuo*. In some cases, NMR-analysis of the crude mixture was performed to determine the regioselectivity of the process. The crude product was then further purified by column chromatography on silica gel using pentane/ether as eluent.

General Procedure (4) for larger-scale (1 mmol) oxidation of alkenes bearing directing groups (isolation): Palladium acetate (11.5 mg, 0.05 mmol, 5 mol%) and benzoquinone (108 mg, 1.00 mmol) were charged in a resealable 20-mL vial under air. A mixture of MeCN (4.5 mL) and water (0.63 mL) was added, followed by the addition of aqueous HBF₄ (0.18 mL, 48% in water, 1.38 mmol). After the addition of the corresponding substrate (1.00 mmol), the homogenous reaction mixture was stirred for 16 h at room temperature. The crude reaction mixture was then diluted with brine (30 mL) and extracted with CH₂Cl₂ (3x30 mL). The combined organic phases were then dried over Na₂SO₄, filtered, and evaporated *in vacuo*. NMR-analysis of the crude mixture was performed to determine the regioselectivity of the process. The crude product was then further purified by column chromatography on silica gel using pentane/ether as eluent.

General Procedure (5) for cross-metathesis reactions using catalyst 1: The corresponding limiting alkene substrate (1 mmol, 1 equiv.) and the excess cross-partner (5.00 mmol, 5 equiv.) were charged in a resealable 20-mL vial in a nitrogen filled drybox. Dry CH₂Cl₂ (2.5 mL) was added, followed by the addition of Grubbs-Hoveyda second generation catalyst (31.3 mg, 0.05 mmol, 5 mol%). The vial was sealed and taken out of the glove-box, put under an Argon atmosphere (balloon) and stirred for 20 h at 40°C before being quenched by addition of ethyl vinyl ether (few drops). The solvent was then evaporated and the *E/Z* ratio was determined by NMR-analysis of the crude reaction mixture. The crude product

was then further purified by column chromatography on silica gel using pentane/ether as eluent.

General Procedure (6) for Z-selective cross-metathesis reactions using

catalyst 2: The corresponding limiting alkene substrate (0.4 mmol) was weighted out in a 4-mL scintillation vial in a nitrogen-filled glovebox. Distilled decene (0.4 mL, 2.1 mmol, 5 equiv) was added, followed by addition of a stock solution of catalyst **2** in THF (0.01 M, 0.8 mL, 0.008 mmol, 2 mol%). The mixture was then stirred open in the glove box for 10 h at the indicated temperature, and was then taken out of the box and quenched by addition of ethyl vinyl ether (few drops). The solvent was evaporated and the *E/Z* ratio was determined by NMR-analysis of the crude reaction mixture. The crude product was then further purified by column chromatography on silica gel using pentane/ether as eluent.

Collection of Reaction Profiles

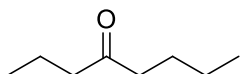
Each profile was generated in triplicate and the values were averaged and graphed using Microsoft Excel to produce the final curves.

Palladium acetate (11.5 mg, 0.05 mmol, 5 mol%) and benzoquinone (108 mg, 1.00 mmol) were charged into 8-mL vials with permeable septum caps under air. 5.4 mL of a stock solution consisting of all of the liquid components was added (stock solution: 9 mL MeCN, 9 mL DMA, 2 mL H₂O, 0.72 mL HBF₄ (48% in water), 250 μL PhNO₂ (to be used as an internal standard) and 628 μL of either

trans-4-octene or *cis*-4-octene (for **A** or **B** respectively)). Time points were taken at the given times and quenched with a 3:1 mixture of EtOAc and Et₃N, followed by analysis with GC.

Product Characterization

octan-4-one (Table 4.2, Entry 1)

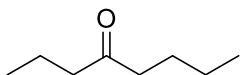


Was obtained as a clear oil (100 mg, 0.78 mmol, 78%) following the general procedure 2. The yield obtained by GC-analysis of the crude was 87%. The difference is attributed to the high volatility of the compound.

¹H NMR: δ 2.35 (q, *J* = 7.0 Hz, 4H), 1.62 – 1.47 (m, 4H), 1.33 – 1.22 (m, 2H), 0.87 (td, *J* = 7.4, 3.3 Hz, 6H). ¹³C NMR: δ 211.5, 44.7, 42.5, 25.9, 22.3, 17.3, 13.8, 13.7.

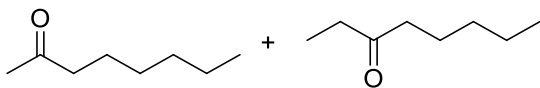
Spectral data were in accordance with a commercial sample.

octan-4-one (Table 4.2, Entry 2)



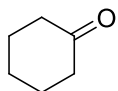
Cis-4-octene was reacted following the general procedure 2. The mixture of crude products was analyzed by GC using tridecane as a standard. Yields of products: 3% 2-octanone, 3% 3-octanone, 70% 4-octanone.

octan-2-one and octan-3-one (Table 4.2, Entry 3)



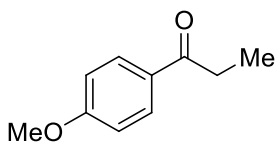
Trans-2-octene was reacted following the general procedure 2. The mixture of crude products was analyzed by GC using tridecane as a standard. Yields of products: 62% 2-octanone, 25% 3-octanone, 3% 4-octanone.

cyclohexanone (Table 4.2, Entry 4)



Cyclohexene was reacted following the general procedure 2. The mixture of crude products was analyzed by GC using tridecane as a standard. 75% yield was obtained. Around 9% cyclohexenone was observed by NMR spectroscopy using mesitylene as an internal standard.

1-(4-methoxyphenyl)propan-1-one (Table 4.2, Entry 5)

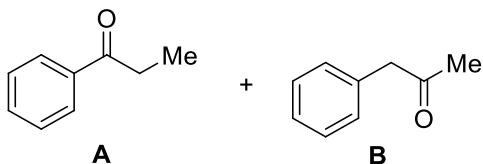


Was obtained as a solid (137 mg, 0.84 mmol, 84%) following the general procedure 2.

¹H NMR: δ 7.92 (d, J = 9.0 Hz, 2H), 6.90 (d, J = 9.0 Hz, 2H), 3.83 (s, 3H), 2.92 (q, J = 7.3 Hz, 2H), 1.18 (t, J = 7.3 Hz, 3H). ¹³C NMR: δ 199.4, 163.3, 130.2, 130.0, 113.6, 55.4, 31.4, 8.4.

Values were in accordance with a commercial sample.

Propiophenone and phenyl acetone (Table 4.2, Entry 6)



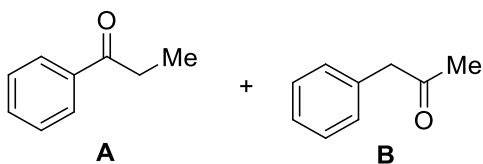
Were obtained from *trans*- β -methyl styrene following a modified general procedure 2 using MeCN/H₂O (4.4 mL/0.63 mL) as the solvent. Crude ratio by NMR was 1:1. The products could be separated by column chromatography, giving two clear oils (A: 62 mg, 0.46 mmol, 46% and B: 60 mg, 0.45 mmol, 45%).

A: ¹H NMR: 7.98 – 7.94 (m, 2H), 7.57 – 7.52 (m, 1H), 7.48 – 7.43 (m, 2H), 3.00 (q, *J* = 7.2 Hz, 2H), 1.22 (t, *J* = 7.2 Hz, 3H). ¹³C NMR: δ 200.8, 136.9, 132.9, 128.5, 128.0, 31.8, 8.2.

B: ¹H NMR: δ 7.36 – 7.32 (m, 2H), 7.30 – 7.25 (m, 1H), 7.23 – 7.19 (m, 2H), 3.70 (s, 2H), 2.15 (s, 3H). ¹³C NMR: δ 206.3, 134.2, 129.4, 128.8, 127.1, 51.0, 29.3.

Values were in accordance with commercial samples.

Propiophenone and phenyl acetone (Table 4.2, Entry 7)



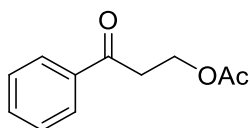
Were obtained from *cis*- β -methyl styrene following a modified general procedure 2 using MeCN/H₂O (4.4 mL/0.63 mL) as the solvent. Crude ratio by NMR was 1.4:1 (A:B). The products could be separated by column chromatography, giving two clear oils (A: 75 mg, 0.56 mmol, 56% and B: 47 mg, 0.35 mmol, 35%).

A: ^1H NMR: 7.98 – 7.94 (m, 2H), 7.57 – 7.52 (m, 1H), 7.48 – 7.43 (m, 2H), 3.00 (q, $J = 7.2$ Hz, 2H), 1.22 (t, $J = 7.2$ Hz, 3H). ^{13}C NMR: δ 200.8, 136.9, 132.9, 128.5, 128.0, 31.8, 8.2.

B: ^1H NMR: δ 7.36 – 7.32 (m, 2H), 7.30 – 7.25 (m, 1H), 7.23 – 7.19 (m, 2H), 3.70 (s, 2H), 2.15 (s, 3H). ^{13}C NMR: δ 206.3, 134.2, 129.4, 128.8, 127.1, 51.0, 29.3.

Values were in accordance with a commercial sample.

3-oxo-3-phenylpropyl acetate (Table 4.2, Entry 8)



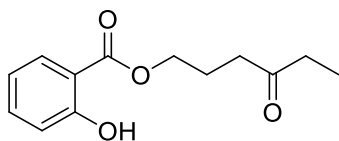
Was obtained as clear oil (153 mg, 0.80 mmol, 80%) following a modified general procedure 2 using MeCN/H₂O (4.4 mL/0.63 mL) as the solvent and 10 mol% palladium acetate.

^1H NMR: δ 7.97 – 7.93 (m, 2H), 7.60 – 7.55 (m, 1H), 7.49 – 7.44 (m, 2H), 4.51 (t, $J = 6.4$ Hz, 2H), 3.31 (t, $J = 6.4$ Hz, 2H), 2.02 (s, 3H). ^{13}C NMR: δ 197.0, 171.0, 136.5, 133.4, 128.7, 128.0, 59.6, 37.3, 20.9.

Values are in accordance with literature.^b

^b *Org. Lett* **2012**, *14*, 2414.

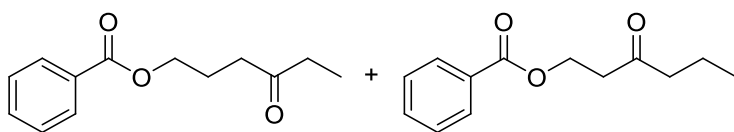
4-oxohexyl 2-hydroxybenzoate (Table 4.2, Entry 9)



Was obtained as an oil (176 mg, 0.75 mmol, 75%) following the general procedure 2. Crude NMR analysis showed the formation of a 4:1 mixture of regioisomers. Only the major product was isolated by column chromatography.

^1H NMR: δ 10.77 (s, 1H), 7.80 (dd, J = 8.0, 1.7 Hz, 1H), 7.45 (ddd, J = 8.6, 7.2, 1.7 Hz, 1H), 6.97 (dd, J = 8.4, 0.8 Hz, 1H), 6.87 (ddd, J = 8.2, 7.2, 1.1 Hz, 1H), 4.35 (t, J = 6.4 Hz, 2H), 2.57 (t, J = 7.1 Hz, 2H), 2.45 (q, J = 7.3 Hz, 2H), 2.13 – 2.01 (m, 2H), 1.06 (t, J = 7.3 Hz, 3H). ^{13}C NMR: δ 210.1, 170.1, 161.7, 135.7, 129.8, 119.1, 117.6, 112.4, 64.6, 38.3, 36.1, 22.7, 7.8. HRMS (EI): calcd (M⁺): 236.2049; measured: 236.2046.

4-oxohexyl benzoate (Table 4.2, Entry 10)



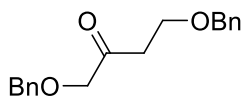
Was obtained as a clear oil (200 mg, 0.91 mmol, 91%, 4:1 mixture) following the general procedure 2.

^1H NMR: δ 8.04 – 7.95 (m, 2H), 7.57 – 7.50 (m, 1H), 7.46 – 7.38 (m, 2H), 4.58 (t, J = 6.4 Hz, 2H, minor), 4.31 (t, J = 6.4 Hz, 2H), 2.86 (t, J = 6.4 Hz, 2H, minor), 2.56 (t, J = 7.2 Hz, 2H), 2.44 (q, J = 7.3 Hz, 2H), 2.12 – 1.97 (m, 2H), 1.70 – 1.51 (m, 2H, minor), 1.04 (t, J = 7.3 Hz, 3H), 0.91 (t, J = 7.4 Hz, 3H, minor). ^{13}C NMR:

δ 210.3, 207.9 (minor), 166.5, 166.4 (minor), 133.0 (minor), 132.9, 130.2 (minor), 129.5 (minor), 129.5, 128.3, 128.3 (minor), 64.2, 60.0 (minor), 45.1 (minor), 41.4 (minor), 38.6, 36.0, 22.9, 17.1 (minor), 13.7 (minor), 7.8.

Values are in accordance with literature.^c

1,4-bis(benzyloxy)butan-2-one (Table 4.2, Entry 11)



Was obtained as a clear oil (150 mg, 0.53 mmol, 53%) following a modified general procedure 2 using 10 mol% palladium acetate.

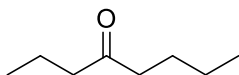
¹H NMR: δ 7.38 – 7.28 (m, 10H), 4.59 (s, 2H), 4.50 (s, 2H), 4.11 (s, 2H), 3.77 (t, $J = 6.2$ Hz, 2H), 2.75 (t, $J = 6.2$ Hz, 2H). ¹³C NMR: δ 207.0, 138.0, 137.2, 128.5, 128.4, 128.0, 127.9, 127.7, 127.7, 75.4, 73.3, 73.3, 65.0, 39.4.

Values are in accordance with literature.^d

^c *Org Lett* **2011**, *13*, 4308.

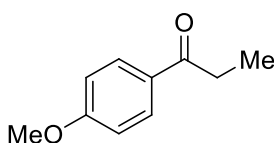
^d *Bull. Chem. Soc. Jap.* **1981**, *54*, 3100.

octan-4-one (Scheme 4.3)



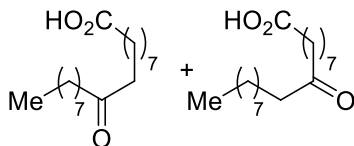
Was obtained following the general procedure 3. A yield of 83% was obtained by GC-analysis of the crude.

1-(4-methoxyphenyl)propan-1-one (Scheme 4.3)



Was obtained as a solid (1.59 g, 9.7 mmol, 72%) on a 2 g-scale following general procedure C. In that case a washing of the ethereal phase with aq. LiCl was necessary to remove DMA prior to chromatography.

10-oxooctadecanoic acid and 9-oxooctadecanoic acid (Scheme 4.3)



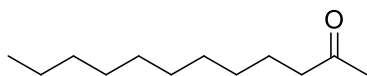
Were obtained as white solids (235 mg, 0.79 mmol, 79%, 1:1) following the general procedure C. Alternatively obtained as white solids (245 mg, 0.82 mmol, 82%, 1:1) following the general procedure B.

$^1\text{H NMR}$: δ 2.37 – 2.33 (m, 6H), 1.66 – 1.49 (m, 6H), 1.35 – 1.20 (m, 18H), 0.86 (t, $J = 7.0$ Hz, 3H). $^{13}\text{C NMR}$: \square 211.8, 211.8, 180.0, 178.0, 42.8, 42.8, 42.7, 42.7, 34.0, 34.0, 31.9, 31.8, 29.4, 29.4, 29.4, 29.3, 29.2, 29.2, 29.1, 29.0, 29.0, 29.0,

28.8, 24.6, 24.6, 23.9, 23.8, 23.7, 22.7, 22.6, 14.1, 14.1. HRMS (EI): calcd $C_{18}H_{34}O_3$ (M^+): 298.2508; measured: 298.2499.

Values are in accordance with literature.^e

dodecan-2-one (Scheme 4.3)

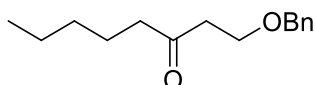


Was obtained as a clear oil (140 mg, 0.76 mmol, 76%) following the general procedure 3.

1H NMR: δ 2.39 (t, $J = 7.5$ Hz, 2H), 2.11 (s, 3H), 1.54 (p, $J = 7.3$ Hz, 2H), 1.30 – 1.15 (m, 14H), 0.86 (t, $J = 7.0$ Hz, 3H). ^{13}C NMR: δ 209.3, 43.8, 31.9, 29.8, 29.5, 29.4, 29.4, 29.3, 29.2, 23.8, 22.6, 14.1.

Spectral data were in accordance with a commercial sample.

1-(benzyloxy)octan-3-one (Table 4.3, Entry 1)

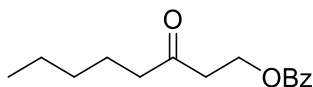


Was obtained in 71% yield (100 mg, 0.43 mmol) following general procedure 4 on a 0.6 mmol scale.

1H NMR (500 MHz, Chloroform- d): δ 7.42–7.19 (m, 5H), 4.51 (s, 2H), 3.74 (t, $J = 6.3$ Hz, 2H), 2.69 (t, $J = 6.3$ Hz, 2H), 2.43 (t, $J = 7.4$ Hz, 2H), 1.58 (p, $J = 7.2$ Hz, 2H), 1.39 – 1.18 (m, 4H), 0.88 (t, $J = 7.0$ Hz, 3H).

Values are in accordance with literature.^f

3-oxooctyl benzoate (Table 4.3, Entry 2)

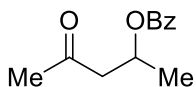


Was obtained in 80% yield (199 mg, 0.80 mmol) following general procedure 4 on a 1 mmol scale.

¹H NMR (500 MHz, Chloroform-d): δ 8.03–7.96 (m, 2H), 7.58–7.52 (m, 1H), 7.43 (t, J = 8.1 Hz, 2H), 4.59 (t, J = 6.4 Hz, 2H), 2.87 (t, J = 6.4 Hz, 2H), 2.47 (t, J = 7.4 Hz, 2H), 1.61 (p, J = 7.5 Hz, 2H), 1.35 – 1.21 (m, 4H), 0.88 (t, J = 7.0 Hz, 3H).

¹³C NMR (125 MHz, Chloroform-d): δ 208.1, 166.4, 133.0, 123.0, 129.6, 128.3, 60.0, 43.3, 41.4, 31.3, 23.3, 22.4, 13.9. HRMS (EI): calcd for C₁₅H₂₁O₃ (M⁺ + H): 249.1491; found 249.1484.

4-oxopentan-2-yl benzoate (Table 4.3, Entry 3)



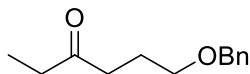
Was obtained in 80% yield (164 mg, 0.80 mmol) following general procedure 4 on a 1 mmol scale.

¹H NMR (500 MHz, Chloroform-d): δ 7.99 (dd, J = 8.4, 1.3 Hz, 2H), 7.56–7.50 (m, 1H), 7.44–7.39 (m, 2H), 5.53 (h, J = 6.3 Hz, 1H), 2.95 (dd, J = 16.3, 6.9 Hz, 1H), 2.69 (dd, J = 16.3, 6.0 Hz, 1H), 2.18 (s, 3H), 1.40 (d, J = 6.3 Hz, 3H).

^f *Tetrahedon. Lett* **52**, 2950.

Values are in accordance with literature.^g

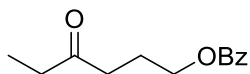
6-(benzyloxy)hexan-3-one (Table 4.3, Entry 4)



Was obtained in 80% yield (33 mg, 0.16 mmol, 9:1 mixture of regioisomers) following general procedure 4 on a 0.2 mmol scale. The isomers ratio was 6.5:1 in the crude reaction mixture as determined by ¹H-NMR.

¹H NMR (500 MHz, Chloroform-d, major): δ 7.31 (m, 5H), 4.48 (s, 2H), 3.48 (t, *J* = 6.1 Hz, 2H), 2.52 (t, *J* = 7.2 Hz, 2H), 2.42 (q, *J* = 7.3 Hz, 2H), 1.90 (p, *J* = 6.7 Hz, 2H), 1.04 (t, *J* = 7.3 Hz, 3H). ¹³C NMR (125 MHz, Chloroform-d, major): δ 211.4, 138.4, 128.4, 127.6, 127.6, 72.8, 69.4, 38.9, 36.0, 23.9, 7.8. HRMS (FAB): calcd for C₁₃H₁₉O₂ (M⁺ + H): 207.1385; found 207.1387.

4-oxohexyl benzoate (Table 4.3, Entry 5)



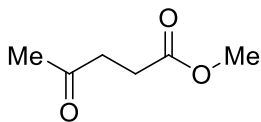
Was obtained in 83% yield (110 mg, 0.50 mmol, 10:1 mixture of regioisomers) following general procedure 4 on a 0.6 mmol scale.

¹H NMR (500 MHz, Chloroform-d): δ 8.03 (d, *J* = 3.0 Hz, 2H), 7.59–7.54 (m, 1H), 7.48–7.42 (m, 2H), 4.33 (t, *J* = 6.4 Hz, 2H), 2.58 (t, *J* = 7.2 Hz, 2H), 2.45 (q, *J* = 7.3 Hz, 2H), 2.12–2.02 (m, 2H), 1.06 (t, *J* = 7.3 Hz, 3H).

Values are in accordance with literature.^h

^g *Tetrahedron Lett.* 49, 3326.

methyl 4-oxopentanoate (Table 4.3, Entry 6)

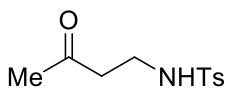


Was obtained in 70% yield (91 mg, 0.7 mmol) following general procedure 4 on a 1 mmol scale.

^1H NMR (500 MHz, Chloroform- d): δ 3.64 (s, 3H), 2.73 (t, J = 6.6 Hz, 2H), 2.54 (t, J = 6.6 Hz, 2H), 2.16 (s, 3H).

Values are in accordance with literature.ⁱ

4-methyl-N-(3-oxobutyl)benzenesulfonamide (Table 4.3, Entry 7)



Was obtained in 72% yield (173 mg, 0.72 mmol) following general procedure 4 on a 1 mmol scale.

^1H NMR (500 MHz, Chloroform- d): δ 7.72 (d, J = 8.3 Hz, 2H), 7.29 (d, J = 8.6 Hz, 2H), 5.22 (t, J = 6.5 Hz, 1H), 3.14 – 3.08 (m, 2H), 2.67 (t, J = 5.8 Hz, 2H), 2.41 (s, 3H), 2.09 (s, 3H).

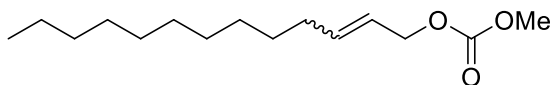
Values are in accordance with literature.^j

^h *Org. Lett.* 13, 4308.

ⁱ *Org. Lett.* 13, 3856.

^j *Tetrahedron* 53, 8887.

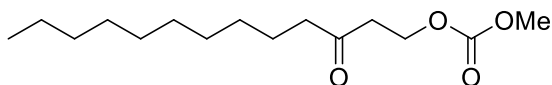
methyl tridec-2-enyl carbonate (Scheme 4.5)



Was obtained in 68% yield (350 mg, 1.37 mmol, 10:1 *E/Z*) following general procedure 5 on a 2 mmol scale using dodecene as the limiting alkene and allyl carbonate as the cross-partner (4 equiv).

^1H NMR (500 MHz, Chloroform-*d*, major): δ 5.85–5.76 (m, 1H), 5.62–5.53 (m, 1H), 4.61–4.52 (m, 2H), 3.78 (s, 3H), 2.05 (q, $J = 7.0$ Hz, 2H), 1.36 (m, 2H), 1.29 (m, 14H), 0.88 (t, $J = 7.0$ Hz, 3H). ^{13}C NMR (125 MHz, Chloroform-*d*, major): δ 155.7, 137.6, 123.0, 68.7, 54.7, 32.2, 31.9, 29.6, 29.6, 29.4, 29.3, 29.1, 28.8, 22.7, 14.1. HRMS (EI): calcd for $\text{C}_{15}\text{H}_{28}\text{O}_3$ (M^+): 256.2038; found 256.2035.

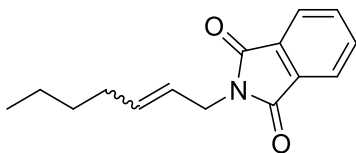
methyl 3-oxotridecyl carbonate (Scheme 4.5)



Was obtained in 80% yield (65 mg, 0.24 mmol) following general procedure 4 on a 0.3 mmol scale.

^1H NMR (500 MHz, Chloroform-*d*): δ 4.39 (t, $J = 6.3$ Hz, 2H), 3.77 (s, 3H), 2.77 (t, $J = 6.3$ Hz, 2H), 2.47–2.37 (m, 2H), 1.64–1.49 (m, 2H), 1.25 (d, $J = 7.2$ Hz, 14H), 0.87 (t, $J = 7.0$ Hz, 3H). ^{13}C NMR (125 MHz, Chloroform-*d*): δ 207.6, 155.5, 62.8, 54.8, 43.3, 41.2, 31.9, 29.5, 29.4, 29.4, 29.3, 29.1, 23.5, 22.7, 14.1. HRMS (EI): calcd for $\text{C}_{15}\text{H}_{29}\text{O}_4$ ($\text{M}+\text{H}^+$): 273.2066; found 273.2067.

2-(hept-2-enyl)isoindoline-1,3-dione (Scheme 4.5)

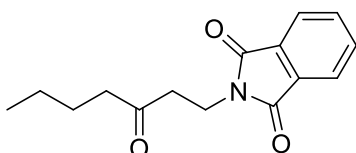


Was obtained in 70% yield (170 mg, 0.70 mmol, 7:1 *E/Z*) following general procedure 5 on a 1 mmol scale using allyl phthalimide as the limiting reagent and hexene as the cross-partner (5 equiv).

^1H NMR (500 MHz, Chloroform-*d*, major): δ 7.84 (dd, $J = 5.4, 3.0$ Hz, 2H), 7.70 (dd, $J = 5.5, 3.0$ Hz, 2H), 5.79–5.69 (m, 1H), 5.55–5.43 (m, 1H), 4.23 (dq, $J = 6.3, 1.0$ Hz, 2H), 2.00 (q, $J = 7.8$ Hz, 2H), 1.43–1.18 (m, 4H), 0.86 (t, $J = 7.2$ Hz, 3H).

^{13}C NMR (125 MHz, Chloroform-*d*, major): δ 168.0, 135.3, 133.8, 132.2, 123.2, 123.0, 39.6, 31.8, 31.0, 22.2, 13.9. HRMS (EI): calcd for $\text{C}_{15}\text{H}_{17}\text{O}_2\text{N}$ (M^+): 243.1259; found 243.1265.

2-(3-oxoheptyl)isoindoline-1,3-dione (Scheme 4.5)

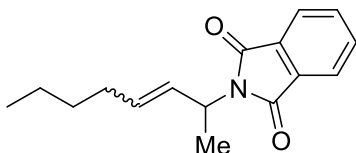


Was obtained in 77% yield (40 mg, 0.15 mmol) following general procedure 4 on a 0.2 mmol scale.

^1H NMR (500 MHz, Chloroform-*d*): δ 7.83 (dd, $J = 5.4, 3.0$ Hz, 2H), 7.70 (dd, $J = 5.5, 3.0$ Hz, 2H), 3.99–3.89 (m, 2H), 2.84 (dd, $J = 7.9, 7.0$ Hz, 2H), 2.46–2.38 (m, 2H), 1.59–1.51 (m, 2H), 1.34–1.25 (m, 2H), 0.88 (t, $J = 7.3$ Hz, 3H). ^{13}C NMR

(125 MHz, Chloroform-d): δ 208.2, 168.1, 134.0, 132.0, 123.2, 42.6, 40.5, 33.0, 25.7, 22.3, 13.8. HRMS (EI): calcd for $C_{15}H_{17}O_3N$ (M^+): 259.1208; found 259.1209.

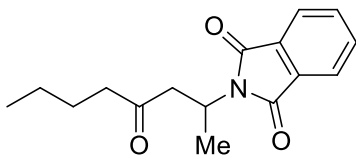
2-(oct-3-en-2-yl)isoindoline-1,3-dione (Scheme 4.5)



Was obtained in 78% yield (100 mg, 0.39 mmol, 10:1 *E/Z*) following general procedure 5 on a 0.5 mmol scale using 2-butenylphthalimide as the limiting reagent and hexene as the cross-partner (5 equiv).

1H NMR (500 MHz, Chloroform-d, major): δ 7.81 (dd, $J = 5.4, 3.0$ Hz, 2H), 7.69 (dd, $J = 5.5, 3.0$ Hz, 2H), 5.87 (ddt, $J = 15.4, 7.6, 1.5$ Hz, 1H), 5.67 (dtd, $J = 15.4, 6.7, 1.1$ Hz, 1H), 4.93–4.84 (m, 1H), 2.06–1.97 (m, 2H), 1.55 (d, $J = 7.1$ Hz, 3H), 1.36–1.25 (m, 4H), 0.87 (t, $J = 7.4$, 3H). ^{13}C NMR (125 MHz, Chloroform-d, major): δ 168.0, 133.8, 133.3, 132.1, 128.4, 123.0, 48.9, 31.8, 31.1, 22.2, 19.0, 13.9. HRMS (EI): calcd for $C_{16}H_{19}O_2N$ (M^+): 257.1416; found 257.1415.

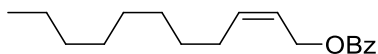
2-(4-oxooctan-2-yl)isoindoline-1,3-dione (Scheme 4.5)



Was obtained in 75% yield (30.6 mg, 0.11 mmol) following general procedure 4 on a 0.15 mmol scale. A single isomer was observed by crude NMR-analysis, accompanied by a small impurity that was not assigned to the minor regioisomer.

^1H NMR (500 MHz, Chloroform- d , major): δ 7.80 (dd, $J = 5.4, 3.1$ Hz, 2H), 7.69 (dd, $J = 5.5, 3.0$ Hz, 2H), 4.90–4.78 (m, 1H), 3.27 (dd, $J = 17.6, 8.1$ Hz, 1H), 2.96 (dd, $J = 17.6, 6.4$ Hz, 1H), 2.39 (td, $J = 7.5, 3.7$ Hz, 2H), 1.54–1.47 (m, 2H), 1.43 (d, $J = 6.9$ Hz, 3H), 1.30–1.22 (m, 2H), 0.85 (t, $J = 7.3$ Hz, 3H). ^{13}C NMR (125 MHz, Chloroform- d , major): δ 208.3, 168.2, 133.8, 131.9, 123.1, 45.7, 42.8, 42.5, 25.7, 22.2, 18.9, 13.8. HRMS (EI): calcd for $\text{C}_{16}\text{H}_{19}\text{O}_3\text{N}$ (M^+): 273.1365; found 273.1366.

(*Z*)-undec-2-enyl benzoate (Scheme 4.6)

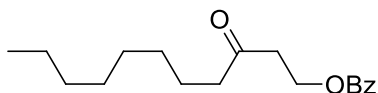


Was obtained in 71% yield (78 mg, 0.29 mmol, > 95% *Z*) following general procedure 6 at 35 °C on a 0.4 mmol scale using allyl benzoate as the limiting reagent.

^1H NMR (500 MHz, Chloroform- d): δ 8.05 (dd, $J = 7.9, 1.7$ Hz, 2H), 7.59 – 7.52 (m, 1H), 7.44 (t, $J = 7.6$ Hz, 2H), 5.69 (tq, $J = 11.2, 6.1, 5.1$ Hz, 2H), 4.87 (d, $J = 6.2$ Hz, 2H), 2.17 (q, $J = 7.1$ Hz, 2H), 1.39 (q, $J = 7.3$ Hz, 2H), 1.35–1.18 (m,

10H), 0.87 (t, $J = 6.7$ Hz, 3H). ^{13}C NMR (125 MHz, Chloroform- d): δ 166.6, 135.8, 132.9, 130.3, 129.6, 128.3, 123.2, 60.9, 31.9, 29.4, 29.4, 29.3, 29.2, 27.6, 22.7, 14.1. HRMS (FAB): calcd for $\text{C}_{18}\text{H}_{27}\text{O}_2$ ($\text{M}^+ + \text{H}$): 275.2011; found 275.2007.

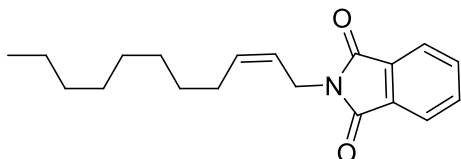
3-oxoundecyl benzoate (Scheme 4.6)



Was obtained in 71% yield (41 mg, 0.14 mmol) following general procedure 4 on a 0.2 mmol scale.

^1H NMR (500 MHz, Chloroform- d , major): δ 7.99 (dd, $J = 8.4, 1.4$ Hz, 2H), 7.57–7.52 (m, 1H), 7.45–7.39 (m, 2H), 4.59 (t, $J = 6.3$ Hz, 2H), 2.87 (t, $J = 6.3$ Hz, 2H), 2.46 (t, $J = 7.4$ Hz, 2H), 1.59 (m, 2H), 1.31–1.22 (m, 10H), 0.87 (t, $J = 6.9$ Hz, 3H). ^{13}C NMR (125 MHz, Chloroform- d , major): δ 208.1, 166.4, 133.0, 129.6, 128.3, 128.3, 60.0, 43.3, 41.4, 31.8, 29.3, 29.2, 29.1, 23.7, 22.6, 14.1. HRMS (FAB): calcd for $\text{C}_{18}\text{H}_{27}\text{O}_3$ ($\text{M}^+ + \text{H}$): 291.1960; found 291.1956.

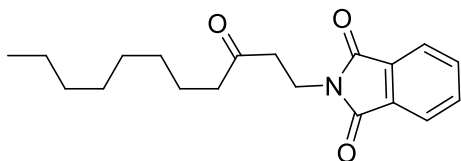
(*Z*)-2-(undec-2-enyl)isoindoline-1,3-dione (Scheme 4.6)



Was obtained in 62% yield (74 mg, 0.25 mmol, >95% *Z*) following general procedure 6 at RT on a 0.4 mmol scale using allyl phthalimide as the limiting reagent.

^1H NMR (500 MHz, Chloroform-d, major): δ 7.84 (dd, $J = 5.4, 3.1$ Hz, 2H), 7.70 (dd, $J = 5.5, 3.0$ Hz, 2H), 5.59 (dtt, $J = 10.4, 7.4, 1.4$ Hz, 1H), 5.50–5.42 (m, 1H), 4.31 (ddt, $J = 7.0, 1.4, 0.6$ Hz, 2H), 2.25 (qd, $J = 7.4, 1.6$ Hz, 2H), 1.44–1.36 (m, 2H), 1.36–1.21 (m, 10H), 0.91–0.85 (m, 3H). ^{13}C NMR (125 MHz, Chloroform-d, major): δ 168.0, 134.7, 133.9, 132.2, 123.2, 122.7, 34.9, 31.9, 29.5, 29.4, 29.3, 29.3, 27.4, 22.7, 14.1. HRMS (EI): calcd for $\text{C}_{19}\text{H}_{25}\text{O}_2\text{N}$ (M^+): 299.1885; found 299.1890.

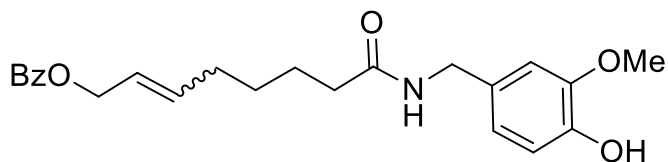
2-(3-oxoundecyl)isoindoline-1,3-dione (Scheme 4.6)



Was obtained in 79% yield (25 mg, 0.08 mmol) following general procedure 4 on a 0.1 mmol scale.

^1H NMR (500 MHz, Chloroform-d): δ 7.83 (dd, $J = 5.4, 3.0$ Hz, 2H), 7.71 (dd, $J = 5.5, 3.0$ Hz, 2H), 3.97–3.93 (m, 2H), 2.84 (dd, $J = 7.9, 7.0$ Hz, 2H), 2.42 (t, $J = 7.5$ Hz, 2H), 1.60–1.50 (m, 2H), 1.31–1.20 (m, 10H), 0.89–0.84 (m, 3H). ^{13}C NMR (125 MHz, Chloroform-d): δ 208.3, 168.1, 134.0, 132.0, 123.3, 42.9, 40.5, 33.0, 31.8, 29.3, 29.2, 29.1, 23.6, 22.6, 14.1. HRMS (EI): calcd for $\text{C}_{19}\text{H}_{25}\text{O}_3\text{N}$ (M^+): 315.1834; found 315.1822.

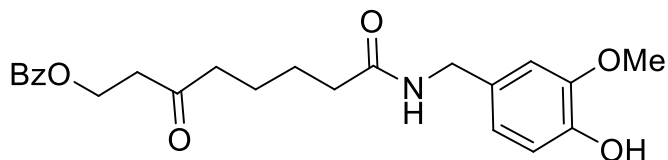
8-(4-hydroxy-3-methoxybenzylamino)-8-oxooct-2-enyl benzoate (Scheme 4.7)



Was obtained in 64% yield (84 mg, 0.21 mmol, *E/Z* 6:1) following general procedure 5 on a 0.33 mmol scale using capsaicin as limiting reagent and *cis*-dibenzoylbutenol (5 equiv) as cross-partner.

^1H NMR (500 MHz, Chloroform-*d*, major): δ 8.07–8.02 (m, 2H), 7.59–7.52 (m, 1H), 7.46–7.39 (m, 2H), 6.86 (d, $J = 8.0$ Hz, 1H), 6.81–6.74 (m, 2H), 5.86–5.79 (m, 1H), 5.73–5.61 (m, 3H), 4.75 (dq, $J = 6.3, 1.0$ Hz, 2H), 4.35 (d, $J = 5.6$ Hz, 2H), 3.86 (s, 3H), 2.21 (t, $J = 7.6$ Hz, 2H), 2.14–2.07 (m, 2H), 1.75–1.58 (m, 2H), 1.45 (tdd, $J = 9.9, 7.2, 5.6$ Hz, 2H). ^{13}C NMR (125 MHz, Chloroform-*d*, major): δ 172.6, 166.4, 146.7, 145.1, 135.8, 132.9, 130.3, 130.3, 129.6, 128.3, 124.3, 120.8, 114.3, 110.7, 65.6, 55.9, 43.5, 36.6, 32.0, 28.4, 25.2. HRMS (FAB): calcd for $\text{C}_{23}\text{H}_{28}\text{O}_5\text{N}$ (M^+): 398.1967; found 398.1966.

8-(4-hydroxy-3-methoxybenzylamino)-3,8-dioxooctyl benzoate (Scheme 4.7)

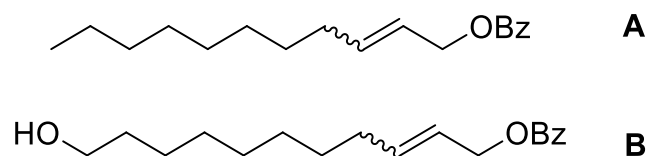


Was obtained in 78% yield (32 mg, 0.08 mmol, 20:1 mixture of isomers) following general procedure 4 on a 0.1 mmol scale.

^1H NMR (500 MHz, Chloroform-d, major): δ 8.01–7.95 (m, 2H), 7.54 (ddt, $J = 7.9$, 7.0, 1.3 Hz, 1H), 7.45–7.38 (m, 2H), 6.85 (d, $J = 8.0$ Hz, 1H), 6.79 (d, $J = 1.9$ Hz, 1H), 6.75 (dd, $J = 8.1$, 2.0 Hz, 1H), 5.86 (t, $J = 5.5$ Hz, 1H), 5.70 (s, 1H), 4.57 (t, $J = 6.3$ Hz, 2H), 4.33 (d, $J = 5.6$ Hz, 2H), 3.86 (s, 3H), 2.85 (t, $J = 6.3$ Hz, 2H), 2.51 (t, $J = 6.6$ Hz, 2H), 2.27–2.16 (m, 2H), 1.65 (m, 4H). ^{13}C NMR (125 MHz, Chloroform-d, major): δ 207.6, 172.3, 166.4, 146.7, 145.1, 133.1, 130.2, 129.9, 129.5, 128.4, 120.8, 114.4, 110.7, 59.9, 55.9, 43.6, 42.8, 41.5, 36.4, 25.0, 23.0. HRMS (FAB): calcd for $\text{C}_{23}\text{H}_{28}\text{O}_6\text{N}$ (M^+): 414.1917; found 414.1928.

(*E*)-undec-2-enyl benzoate (A) and (*E*)-11-hydroxyundec-2-enyl benzoate (B)

(Scheme 4.8)



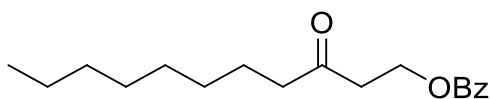
A and **B** were obtained in 62% yield (170 mg, 0.62 mmol, *E/Z* 7:1, **A**) and 63% yield (182 mg, 0.63 mmol, *E/Z* 8:1, **B**) following general procedure 5 on a 1 mmol scale using oleyl alcohol as limiting reagent and *cis*-dibenzoylbutenol (5 equiv) as cross-partner.

A: see below

B: ^1H NMR (500 MHz, Chloroform-d, major): δ 8.09–8.02 (m, 2H), 7.58–7.53 (m, 1H), 7.46–7.41 (m, 2H), 5.91–5.80 (m, 1H), 5.73–5.63 (m, 1H), 4.77 (dq, $J = 6.4$, 1.0 Hz, 2H), 3.64 (t, $J = 6.6$ Hz, 2H), 2.11–2.05 (m, 2H), 1.61–1.25 (m, 13H). ^{13}C NMR (125 MHz, Chloroform-d, major): δ 166.5, 136.6, 132.9, 130.4, 129.6,

128.3, 123.8, 65.8, 63.1, 32.8, 32.3, 29.4, 29.3, 29.1, 28.8, 25.7. HRMS (FAB):
calcd for C₁₈H₂₇O₃ (M⁺ + H): 291.1960; found 291.1965.

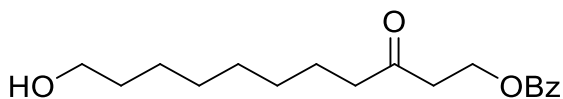
3-oxoundecyl benzoate (Scheme 4.8)



Was obtained in 78% yield (45 mg, 0.16 mmol) following general procedure 4 on a 0.2 mmol scale. Isomeric ratio was 20:1 by NMR-analysis of the crude.

¹H NMR (500 MHz, Chloroform-d): δ 7.99 (dd, *J* = 8.4, 1.4 Hz, 2H), 7.58–7.52 (m, 1H), 7.46–7.38 (m, 2H), 4.59 (t, *J* = 6.3 Hz, 2H), 2.87 (t, *J* = 6.3 Hz, 2H), 2.46 (t, *J* = 7.4 Hz, 2H), 1.60 (t, *J* = 7.3 Hz, 2H), 1.32 – 1.18 (m, 10H), 0.87 (t, *J* = 6.9 Hz, 3H). ¹³C NMR (125 MHz, Chloroform-d): δ 208.1, 166.4, 133.0, 129.6, 128.3, 128.3, 60.0, 43.3, 41.4, 31.8, 29.3, 29.2, 29.1, 23.7, 22.6, 14.1. HRMS (FAB):
calcd for C₁₈H₂₇O₃ (M⁺+H): 291.1960; found 291.1956.

11-hydroxy-3-oxoundecyl benzoate (Scheme 4.8)



Was obtained in 77% yield (47 mg, 0.15 mmol, *E/Z* 6:1) following general procedure 4 on a 0.2 mmol scale.

¹H NMR (500 MHz, Chloroform-d): 8.01–7.96 (m, 2H), 7.57–7.52 (m, 1H), 7.44–7.39 (m, 2H), 4.58 (t, *J* = 6.3 Hz, 2H), 3.62 (t, *J* = 6.6 Hz, 2H), 2.86 (t, *J* = 6.3 Hz, 2H), 2.46 (t, *J* = 7.4 Hz, 2H), 1.64–1.49 (m, 3H), 1.36–1.24 (m, 10H). ¹³C NMR

(125 MHz, Chloroform-d): δ 208.1, 166.4, 133.0, 123.0, 129.6, 128.3, 63.0, 60.0, 43.2, 41.4, 32.7, 29.3, 29.2, 29.0, 25.6, 23.6. HRMS (FAB): calcd for C₁₈H₂₇O₄ (M⁺+H): 307.1909; found 307.1919.

References

- (1) Siegel, H.; Eggersdorfer, M. *Ullmanns Encyclopedia of Industrial Chemistry*, Vol. 18, 6th ed. (Eds.: M. Bohnet), VCH, Weinheim, **2003**, p. 739.
- (2) Takeda, T. *Modern Carbonyl Olefination: Methods and Applications*, Wiley-VCH **2004**.
- (3) Grubbs, R. H. *Handbook of metathesis*, Wiley-VCH **2003**.
- (4) Chen, X.; Mihalic, J.; Fan, P.; Liang, L.; Lindstrom, M.; Wong, S.; Ye, Q.; Fu, Y.; Jaen, J.; Chen, J.-L.; Dai, K.; Li, L. *Bioorg. Med. Chem. Lett.* **2012**, *22*, 363.
- (5) Hudson, A. R.; Higuchi, R. I.; Roach, S. L.; Valdez, L. J.; Adams, M. E.; Vassar, A.; Rungta, D.; Syka, P. M.; Mais, D. E.; Marschke, K. B.; Zhi, L. *Bioorg. Med. Chem. Lett.* **2011**, *21*, 1654.
- (6) Sun, H.; Lu, J.; Liu, L.; Yi, H.; Qiu, S.; Yang, C.-Y.; Deschamps, J. R.; Wang, S. *J. Med. Chem.* **2010**, *53*, 6361
- (7) Dounay, A. B.; Humphreys, P. G.; Overman, L. E.; Wroblewski, A. D. *J. Am. Chem. Soc.* **2008**, *130*, 5368
- (8) Harrak, Y.; Barra, C. M.; Delgado, A.; Castano, A. R.; Llebaria, A. *J. Am.*

- Chem. Soc.* **2011**, *133*, 12079.
- (9) Tsuji, J. *Synthesis* **1984**, 369.
- (10) Cornell, C. N.; Sigman, M. S. *Org. Lett.* **2006**, *8*, 4117.
- (11) B. M. Trost, T. L. Calkins *Tetrahedron Lett.* **1995**, *36*, 6021.
- (12) Y. Sato, N. Saito, M. Mori, *J. Org. Chem.* **2002**, *67*, 9310.
- (13) S. B. Narute, N. C. Kiran, C. V. Ramana, *Org. Biomol. Chem.* **2011**, *9*, 5469.
- (14) Raffier, L.; Izquierdo, F.; Piva, O. *Synthesis* **2011**, 4037.
- (15) Lee, K.; Kim, H.; Hong, J. *Org. Lett.* **2009**, *11*, 5202;
- (16) Mukherjee, P.; Roy, S. J. S.; Sarkar, T. K. *Org. Lett.* **2010**, *12*, 2472.
- (17) T. Mitsudome, T.; Mizumoto, K.; Mizugaki, T.; Jitsukawa, K.; Kaneda, K. *Angew. Chem. Int. Ed.* **2010**, *49*, 1238.
- (18) Gligorich, K. M.; Sigman, M. S. *Chem. Commun.* **2009**, 3854.
- (19) Cornell, C. N.; Sigman, M. S. *Inorg. Chem.* **2007**, *46*, 1903
- (20) Hoover, J. M.; Stahl, S. S. *J. Am. Chem. Soc.* **2011**, *133*, 16901
- (21) Y. Fujiwara, Y.; Domingo, V.; Seiple, I. B.; Gianatassio, R.; Bel, M. D.; Baran, P. S. *J. Am. Chem. Soc.* **2011**, *133*, 3292.
- (22) Kwong, F. Y.; Buchwald, S. L. *Org. Lett.* **2002**, *4*, 3517.
- (23) Zhou, S.; Junge, K.; Addis, D.; Das, S.; Beller, M. *Org. Lett.* **2009**, *11*, 2461.
- (24) Mitsudome, T.; Umetani, T.; Nosaka, N. Mori, K.; Mizugaki, T.; Ebitani, K.; Kaneda, K. *Angew. Chem. Int. Ed.* **2006**, *45*, 481.

- (25) H. Grennberg, A. Gogoll, J.-E. Bäckvall, *Organometallics* **1993**, *12*, 1790.
- (26) D. G. Miller, D. D. M. Wayner, *J. Org. Chem.* **1990**, *55*, 2924.
- (27) D. G. Miller, D. D. M. Wayner, *Can. J. Chem.* **1992**, *70*, 2485.
- (28) J.-E. Bäckvall, R. B. Hopkins, *Tetrahedron Lett.* **1988**, *29*, 2885.
- (29) Wang, A.; Jiang, H. *J. Org. Chem.* **2010**, *75*, 2321.
- (30) Wang, J.-Q.; Cai, F.; Wang, E.; He, L.-N. *Green Chem.* **2007**, *9*, 882
- (31) Mori, A.; Lehmann, S.; O'Kelly, J.; Kumagai, T.; Desmond, J. C.; Pervan, M.; McBride, W. H.; Kizaki, M.; Koeffler, H. P. *Cancer Res.* **2006**, *66*, 3222
- (32) K. Ito, K.; Nakazato, T.; Yamato, K.; Miyakawa, Y.; Yamada, T.; Hozumi, N.; Segawa, K.; Ikeda, Y.; Kizaki, M. *Cancer Res.* **2004**, *64*, 1071.
- (33) Caterina, M. J.; Schumacher, M. A.; Tominaga, M.; Rosen, T. A.; Levine, J. D.; Julius, D. *Nature* **1997**, *389*, 816.
- (34) Piera, J.; Bäckvall, J.-E. *Angew. Chem. Int. Ed.* **2008**, *47*, 3506.
- (35) Bäckvall, J.-E.; Awasthi, A. K.; Renko, Z. D. *J. Am. Chem. Soc.* **1987**, *109*, 4750
- (36) Bäckvall, J.-E.; Hopkins, R. B.; Grennberg, H.; Mader, M. M.; Awasthi, A. K. *J. Am. Chem. Soc.* **1990**, *112*, 5160.
- (37) Decharin, N.; Stahl, S. S. *J. Am. Chem. Soc.* **2011**, *133*, 5732.
- (38) Hull, K. L.; Sanford, M. S. *J. Am. Chem. Soc.* **2009**, *131*, 9651
- (39) Chen, M. S.; Prabakaran, N.; Labenz, N. A.; White, M. C. *J. Am. Chem. Soc.* **2005**, *127*, 6970.
- (40) Bäckvall, J.-E.; Bystroem, S. E.; Nordberg, R. E. *J. Org. Chem.* **1984**, *49*,

4619.

- (41) Stahl, S. S. *Angew. Chem. Int. Ed.* **2004**, *43*, 3400.
- (42) Campbell, A. N.; Stahl, S. S. *Acc. Chem. Res.* **2012**, *45*, 851.
- (43) Carreira, E. M.; Kvaerno, L. *Classics in Stereoselective Synthesis* (Wiley-VCH, ed. 1, **2009**).
- (44) Dong, J. J.; Fañanás-Mastral, M.; Alsters, P. L.; Browne, W. R.; Feringa, B. L. *Angew. Chem. Int. Ed.* **2013**, *52*, 5561–5565.
- (45) B. W. Michel, B. W.; McCombs, J. R.; Winkler, A.; Sigman, M. S. *Angew. Chem. Int. Ed.* **2010**, *49*, 7312.
- (46) R. J. DeLuca, R. J.; Edwards, J. L.; Steffens, L. D.; Michel, B. W.; Qiao, X.; Zhu, C.; Cook, S. P.; Sigman, M. S. *J. Org. Chem.* **2013**, *78*, 1682
- (47) Morandi, B.; Wickens, Z. K.; Grubbs, R. H. *Angew. Chem. Int. Ed.* **2013**, *52*, 2944.
- (48) Rosebrugh, L. E.; Herbert, M. B.; Marx, V. M.; Keitz, B. K.; Grubbs, R. H. *J. Am. Chem. Soc.* **2011**, *135*, 1276.
- (49) Corma, A.; Iborra, S.; Velty, A. *Chem. Rev.* **2007**, *107*, 2411.
- (50) Beller, M. *Eur. J. Lipid Sci. Technol.* **2008**, *110*, 789.

CHAPTER 5

UNDERSTANDING AND MANIPULATING INNATE NUCLEOPALLADATION REGIOSELECTIVITY

The text in this chapter was reproduced in part with permission from:

Morandi, B.; Wickens, Z. K.; Grubbs, R. H. *Angew. Chem. Int. Ed.* **2013**, *52*, 2944–2948.

Copyright 2013 John Wiley and Sons

Lerch, M. M.; Morandi, B.; Wickens, Z. K.; Grubbs, R. H. *Angew. Chem. Int. Ed.* **2014**, *53*, 8654–8658.

Copyright 2014 John Wiley and Sons

Abstract

Inductive effects were identified as important factors in controlling innate regioselectivity in the Wacker-type oxidation of internal alkenes. A systematic study of electronically differentiated internal alkene substrates initially suggested to us that alkene electronics substantially influence regioselectivity. To further investigate this hypothesis, the ability of non-coordinating, inductively withdrawing trifluoromethyl groups to be effective directing groups for Wacker-type oxidations was evaluated. Despite being incapable of strong coordination to the palladium center, trifluoromethyl groups were extraordinarily effective in controlling Wacker regioselectivity. Next, a series of sterically and electronically differentiated oxygen directing groups were shown to provide predictable selectivity purely on the basis of electronic variation. The understanding of innate selectivity developed over the course of these studies led to the discovery of Wacker oxidation conditions capable of maintaining high Markovnikov selectivity even with classically challenging substrates.

Introduction

In stark contrast to the high Markovnikov selectivity observed with unfunctionalized terminal alkenes, allylic functional groups diminish selectivity and often result in mixtures of aldehyde and methyl ketone products. Further discussion of this effect was provided in Chapter 1 and is the subject of a well-written and detailed review.¹ Due to the potential involvement of a variety of

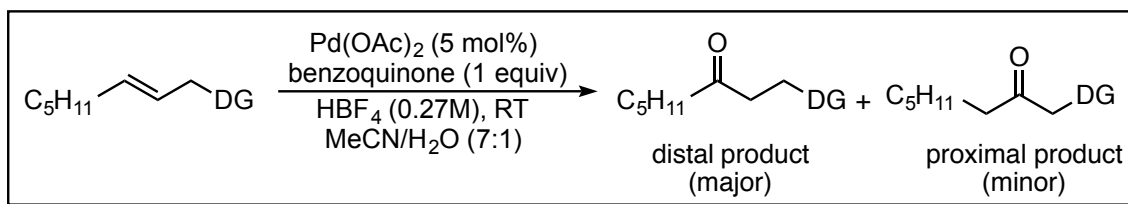
substrate-derived influences (e.g., electronic and steric effects or coordination to palladium) selectivity can be extraordinarily difficult to predict *a priori*, much less control.^{1,2} Coordination of proximal heteroatoms to the palladium center is most frequently invoked to explain the disruption of the expected Markovnikov selectivity.^{1,3-8} However, consideration of the relative Lewis basicity of proximal functional groups is insufficient to qualitatively predict regiochemical outcomes of new substrates. By improving our understanding of the factors that contribute to innate regioselectivity in Wacker-type oxidations, we can ultimately develop catalytic systems that are controlled primarily by one specific contributing factor (i.e., electronegativity, Lewis basicity, etc.).⁹ Ideally, such transformations would retain the practicality and generality of the traditional Tsuji–Wacker conditions.^{10,11}

Direct deconvolution of the factors contributing to the regioselectivity in Wacker-type oxidations of allylic functionalized alkenes has been particularly challenging due to the inherent steric and electronic asymmetry of terminal alkenes. While internal olefins would avoid this bias, this class of substrates exhibits initial reactivity under Tsuji–Wacker conditions. One notable exception to this limitation is the β -methylstyrene subclass. Prior to the current studies, Spencer and coworkers exploited these moderately activated substrates to illustrate that the nucleopalladation regioselectivity in Wacker-type oxidations had an electronic component.¹² However, due to the potential for an η^3 -benzylpalladium intermediate,^{13,14} drawing conclusions from these results outside

of the context of styrenyl substrates is difficult. However, in the mechanistically related Heck reaction, nucleopalladation has been demonstrated to be strongly influenced by alkene electronics.^{15,16} In Chapter 4, the development of a highly efficient and general catalytic system for the Wacker-type oxidation of internal alkenes was outlined.^{17,18} Below, the use of this new catalytic system to probe mechanistic features of regiocontrol in Wacker oxidations is reported and discussed.

Results and Discussion

For our initial experiments, we took advantage of the synthetic flexibility offered by an allylic benzoate group to qualitatively study the electronic effects of the substituents on the reaction outcome. Competition experiments were performed between the unfunctionalized benzoate derivative and the corresponding 4-NO₂ and 4-MeO derivatives. The relative rates followed the order NO₂ < H < MeO and the product selectivity was inversely proportional to rate (Scheme 5.1). This long-range electronic effect suggests the significant build-up of a positive charge in the transition state.¹⁹ While we initially anticipated the regioselectivity might be chelation controlled,^{5,6} the increased selectivity obtained using the NO₂-substituent indicates that the regioselectivity of the process has a significant inductive component. An inductive model is also consistent with the selectivity obtained with the more electron withdrawing benzoate as compared to the allylic benzyl protected alcohol.

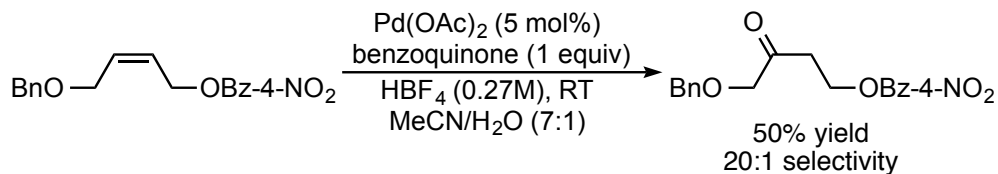


DG = Directing Group		>		>		>	
Selectivity	28:1		20:1		16:1		9:1
Relative rate	1	<	2	<	2.4	<	7.0

Scheme 5.1 Qualitative study of the role of directing group

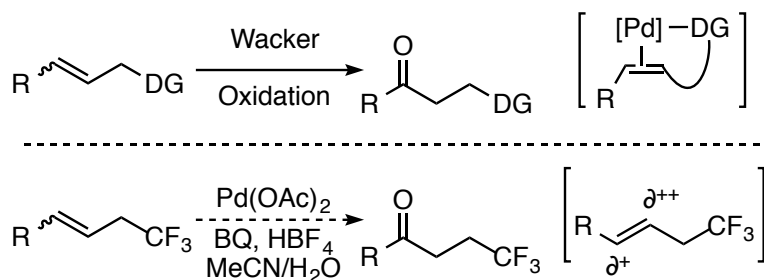
electronics on regioselectivity and relative rate.

To further probe the effect of electron density on the relative oxidation rate, an intramolecular competition experiment using a substrate bearing both an allylic OBn and an allylic 4-NO₂-BzO was performed (Scheme 5.2). The product from the oxidation of the most electron-rich position (distal to the 4-NO₂-BzO group), was oxidized with greater than 20:1 regioselectivity. This outcome supplements the results of the intermolecular experiments and demonstrates that protecting-group selection can enable selective oxidation, even when potentially competing directing groups are proximal to the alkene. Benzoyl and benzyl groups are orthogonal protecting groups, and thus, this result will have significant implications in target-oriented synthesis.



Scheme 5.2 intramolecular competition experiments.

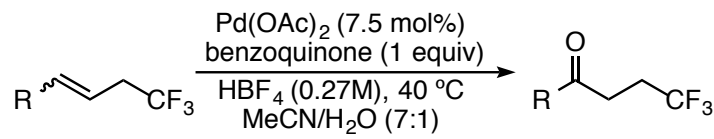
Coordination to the palladium center is frequently postulated to be the source of the regiochemical influence exhibited by proximal polar functional groups. Although the results discussed thus far in this chapter are suggestive of an inductive influence on regioselectivity, the oxygen-based functional groups examined are also capable of coordination to the palladium center and alternative hypotheses are difficult to eliminate. In contrast, trifluoromethyl groups are relatively non-coordinating and their influence on regioselectivity remains to be established. If inductive effects alone were sufficient to engender high selectivity, trifluoromethyl groups could enable the highly regioselective oxidation of internal alkenes at the distal position despite the lack of chelation-assistance (Scheme 5.3).

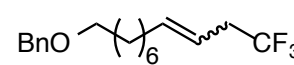
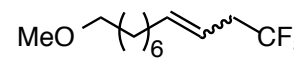
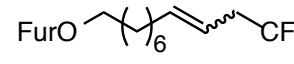
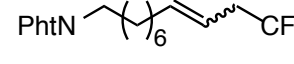
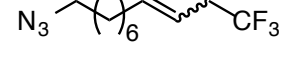
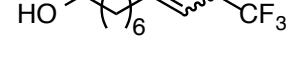
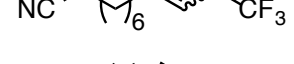
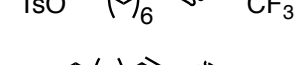
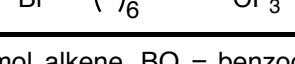


Scheme 5.3 Regiocontrol in Wacker oxidations of internal alkenes. BQ = benzoquinone; DG = coordinating directing group

After a brief survey of reaction conditions, the dicationic Wacker-type oxidation conditions were found to provide good conversions and excellent regioselectivities with allylic trifluoromethyl substituted alkenes. Under these conditions, a variety of alkenes bearing allylic trifluoromethyl groups could be oxidized in 70–91% yield. As predicted by the inductive hypothesis, each example exhibited excellent ($\geq 20:1$) regioselectivity for the distal oxidation product (Table 5.1). Relative to previously examined internal alkenes, the trifluoromethyl substituted alkene substrates exhibited lower reactivity and thus required increased temperature (40 °C) and catalyst loading (7.5 mol%). This is consistent with our observations regarding the influence of electronics on reaction rate (Scheme 5.1). The newly developed protocol tolerates a variety of synthetically useful alcohol protecting groups (entry 1 to 3) and amine precursors (entry 4 and 5). Even alkenes containing unprotected alcohols (entry 6) could be chemoselectively oxidized. The excellent functional group tolerance of this reaction was further demonstrated by its compatibility with nitriles (entry 7), tosylates (entry 8) and primary alkyl halides (entry 9). In all cases, selectivities of $\geq 20:1$ (distal:proximal) were obtained and further establish the powerful directing effect of the trifluoromethyl group in Wacker-type oxidations of internal alkenes.

Table 5.1 Substrate scope for the CF₃-directed Wacker Oxidation.^a



Entry	Substrate ^b	Yield ^c	Selectivity ^d
1 ^e		72	≥95:5
2		91	≥95:5
3		75	≥95:5
4		85	≥95:5
5		77	≥95:5
6		84	≥95:5
7		75	≥95:5
8		82	≥95:5
9 ^f		74	≥95:5

^a0.25 mmol alkene, BQ = benzoquinone ^b*E/Z*-ratio between 5:1–10:1; ^cisolated yields; ^dSelectivity = ratio of distal oxidation to proximal oxidation, as determined by ¹⁹F- and ¹H-NMR analysis of the crude reaction mixture; ^e0.5 mmol alkene ^f0.21 mmol alkene. PhtN = phthalimide; Fur = 2-furoyl.

Next, we sought to probe the directing power of the trifluoromethyl group relative to classical Wacker directing groups. For direct comparison, substrates with an allylic trifluoromethyl group and an allylic directing group (–OBn, –OBz, –OFur) on opposite sides of the alkene were synthesized and tested. However, these substrates underwent oxidation in very low conversion, presumably due to

the electron deficiency of the alkene. Thus, we designed and executed an alternative series of intramolecular competition experiments in order to compare the influence of functional groups proximal to the double bond (Figure 5.2). To more precisely evaluate the influence of the trifluoromethyl group on the observed selectivities, we additionally probed substrates bearing a non-directing alkyl group in place of the trifluoromethyl group. In each of the investigated cases, the replacement of an alkyl substituent with a trifluoromethyl group led to an inversion of selectivity, demonstrating that the predominantly inductive trifluoromethyl group can override the regioselectivity induced by traditional coordinating groups. These competition experiments thus further illustrate the powerful directing ability of the trifluoromethyl group for the synthesis of valuable fluorinated products. Moreover, these observations offer a platform to predict the regioselectivity of Wacker-type oxidations of internal alkenes bearing potentially competing directing groups, which is critical for the adoption of this oxidation methodology in target-oriented synthesis.

BzO			BnO			PhtN		
R	Selectivity	Yield	R	Selectivity	Yield	R	Selectivity	Yield
Me	9: 91	83%	Me	13: 87	80%	C ₇ H ₁₅	33: 66	77%
CF ₃	94 :6	53%	CF ₃	≥95 :5	79%	CF ₃	95 :5	51%

Figure 5.2 Intramolecular competition experiments between a traditional coordinating directing group and the purely inductive trifluoromethyl directing group. See Table 5.1 for oxidation conditions. PhtN = phthalimide.

To probe the distance dependence of the observed directing effects, a series of alkenes bearing trifluoromethyl groups at increasing distance from the alkene were subjected to the catalytic conditions (Table 5.2). When the distance from the site of unsaturation was increased, the selectivity for the distal oxidation decreased steadily in accordance with an inductive model. The synthetically useful selectivity (84:16) obtained with a homoallylic trifluoromethyl-substituted substrate (entry 2) illustrates the applicability of this strategy to prepare γ -trifluoromethyl-substituted ketones. Even a trifluoromethyl group four bonds away from the alkene (entry 3) exerts an appreciable influence on regioselectivity (66:34).

Table 5.2 Distance-dependence of the CF₃-directed Wacker Oxidation.^a

Entry	Substrate	Yield ^b	Selectivity ^c
1 ^{d,e}	Br-CH ₂ -CH ₂ -CH ₂ -CH ₂ -CH ₂ -CH=CH-CF ₃	74	≥95:5
2 ^f	Br-CH ₂ -CH ₂ -CH ₂ -CH=CH-CH ₂ -CH ₂ -CF ₃	86	84:16
3 ^g	Br-CH ₂ -CH ₂ -CH ₂ -CH=CH-CH ₂ -CH ₂ -CH ₂ -CF ₃	74	66:34

^a0.1 mmol alkene, BQ = benzoquinone; ^bIsolated yields; ^cSelectivity = ratio of distal oxidation to proximal oxidation, as determined by ¹⁹F- and ¹H-NMR analysis of the crude reaction mixture; ^d0.21 mmol alkene, see Table 1, entry 10; ^eE/Z-ratio 5:1; ^fE/Z-ratio 1:6; ^gE/Z-ratio 1:16.

Having demonstrated that inductive effects alone were capable of greatly impacting nucleopalladation regioselectivity using allylic trifluoromethyl substrates, we returned to 1,2-disubstituted allylic alcohol derivatives for a systematic study aiming to understand whether coordination plays a significant role in such substrates or whether the selectivity can be explained purely on the basis of inductive effects.

The difference in ^{13}C shift between the two unsaturated carbon atoms has been established as a means to estimate changes in ground state electronics due to the inductive effect.²⁰⁻²³ Thus, if inductive effects are the dominant factor influencing selectivity, comparison of the difference in alkene carbon shifts to observed selectivity might offer a practical mnemonic for predicting selectivity *a priori*. Indeed, we found that the difference in alkene ^{13}C signals correlated strongly ($R^2 = 0.99$) with Wacker selectivity using a Brønsted acid free variant of the Wacker-type oxidation developed in Chapter 4 (Figure 5.3).²⁴ Importantly, although the carbon skeleton of the substrate remained the same throughout each substrate, the oxygen-based directing group structure was significantly varied (silyl ethers, aryl ethers, alkyl ethers and esters). If coordination to palladium were a significant factor, this steric and conformational variation would be expected to have substantial effects upon selectivity that would not be reflected in a simple $\Delta^{13}\text{C}$ model. Thus, these results are inconsistent with a significant influence of coordination to palladium on regioselectivity and, as an alternative, suggest that inductive effects are highly influential.

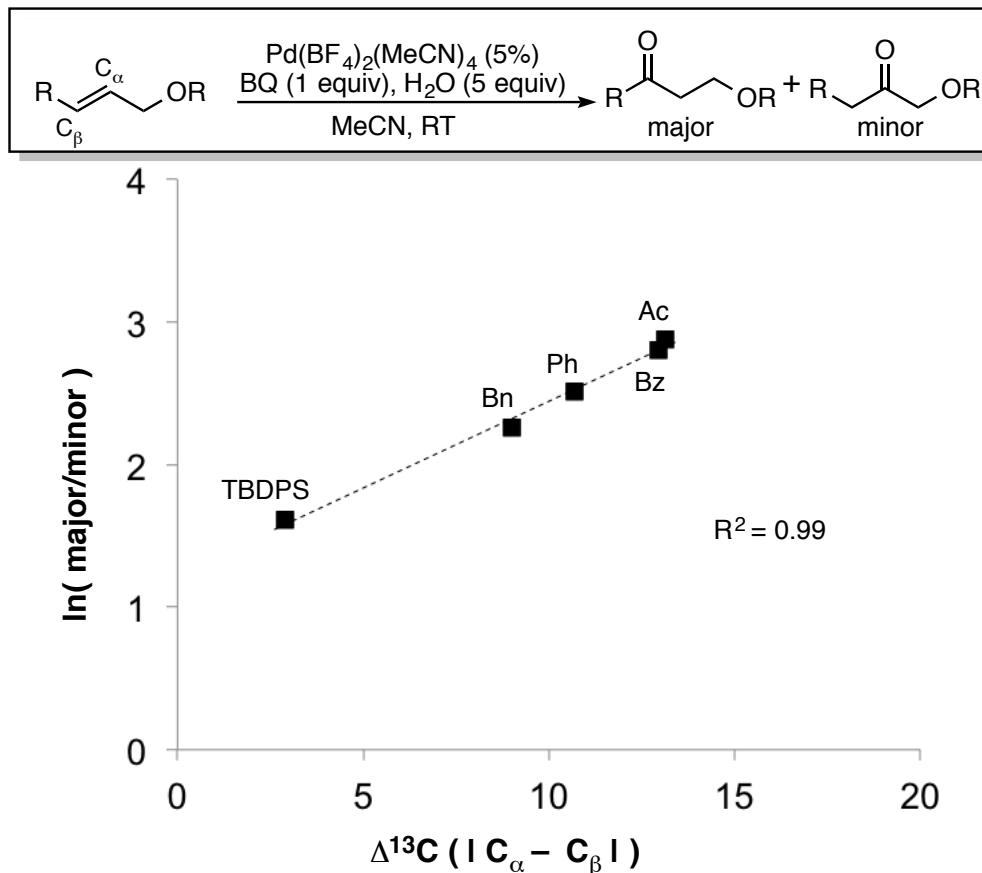


Figure 5.3 Correlation between inductive effects (as estimated by alkene ^{13}C chemical shifts) and selectivity in the oxidation of internal alkenes.

To further support a largely inductive explanation for selectivity, the best fit line generated from this dataset predicts the experimental results observed in Table 5.2 with reasonable accuracy (42:1 selectivity predicted for entry 1 and 6.4:1 selectivity predicted for entry 2). Thus, despite replacement of the potentially coordinating oxygen atom with a purely inductive trifluoromethyl group, a similar model is qualitatively accurate. Overall, although alternative explanations cannot

be discarded, these results are consistent with predominantly inductively controlled oxidation regioselectivity.

Based on these results, we suggest that under these modified Wacker conditions, the oxidation occurs at the position most able to stabilize a cationic transition state and other factors play a minimal role in influencing regioselectivity. To evaluate this hypothesis we subjected five structurally and electronically diverse allylic alcohol derivatives to the reaction conditions (Figure 5.4).

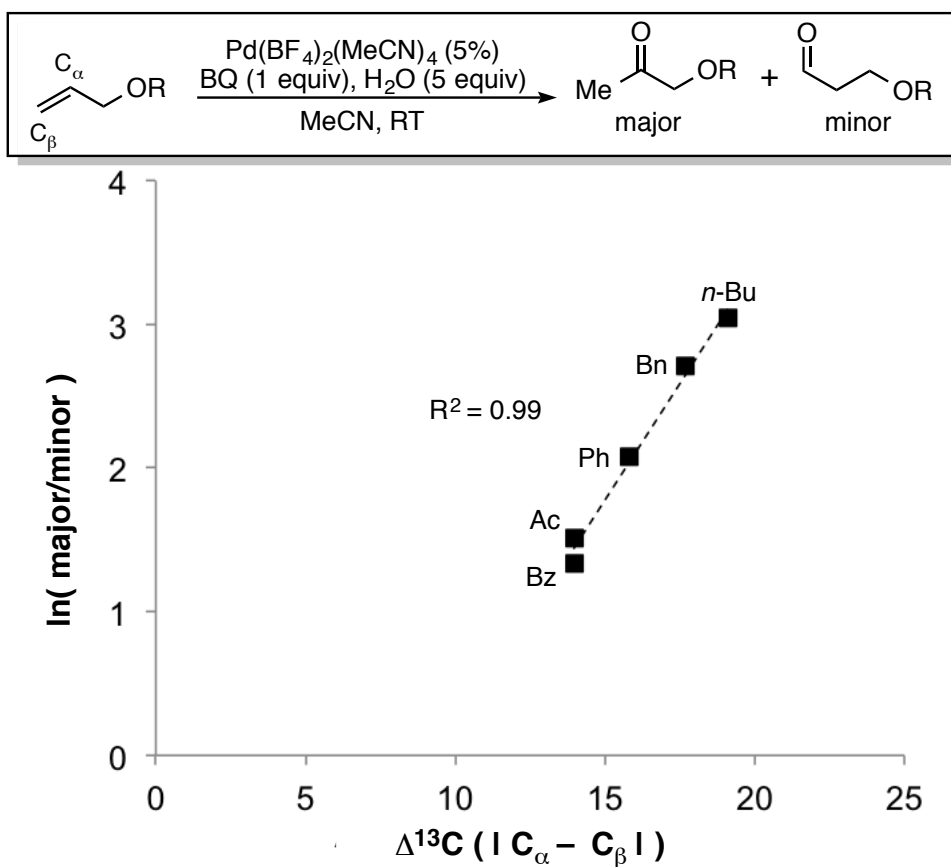


Figure 5.4 Correlation between inductive effects (as estimated by alkene ^{13}C chemical shifts) and selectivity in the oxidation of terminal alkenes.

As anticipated based on the results presented in Figure 5.3, $\Delta^{13}\text{C}$ was strongly correlated with selectivity in this subset of terminal alkenes. Importantly, although the selectivity is clearly dependent upon substrate identity, the catalyst system emphasizes Markovnikov selectivity (all substrates in this series $\geq 80:20$) and the selectivity is predictable on the basis of electronic effects.

Due to its operational simplicity, inexpensive reagents and predictable Markovnikov selectivity, this methodology will be a valuable complementary method to the catalyst controlled ketone-selective Wacker developed by Sigman and co-workers.⁸ Thus, we have begun to explore the substrate scope of the transformation (Table 5.4).

Table 5.3 Initial substrate scope with functionalized alkenes

Entry	Substrate	Yield (%) ^b	Selectivity ^c
1		88	89:11
2		83	80:20
3 ^d		76	82:18
4		87	94:6
5 ^d		86	95:5
6		90	95:5
7		91	94:6

^a0.5 mmol alkene, 2 hours; ^bIsolated yield
^cselectivity = ratio of ketone to aldehyde ^dYield determined by ¹H NMR analysis of the crude reaction mixture

Conclusion

Overall, the results in this chapter further our understanding of the regioselectivity of nucleopalladation events and have led to improved predictability in the Wacker oxidation of unsymmetrical olefins. These insights have led to the development of a catalytic system capable of enforcing unusually high Markovnikov selectivity in substrates that have previously provided poor regioselectivity in Wacker-type oxidations. This detailed understanding of the factors contributing to innate Wacker selectivity will continue to prove highly valuable in developing methods aiming to manipulate nucleopalladation regioselectivity in Wacker-type oxidations by modification of the catalytic system.

Experimental Section

Materials and methods

General Reagent Information: Preparation of non-commercial substrates: Unless stated otherwise, all reactions except for the Wacker oxidations were carried out in oven- and flame-dried glassware (200 °C) using standard Schlenk techniques and were run under argon atmosphere. Wacker oxidations were carried out without exclusion of air. The reaction progress was monitored by TLC. Starting materials and reagents were purchased from *Sigma Aldrich, Acros, Fluka, Fischer, TCI or Synquest Laboratories* and were used without further purification, unless stated otherwise. Solvents for the reactions were of quality

puriss., p.a. of the companies *Fluka* or *J.T. Baker* or of comparable quality. Anhydrous solvents were purified by passage through solvent purification columns. For aqueous solutions, deionized water was used.

General Analytical Information: Nuclear Magnetic Resonance spectra were measured with a *Varian-Inova 500* spectrometer (500 MHz), a *Varian-Inova 400* spectrometer (400 MHz), or a *Varian-Mercury Plus 300* spectrometer (300 MHz). The solvent used for the measurements is indicated. All spectra were measured at room temperature (22–25 °C). Chemical shifts for the specific NMR spectra were reported relative to the residual solvent peak [CDCl_3 : $\delta_{\text{H}} = 7.26$; CDCl_3 : $\delta_{\text{C}} = 77.16$]. The multiplicities of the signals are denoted by *s* (singlet), *d* (doublet), *t* (triplet), *q* (quartet), *p* (pentet) and *m* (multiplet). The coupling constants *J* are given in Hz. All ^{13}C -NMR spectra are ^1H -broadband decoupled, unless stated otherwise. High-resolution mass spectrometric measurements were provided by the California Institute of Technology Mass Spectrometry Facility using a JEOL JMS-600H High Resolution Mass Spectrometer. The molecule-ion M^+ , $[\text{M} + \text{H}]^+$, and $[\text{M}-\text{X}]^+$, respectively, or the anion are given in *m/z*-units.

General Considerations: Thin Layer Chromatography analyses were performed on silica gel coated glass plates (0.25 mm) with fluorescence-indicator UV_{254} (*Merck*, TLC silica gel 60 F_{254}). For detection of spots, UV light at 254 nm or 366 nm was used. Alternatively, oxidative staining using aqueous basic

potassium permanganate solution (KMnO₄) was performed. Flash column chromatography was conducted with *Silicagel 60* (Fluka; particle size 40–63 μM) at 24 °C and 0–0.3 bar excess pressure (compressed air) using Et₂O/pentane unless state otherwise.

General procedures

General procedure (1) for the Wacker-type oxidation of internal alkenes bearing allylic trifluoromethyl directing groups: A resealable 8-mL vial equipped with a magnetic stir bar and Teflon septum was charged (under air) with palladium acetate (4.2 mg, 0.02 mmol, 7.5 mol%) and benzoquinone (27 mg, 0.25 mmol, 1.0 eq.). A mixture of MeCN (1.10 mL) and water (0.16 mL) was added, followed by the addition of aqueous HBF₄ (0.045 mL, 0.35 mmol, 48% in water). The corresponding substrate (0.25 mmol, 1.0 eq.) was added and the homogeneous, dark red reaction mixture was stirred for 24 h at 40 °C. The crude reaction mixture was diluted with sat. aq. NaCl solution (7.5 mL) and extracted with CH₂Cl₂ (3x7.5 mL). The combined organic phases were dried over Na₂SO₄, filtered and concentrated *in vacuo*. NMR-analysis of the crude mixture was performed to determine the regioselectivity of the process. The crude product was then further purified by flash column chromatography on silica gel using pentane/Et₂O as eluent to furnish the desired pure product.

General Procedure (2) for cross-metathesis reactions using the Grubbs 2nd

generation catalyst: An oven-dried resealable 20-mL vial equipped with a magnetic stir bar and Teflon septum was charged with the corresponding limiting alkene substrate (1.0 mmol, 1.0 eq.) and the excess cross-partner (5.0 mmol, 5.0 eq.) and dissolved in anhydrous CH₂Cl₂ (2.5 mL) and put under argon atmosphere (argon balloon). Then Grubbs 2nd generation catalyst (31.3 mg, 0.05 mmol, 5 mol%) was added. The reaction mixture was stirred for 20 h at 40°C and was then quenched by addition of ethyl vinyl ether (few drops).

The solvent was evaporated and the *E/Z* ratio was determined by NMR-analysis of the crude reaction mixture. The crude product was then further purified by flash column chromatography on silica gel using pentane/Et₂O as eluent.

General Procedure (3) for the oxidation of terminal alkenes bearing

directing groups (isolation): Pd(MeCN)₄(BF₄)₂ (22.2 mg, 0.05 mmol, 5 mol%) and benzoquinone (108 mg, 1.00 mmol) were charged in a resealable 20-mL vial under air. MeCN (4.5 mL) was added, followed by the addition of water (90 μL, 5 mmol). After the addition of the corresponding substrate (1.00 mmol), the homogenous reaction mixture was stirred for 2 h at room temperature. The crude reaction mixture was then diluted with brine (30 mL) and extracted with CH₂Cl₂ (3x30 mL). The combined organic phases were then dried over Na₂SO₄, filtered, and evaporated *in vacuo*. NMR-analysis of the crude mixture was performed to

determine the regioselectivity of the process. The crude product was then further purified by column chromatography on silica gel using pentane/ether as eluent.

Intermolecular Competition Experiments

Three competition experiments were run using 5 mol% palladium and only 10 mol% benzoquinone to ensure only low conversions to be achieved. A 1:1 ratio of competing substrates was used, and after two hours the ratio of products was determined by analysis of the proton NMR. Results:

MeO vs H: **1.2 to 1**

NO₂ vs H: **0.5 to 1**

MeO vs NO₂: **2.4 to 1**

OBz vs OBn **1 to 3.5**

OBn vs CH₂OBz **1 to 2.2** (therefore CH₂OBz is 2.2*3.5 = 7.7 faster than OBz)

Intramolecular Competition Experiment

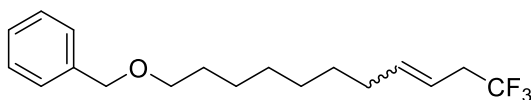


Palladium acetate (0.01 mmol, 5 mol%) and benzoquinone (21.6 mg, 0.2 mmol, 1 equiv) were charged in a resealable resealable 4-mL vial under air. A mixture of MeCN (0.9 mL) and water (126 μ L) was added, followed by the addition of aqueous HBF₄ (36 μ L, 48% in water, 0.28 mmol). After the addition of the substrate (0.2 mmol), the homogenous reaction mixture was stirred for 16 h at

room temperature. The crude reaction mixture was then diluted with brine (30 mL) and extracted with CH₂Cl₂ (3x30 mL). The combined organic phases were then dried over Na₂SO₄, filtered, and evaporated *in vacuo*. NMR-analysis of the crude mixture was performed to determine an isomeric ratio of 31:1 (major, triplet next to 4-NO₂BzO: 4.62; minor, triplet next to OBn: 3.77). The crude product was then further purified by column chromatography on silica gel using pentane/ether as eluent and the oxidized product obtained in 50% yield (34.3 mg, 0.1 mmol).

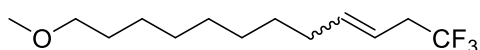
¹H NMR (500 MHz, Chloroform-d, major): δ 8.26 (d, *J* = 9.0 Hz, 2H), 8.15 (d, *J* = 9.0 Hz, 2H), 7.39 – 7.32 (m, 5H), 4.66 (t, *J* = 6.2 Hz, 2H), 4.61 (s, 2H), 4.11 (s, 2H), 3.02 (t, *J* = 6.2 Hz, 2H). ¹³C NMR (125 MHz, Chloroform-d, major): δ 205.8, 164.5, 150.6, 136.8, 135.3, 130.7, 128.6, 128.2, 127.9, 123.8, 75.2, 73.5, 60.3, 38.0. HRMS (EI): calcd for C₁₈H₁₈NO₆ (M + H⁺): 344.1134; found 344.1121.

Alkene Syntheses

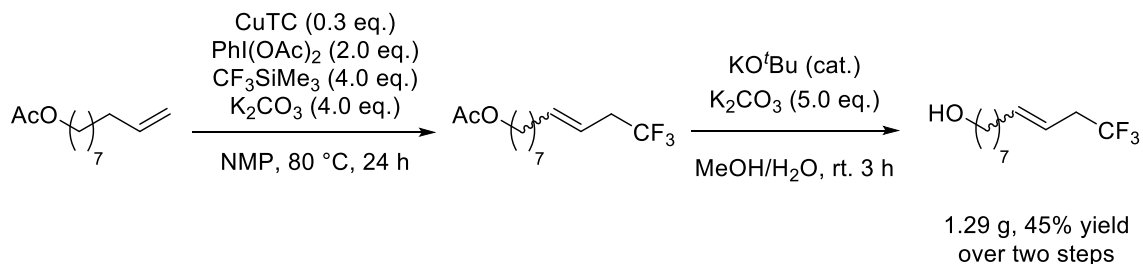


(((11,11,11-trifluoroundec-8-en-1-yl)oxy)methyl)benzene: prepared according to a reported protocol.²⁵ Purification by flash column chromatography (SiO₂, Et₂O/pentane) afforded the product (1.40 g, 60% yield): ***E/Z*-ratio:** 6.7:1; ***E*-isomer:** ¹H NMR (500 MHz, CDCl₃) δ = 7.38 – 7.26 (m, 5H), 5.73 – 5.65 (m, 1H), 5.36 (dt, *J*=15.5, 7.1, 1.5, 1H), 4.50 (s, 2H), 3.46 (t, *J*=6.6, 2H), 2.89 – 2.68 (m, 2H), 2.10 – 2.00 (m, 2H), 1.61 (dq, *J*=7.9, 6.6, 2H), 1.42 – 1.25 (m, 8H); ¹³C NMR (126 MHz, CDCl₃) δ = 138.82, 138.57, 128.48, 127.76, 127.62, 126.21 (q,

$J=276.4$), 117.62 (q, $J=3.6$), 73.01, 70.61, 37.52 (q, $J=29.4$), 32.59, 29.88, 29.39, 29.12, 28.96, 26.27; ^{19}F NMR (376 MHz, CDCl_3) $\delta = -66.77$ (t, $J=10.8$); HRMS (FAB+): Calcd. for $\text{C}_{18}\text{H}_{24}\text{OF}_3$ $[(\text{M} + \text{H}) - \text{H}_2]^+$: 313.1779; found 313.1774.



1,1,1-trifluoro-12-methoxydodec-3-ene: prepared according to a reported protocol.²⁵ Purification by flash column chromatography (SiO_2 , EtOAc/pentane) afforded the product (1.61 g, 68% yield): **E/Z-ratio**: 8.3:1; **E-isomer**: ^1H NMR (300 MHz, CDCl_3) $\delta = 5.69$ (dt, $J=15.2, 6.7$, 1H), 5.35 (dt, $J=15.5, 7.0, 1.5$, 1H), 3.36 (t, $J=6.7$, 2H), 3.33 (d, $J=0.6$, 3H), 2.75 (dtdd, $J=12.0, 9.8, 7.0, 1.1$, 2H), 2.04 (q, $J=6.6$, 2H), 1.62 – 1.50 (m, 2H), 1.43 – 1.23 (m, 10H); ^{13}C NMR (126 MHz, CDCl_3) $\delta = 138.54, 126.21$ (q, $J=276.4$), 117.61 (q, $J=3.5$), 73.05, 58.57, 37.49 (q, $J=29.5$), 32.58, 29.78, 29.54, 29.49, 29.09, 29.01, 26.25; ^{19}F NMR (282 MHz, CDCl_3) $\delta = -66.78$ (t, $J=10.8$); HRMS (FAB+): Calcd. for $\text{C}_{13}\text{H}_{24}\text{F}_3\text{O}$ $[\text{M} + \text{H}]^+$: 253.1779; found 253.1768.

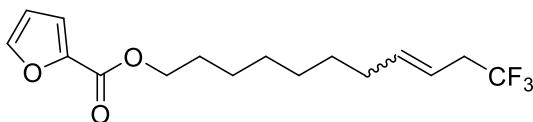


11,11,11-trifluoroundec-8-en-1-ol: A flame-dried round-bottomed flask (250 mL) with a magnetic stir bar was charged with copper(I) thiophene-2-carboxylate (0.73 g, 3.84 mmol, 0.3 eq.), K_2CO_3 (7.08 g, 51.2 mmol, 4.0 eq.) and $\text{PhI}(\text{OAc})_2$

(8.25 g, 25.6 mmol, 2.0 eq.). The reaction vessel was evacuated and put under argon-atmosphere (argon-filled balloon). The salts were dissolved in anhydrous *N*-methyl pyrrolidinone (43 mL) and the terminal alkene (2.54 g, 12.80 mmol, 1.0 eq.) was subsequently added. Finally CF_3SiMe_3 (7.28 g, 51.2 mmol, 4.0 eq.) was added dropwise at 0°C (ice-water bath) and the heterogeneous, blue/cyan reaction mixture was heated to 80 °C and stirred for 24 h. The crude reaction mixture was diluted with Et_2O (100 mL) and filtered through a short pad of Celite[®]. The filtrate was washed with sat. aq. NaCl solution (1x100 mL) and water (1x100 mL), dried over Na_2SO_4 , filtered and concentrated *in vacuo*.

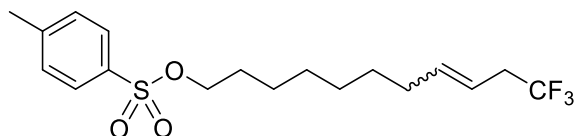
The crude product was then deprotected using K_2CO_3 (8.85 g, 64 mmol, 5.0 eq.) and catalytic KO^tBu in aqueous MeOH (64 mL MeOH and 10 mL water) for 3 h at room temperature.²⁶ The crude mixture was extracted with Et_2O (3x50 mL) and the combined organic extracts were washed water (2x100 mL) and sat. aq. NaCl solution (1x100 mL). The organic phase was then dried over Na_2SO_4 , filtered and concentrated *in vacuo*. Purification by flash column chromatography (SiO_2 , Et_2O /pentane) afforded the final product (1.29 g, 45% yield over two steps): ***E/Z*-ratio: 7.1:1; *E*-isomer: ¹H NMR** (500 MHz, CDCl_3) δ = 5.74 – 5.63 (m, 1H), 5.36 (dt, $J=15.6, 7.1, 1.5, 1\text{H}$), 3.64 (td, $J=6.7, 1.4, 2\text{H}$), 2.81 – 2.71 (m, 2H), 2.08 – 2.01 (m, 2H), 1.61 – 1.52 (m, 2H), 1.43 – 1.24 (m, 8H); **¹³C NMR** (126 MHz, CDCl_3) δ = 138.53, 126.21 (q, $J=276.5$), 117.67 (q, $J=3.6$), 63.19, 37.51 (q, $J=29.5$), 32.89, 32.58, 29.34, 29.11, 28.94, 25.81; **¹⁹F NMR** (376 MHz, CDCl_3) δ

= -66.78 (t, $J=10.9$); **HRMS (EI+)**: Calcd. for $C_{11}H_{17}F_3$ $[M - H_2O]^+$: 206.1282; found 206.1273.



11,11,11-trifluoroundec-8-en-1-yl furan-2-carboxylate: In a flame-dried round-bottomed flask (50 mL) 11,11,11-trifluoroundec-8-en-1-ol (0.20 g, 0.89 mmol, 1.0 eq) was dissolved in anhydrous CH_2Cl_2 (4.5 mL) and pyridine (0.14 mL, 1.78 mmol, 2.0 eq.). Then, furan-2-carbonyl chloride (0.097 g, 0.98 mmol, 1.1 eq.) and catalytic 4-dimethylaminopyridine was added at 0 °C (ice-water bath). The reaction mixture was stirred for 20 h. The crude reaction mixture was diluted with sat. aq. NaCl solution (5 mL) and extracted with CH_2Cl_2 (3x5 mL). The combined organic extracts were washed with aq. HCl solution (1 M; 2x5 mL), water (2x5 mL) and sat. aq. NaCl solution (1x5 mL). The organic phase was then dried over Na_2SO_4 , filtered and concentrated *in vacuo*. Purification by flash column chromatography (SiO_2 , Et_2O /pentane) afforded the product (0.22 g, 78% yield): **E/Z-ratio**: 6.7:1; **E-isomer**: 1H NMR (500 MHz, $CDCl_3$) δ = 7.57 (dt, $J=1.8$, 0.8, 1H), 7.17 (dt, $J=3.5$, 0.8, 1H), 6.50 (ddd, $J=3.5$, 1.7, 0.8, 1H), 5.68 (dt, $J=14.2$, 6.9, 1H), 5.41 – 5.31 (m, 1H), 4.29 (t, $J=6.7$, 2H), 2.75 (dddd, $J=12.0$, 10.9, 9.2, 6.7, 2H), 2.04 (q, $J=7.1$, 2H), 1.74 (p, $J=6.8$, 2H), 1.45 – 1.27 (m, 8H); ^{13}C NMR (126 MHz, $CDCl_3$) δ = 159.00, 146.32, 145.02, 138.47, 126.20 (q, $J=276.4$), 117.83, 117.71 (q, $J=3.7$), 111.92, 65.17, 37.51 (q, $J=29.5$); 32.56,

29.15, 29.01, 28.91, 28.79, 25.96; ^{19}F NMR (282 MHz, CDCl_3) $\delta = -66.88$ (t, $J=10.8$); HRMS (FAB+): Calcd. for $\text{C}_{16}\text{H}_{22}\text{O}_3\text{F}_3$ $[\text{M} + \text{H}]^+$: 319.1521; found 319.1531.

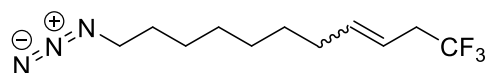


11,11,11-trifluoroundec-8-en-1-yl 4-methylbenzenesulfonate: A round-bottomed flask (100 mL) with magnetic stir bar was charged with 11,11,11-trifluoroundec-8-en-1-ol (0.50 g, 2.23 mmol, 1.0 eq.) dissolved in anhydrous CH_2Cl_2 (7.2 mL). Then triethylamine (0.37 mL, 2.68 mmol, 1.2 eq.), *p*-toluolsulfonyl chloride (0.53 g, 2.79 mmol, 1.25 eq.) and catalytic 4-dimethylaminopyridine was added at 0 °C (ice-water bath). The reaction mixture was stirred at 0 °C for 10 min. and then stirred for 16 h at room temperature.

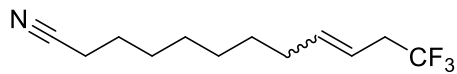
The reaction mixture was diluted with sat. aq. NaCl solution (20 mL) and extracted with CH_2Cl_2 (3x10 mL). The combined organic extracts were then dried over Na_2SO_4 , filtered and concentrated *in vacuo*. Purification by flash column chromatography (SiO_2 , Et_2O /pentane) afforded the product (0.722 g, 86% yield):

E/Z-ratio: 7.2:1; **E-isomer:** ^1H NMR (500 MHz, CDCl_3) $\delta = 7.80 - 7.77$ (m, 2H), 7.36 - 7.32 (m, 2H), 5.71 - 5.63 (m, 1H), 5.39 - 5.31 (m, 1H), 4.01 (td, $J=6.5, 1.0$, 2H), 2.80 - 2.71 (m, 2H), 2.45 (s, 3H), 2.05 - 1.98 (m, 2H), 1.63 (ddt, $J=9.0, 7.9, 5.6$, 2H), 1.36 - 1.19 (m, 8H); ^{13}C NMR (126 MHz, CDCl_3) $\delta = 144.77, 138.39, 133.34, 129.92, 128.01, 126.04$ (q, $J=276.5$), 117.58 (q, $J=3.6$), 70.76, 37.33 (q,

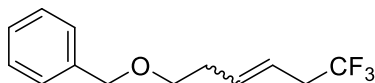
$J=29.6$), 32.49, 28.90, 28.87, 28.82, 25.40, 25.39, 21.76; ^{19}F NMR (282 MHz, CDCl_3) $\delta = -66.75$ (t, $J=10.8$); **HRMS (FAB+)**: Calcd. for $\text{C}_{18}\text{H}_{26}\text{O}_3\text{F}_3\text{S}$ $[\text{M} + \text{H}]^+$: 379.1555; found 379.1563.



11-azido-1,1,1-trifluoroundec-3-ene: In an oven-dried vial (20 mL) with septum, 11,11,11-trifluoroundec-8-en-1-yl 4-methylbenzenesulfonate (200 mg, 0.53 mmol, 1.0 eq.) was dissolved in DMSO (1.1 mL). Then, NaN_3 (41 mg, 0.64 mmol, 1.2 eq.) was added and the reaction mixture was stirred for 20 h at room temperature. The reaction mixture was diluted with water (5 mL) and extracted with Et_2O (3x5 mL). The combined organic extracts were then washed with water (1x10 mL) and sat. aq. NaCl solution (1x10 mL). The organic phase was dried over Na_2SO_4 , filtered and concentrated *in vacuo*. Purification by flash column chromatography (SiO_2 , Et_2O /pentane) afforded the product (129 mg, 98% yield): **E/Z-ratio**: 7.1:1; **E-isomer**: ^1H NMR (500 MHz, CDCl_3) $\delta = 5.68$ (ddd, $J=15.5, 7.5, 6.1$, 1H), 5.37 (dt, $J=15.6, 7.1, 1.5$, 1H), 3.26 (t, $J=6.9$, 2H), 2.81 – 2.71 (m, 2H), 2.08 – 2.02 (m, 2H), 1.59 (dq, $J=8.3, 6.8$, 2H), 1.42 – 1.27 (m, 8H); ^{13}C NMR (126 MHz, CDCl_3) $\delta = 138.44, 126.20$ (q, $J=276.5$), 117.76 (q, $J=3.6$), 51.60, 37.51 (q, $J=29.5$), 32.54, 29.07, 28.98, 28.94, 28.89, 26.79; ^{19}F NMR (376 MHz, CDCl_3) $\delta = -66.76$ (t, $J=10.8$); **HRMS (FAB+)**: Calcd. for $\text{C}_{11}\text{H}_{19}\text{F}_3\text{N}_3$ $[\text{M} + \text{H}]^+$: 250.1531; found 250.1527.

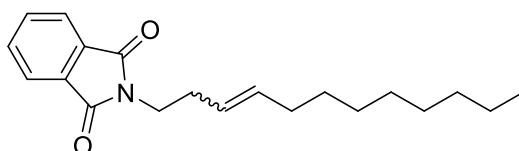


12,12,12-trifluorododec-9-enitrile: In an oven-dried vial (20 mL) with septum, 11,11,11-trifluoroundec-8-en-1-yl 4-methylbenzenesulfonate (200 mg, 0.53 mmol, 1.0 eq.) was dissolved in DMSO (1.1 mL). Then, NaCN (31 mg, 0.64 mmol, 1.2 eq.) was added and the reaction mixture was stirred for 20 h at room temperature. The reaction mixture was diluted with water (5 mL) and extracted with Et₂O (3x5 mL). The combined organic extracts were then washed with water (1x10 mL) and sat. aq. NaCl solution (1x10 mL). The organic phase was dried over Na₂SO₄, filtered and concentrated *in vacuo*. Purification by flash column chromatography (SiO₂, Et₂O/pentane) afforded the product (105 mg, 85% yield): ***E/Z*-ratio:** 10.0:1; ***E*-isomer:** ¹H NMR (500 MHz, CDCl₃) δ = 5.74 – 5.64 (m, 1H), 5.37 (dt, *J*=15.6, 7.1, 1.5, 1H), 2.82 – 2.71 (m, 2H), 2.34 (t, *J*=7.1, 2H), 2.08 – 2.02 (m, 2H), 1.69 – 1.62 (m, 2H), 1.48 – 1.27 (m, 8H); ¹³C NMR (126 MHz, CDCl₃) δ = 138.33, 126.19 (q, *J*=276.5), 119.95, 117.84 (q, *J*=3.5), 37.49 (q, *J*=29.4), 32.49, 28.82, 28.79, 28.71, 28.68, 25.45, 17.26; ¹⁹F NMR (376 MHz, CDCl₃) δ = -66.77 (t, *J*=10.9); **HRMS (FAB+):** Calcd. for C₁₂H₁₉NF₃ [M + H]⁺: 234.1470; found 234.1466.



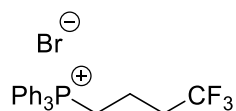
(((6,6,6-trifluorohex-3-en-1-yl)oxy)methyl)benzene: prepared according to a reported protocol.²⁵ Purification by flash column chromatography (SiO₂,

Et₂O/pentane) afforded the product (0.59 g, 38% yield): **E/Z-ratio:** 5.6:1; **E-isomer:** ¹H NMR (500 MHz, CDCl₃) δ = 7.39 – 7.27 (m, 5H), 5.76 (dt, *J*=15.5, 6.8, 1H), 5.49 (dt, *J*=15.6, 7.1, 1.5, 1H), 4.53 (s, 2H), 3.54 (t, *J*=6.6, 2H), 2.80 (ttdd, *J*=10.8, 9.6, 7.1, 1.2, 2H), 2.40 (qq, *J*=6.6, 1.2, 2H); ¹³C NMR (126 MHz, CDCl₃) δ = 138.57, 134.82, 128.52, 127.76, 127.73, 126.14 (q, *J*=276.5), 119.74 (q, *J*=3.6), 73.09, 69.56, 37.58 (q, *J*=29.7), 33.12; ¹⁹F NMR (376 MHz, CDCl₃) δ = -66.63 (t, *J*=10.8); **HRMS (FAB+):** Calcd. for C₁₃H₁₆OF₃ [M + H]⁺: 245.1153; found 245.1152.



2-(dodec-3-en-1-yl)isoindoline-1,3-dione: prepared according to general procedure 2 (1.00 g, 6.02 mmol, 1.0 eq.) and dec-1-ene (5.70 mL, 30.1 mmol, 5.0 eq.). Purification by flash column chromatography (SiO₂, Et₂O/pentane) afforded the product (0.296 g, 38% yield): **E/Z-ratio:** 5.3:1; **E-isomer:** ¹H NMR (500 MHz, CDCl₃) δ = 7.86 – 7.81 (m, 2H), 7.73 – 7.68 (m, 2H), 5.47 – 5.40 (m, 1H), 5.40 – 5.32 (m, 1H), 3.72 (dd, *J*=7.5, 6.7, 2H), 2.37 (qd, *J*=6.8, 1.0, 2H), 1.91 (q, *J*=6.5, 2H), 1.36 – 1.12 (m, 12H), 0.87 (t, *J*=7.2, 3H); ¹³C NMR (126 MHz, CDCl₃) δ = 168.46, 134.11, 133.95, 133.91, 125.75, 123.26, 38.03, 32.62, 32.05, 31.81, 29.58, 29.49, 29.35, 29.20, 22.80, 14.22; **HRMS (FAB+):** Calcd. for C₂₀H₂₈O₂N [M + H]⁺: 314.2120; found 314.2121.

6-bromohexanal was accessed by following a literature procedure.²⁶

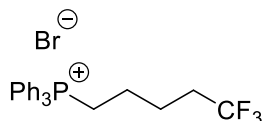


triphenyl(4,4,4-trifluorobutyl)phosphonium bromide: An oven-dried seal tube (15 mL) with stir bar, was charged with triphenylphosphine (1.37 g, 5.24 mmol, 1.0 eq.), 4-bromo-1,1,1-trifluorobutane (1.00 g, 5.24 mmol, 1.0 eq.) and toluene (5.3 mL). The reaction mixture was refluxed for 48 h and then cooled down to room temperature. The yellowish viscous phase was dissolved in CH₂Cl₂ and concentrated *in vacuo* to yield the crude product (1.96 g, quantitative yield). The Wittig salt was used without further purification: **¹H NMR** (500 MHz, CDCl₃) δ = 7.81 (ddt, *J*=12.7, 7.2, 1.4, 6H), 7.75 (tt, *J*=7.5, 1.5, 3H), 7.65 (ddd, *J*=8.7, 7.1, 3.4, 6H), 4.10 – 4.00 (m, 2H), 2.63 (dtd, *J*=18.2, 10.6, 7.5, 2H), 1.88 – 1.76 (m, 2H); **¹³C NMR** (126 MHz, CDCl₃) δ = 135.24 (d, *J*=3.1), 133.70 (d, *J*=10.1), 130.63 (d, *J*=12.6), 126.54 (q, *J*=277.7), 117.82 (dd, *J*=86.4, 3.0), 33.68 (qd, *J*=28.9, 18.0), 21.94 (d, *J*=52.1), 16.01; **¹⁹F NMR** (282 MHz, CDCl₃) δ = -65.98 (td, *J*=10.7, 1.7); **³¹P NMR** (121 MHz, CDCl₃) δ = 24.31 (d, *J*=1.9); **HRMS (FAB+):** Calcd. for C₂₂H₂₁PF₃ [M]⁺: 373.1333; found 373.1345.

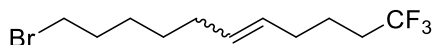


10-bromo-1,1,1-trifluorodec-4-ene: A flame-dried round-bottomed flask (100 mL) was charged with triphenyl(4,4,4-trifluorobutyl)phosphonium bromide

(0.500 g, 1.10 mmol, 1.2 eq.) and anhydrous THF (6.0 mL) at 0 °C (ice-water bath). Potassium *tert*-butoxide (0.134 g, 1.20 mmol, 1.3 eq.) was added to the cooled suspension and the reaction mixture was stirred for 10 min. at 0 °C and 50 min at room temperature. A color change to dark red/orange was observed. Then, the reaction mixture was re-cooled to 0 °C (ice-water bath) and a solution of 6-bromohexanal (0.165 g, 0.92 mmol, 1.0 eq.) in anhydrous THF (1.5 mL) was added dropwise. The reaction mixture was stirred for a further 10 min at 0 °C and 12 h at room temperature. Upon completion of the reaction (as indicated by TLC analysis), the crude reaction mixture was concentrated *in vacuo*. Then, cold pentane was added to precipitate the triphenylphosphine oxide, that was removed by filtration and the filtrate was concentrated *in vacuo*. The so obtained product mixture was purified by flash column chromatography (SiO₂, 100% pentane) to yield the product (0.147 g, 58% yield): ***E/Z*-ratio**: 1:6.2; ***Z*-isomer**: ¹H NMR (500 MHz, CDCl₃) δ = 5.45 (dt, *J*=10.4, 7.2, 1.5, 1H), 5.37 – 5.31 (m, 1H), 3.41 (t, *J*=6.8, 2H), 2.33 – 2.26 (m, 2H), 2.17 – 2.03 (m, 4H), 1.90 – 1.83 (m, 2H), 1.49 – 1.35 (m, 4H); ¹³C NMR (126 MHz, CDCl₃) δ = 131.76, 127.09 (d, *J*=276.7), 126.57, 34.06 (q, *J*=28.2), 33.76, 32.85, 28.78, 27.95, 27.07, 20.15 (q, *J*=3.3); ¹⁹F NMR (282 MHz, CDCl₃) δ = -66.31 (t, *J*=10.9); **HRMS (FAB+)**: Calcd. for C₁₀H₁₆BrF₃ [M + H]⁺: 272.0387; found 272.0363.



triphenyl(5,5,5-trifluoropentyl)phosphonium bromide: An oven-dried seal tube (7 mL) with stir bar, was charged with triphenylphosphine (0.38 g, 1.46 mmol, 1.0 eq.), 5-bromo-1,1,1-trifluoropentane (0.30 g, 1.46 mmol, 1.0 eq.) and toluene (1.5 mL). The reaction mixture was refluxed for 48 h and then cooled down to room temperature. The yellowish viscous phase was dissolved in CH₂Cl₂ and concentrated *in vacuo* to yield the crude product (526 mg, 93% yield). The Wittig salt was used without further purification: **¹H NMR** (500 MHz, CDCl₃) δ = 7.91 – 7.85 (m, 6H), 7.82 – 7.77 (m, 3H), 7.73 – 7.67 (m, 6H), 4.00 (dddd, *J*=13.1, 8.1, 5.5, 2.6, 2H), 2.20 (qt, *J*=11.1, 7.1, 2H), 1.99 (p, *J*=7.3, 2H), 1.74 (td, *J*=16.3, 8.8, 2H); **¹³C NMR** (126 MHz, CDCl₃) δ = 135.18 (d, *J*=3.1), 133.93 (d, *J*=10.0), 130.65 (d, *J*=12.4), 127.23 (q, *J*=276.9), 118.51 (d, *J*=85.4), 32.95 (q, *J*=28.5, 27.8), 22.96 (d, *J*=51.2), 22.89 (ddd, *J*=18.4, 6.5, 3.6), 21.80 (q, *J*=3.7); **¹⁹F NMR** (282 MHz, CDCl₃) δ = -65.37 (t, *J*=11.1); **³¹P NMR** (121 MHz, CDCl₃) δ = 24.53; **HRMS (FAB+):** Calcd. for C₂₂H₂₃PF₃ [M]⁺: 387.1489; found 387.1473.

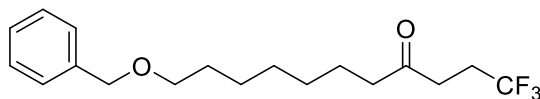


11-bromo-1,1,1-trifluoroundec-5-ene: A flame-dried round-bottomed flask (100 mL) was charged with triphenyl(5,5,5-trifluoropentyl)phosphonium bromide and anhydrous THF (6.0 mL) at 0°C (ice-water bath). Potassium *tert*-butoxide (0.130 g, 1.16 mmol, 1.3 eq.) was added to the cooled suspension and the

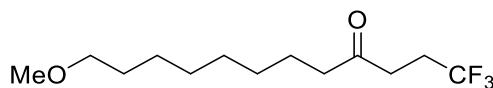
reaction mixture was stirred for 10 min. at 0 °C and 50 min at room temperature. A color change to dark red/orange was observed. Then, the reaction mixture was re-cooled to 0 °C (ice-water bath) and a solution of 6-bromohexanal (0.160 g, 0.89 mmol, 1.0 eq.) in anhydrous THF (1.5 mL) was added dropwise. The reaction mixture was stirred for a further 10 min at 0 °C and 14 h at room temperature.

Upon completion of the reaction (as indicated by TLC analysis), the crude reaction mixture was concentrated *in vacuo*. Then, cold pentane was added to precipitate the triphenylphosphine, which was removed by filtration, and the filtrate was concentrated *in vacuo*. The so obtained product mixture was purified by flash column chromatography (SiO₂, 100% pentane) (0.101 g, 40% yield): **E/Z-ratio:** 1:16; **Z-isomer:** ¹H NMR (500 MHz, CDCl₃) δ = 5.46 – 5.39 (m, 1H), 5.36 – 5.29 (m, 1H), 3.41 (t, *J*=6.8, 2H), 2.15 – 2.00 (m, 6H), 1.89 – 1.82 (m, 2H), 1.65 – 1.58 (m, 2H), 1.48 – 1.41 (m, 2H), 1.41 – 1.34 (m, 2H); ¹³C NMR (126 MHz, CDCl₃) δ = 131.21, 128.38, 127.41 (q, *J*=276.2), 33.81, 33.33 (q, *J*=28.5), 32.87, 28.91, 27.99, 27.19, 26.25, 22.06 (q, *J*=2.9); ¹⁹F NMR (282 MHz, CDCl₃) δ = -66.31 (t, *J*=10.9); **HRMS (FAB+):** Calcd. for C₁₁H₁₈BrF₃ [M + H]⁺: 286.0544; found 286.0509.

Product Characterization

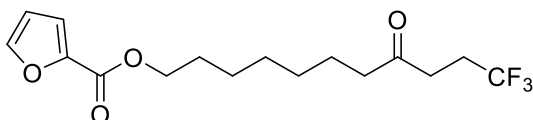


11-(benzyloxy)-1,1,1-trifluoroundecan-4-one (Table 5.1, Entry 1): prepared according to general procedure 1. Purification by flash column chromatography (SiO₂) provided 119 mg (72% yield) in \geq 20:1 selectivity: **¹H NMR** (500 MHz, CDCl₃) δ = 7.37 – 7.26 (m, 5H), 4.50 (s, 2H), 3.46 (t, J =6.6, 2H), 2.70 – 2.63 (m, 2H), 2.47 – 2.35 (m, 4H), 1.64 – 1.55 (m, 4H), 1.41 – 1.25 (m, 6H); **¹³C NMR** (126 MHz, CDCl₃) δ = 207.29, 138.77, 128.45, 127.72, 127.59, 127.10 (q, J =275.7), 72.98, 70.49, 42.87, 34.94 (q, J =2.7), 29.80, 29.29, 29.18, 28.00 (q, J =29.8), 26.13, 23.78; **¹⁹F NMR** (376 MHz, CDCl₃) δ = -66.65 (t, J =10.9); **HRMS (EI+):** Calcd. for C₁₈H₂₅O₂F₃ [M]⁺: 330.1807; found 330.1809.



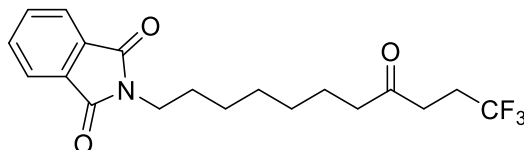
1,1,1-trifluoro-12-methoxydodecan-4-one (Table 5.1, Entry 2): prepared according to general procedure 1. Purification by flash column chromatography (SiO₂) provided 61 mg (91% yield) in \geq 20:1 selectivity. The Wacker-type oxidation was also performed on a larger scale (1.0 g, 4.0 mmol, 1.0 eq.) to yield (after purification) 747 mg (70% yield) in \geq 20:1 selectivity: **¹H NMR** (500 MHz, CDCl₃) δ = 3.35 (t, J =6.6, 2H), 3.32 (s, 3H), 2.67 – 2.62 (m, 2H), 2.46 – 2.34 (m, 4H), 1.62 – 1.52 (m, 4H), 1.36 – 1.23 (m, 8H); **¹³C NMR** (126 MHz, CDCl₃) δ =

207.22, 127.11 (q, $J=275.7$), 73.00, 58.61, 42.91, 34.94 (q, $J=2.6$), 29.73, 29.39, 29.37, 29.18, 28.04 (q, $J=29.8$), 26.19, 23.85; ^{19}F NMR (282 MHz, CDCl_3) $\delta = -66.64$ (t, $J=10.8$); **HRMS (FAB+)**: Calcd. for $\text{C}_{13}\text{H}_{24}\text{O}_2\text{F}_3$ $[\text{M} + \text{H}]^+$: 269.1728; found 269.1741.



11,11,11-trifluoro-8-oxoundecyl furan-2-carboxylate (Table 5.1, Entry 3):

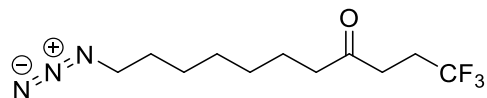
prepared according to general procedure 1. Purification by flash column chromatography (SiO_2) provided 63 mg (75% yield) in $\geq 20:1$ selectivity; ^1H NMR (500 MHz, CDCl_3) $\delta = 7.57$ (dd, $J=1.7, 0.9$, 1H), 7.17 (dd, $J=3.5, 0.9$, 1H), 6.50 (dd, $J=3.5, 1.7$, 1H), 4.29 (t, $J=6.7$, 2H), 2.70 – 2.64 (m, 2H), 2.47 – 2.42 (m, 2H), 1.74 (dq, $J=8.2, 6.7$, 2H), 1.63 – 1.57 (m, 2H), 1.46 – 1.26 (m, 8H); ^{13}C NMR (126 MHz, CDCl_3) $\delta = 207.25, 158.98, 146.34, 144.99, 127.11$ (q, $J=275.8$), 117.88, 111.94, 65.10, 42.87, 35.03 (q, $J=2.5$), 29.12, 29.10, 28.76, 28.04 (q, $J=29.9$), 25.85, 23.74; ^{19}F NMR (282 MHz, CDCl_3) $\delta = -66.64$ (t, $J=10.9$); **HRMS (FAB+)**: Calcd. for $\text{C}_{16}\text{H}_{22}\text{O}_4\text{F}_3$ $[\text{M} + \text{H}]^+$: 335.1470; found 335.1483.



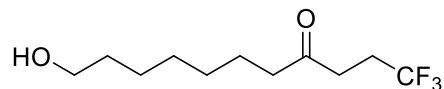
2-(11,11,11-trifluoro-8-oxoundecyl)isoindoline-1,3-dione (Table 5.1, Entry 4):

prepared according to general procedure 1. Purification by flash column

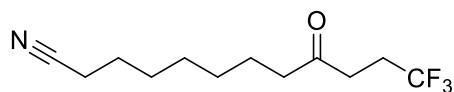
chromatography (SiO₂) provided 78 mg (85% yield) in \geq 20:1 selectivity: **¹H NMR** (500 MHz, CDCl₃) δ = 7.85 – 7.80 (m, 2H), 7.72 – 7.68 (m, 2H), 3.68 – 3.64 (m, 2H), 2.68 – 2.63 (m, 2H), 2.46 – 2.33 (m, 4H), 1.70 – 1.62 (m, 2H), 1.61 – 1.53 (m, 2H), 1.36 – 1.23 (m, 6H); **¹³C NMR** (126 MHz, CDCl₃) δ = 207.25, 168.59, 133.99, 132.27, 127.11 (q, J =275.8), 123.28, 42.82, 38.04, 34.99 (q, J =2.5), 29.06, 28.96, 28.61, 28.02 (q, J =29.8), 26.72, 23.71; **¹⁹F NMR** (282 MHz, CDCl₃) δ = -66.64 (t, J =10.9); **HRMS (FAB+)**: Calcd. for C₁₉H₂₃NO₃F₃ [M + H]⁺: 370.1630; found 370.1648.



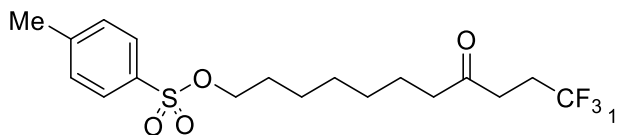
11-azido-1,1,1-trifluoroundecan-4-one (Table 5.1, Entry 5): prepared according to general procedure 1. Purification by flash column chromatography (SiO₂) provided 51 mg (77% yield) in \geq 20:1 selectivity: **¹H NMR** (300 MHz, CDCl₃) δ = 3.26 (t, J =6.9, 2H), 2.67 (dd, J =8.7, 6.7, 2H), 2.50 – 2.32 (m, 4H), 1.66 – 1.56 (m, 4H), 1.42 – 1.24 (m, 6H); **¹³C NMR** (126 MHz, CDCl₃) δ = 207.22, 127.10 (q, J =275.6), 51.56, 42.86, 35.04 (q, J =2.6), 29.11, 29.04, 28.91, 28.05 (q, J =29.8), 26.66, 23.71; **¹⁹F NMR** (376 MHz, CDCl₃) δ = -66.65 (t, J =10.9); **HRMS (FAB+)**: Calcd. for C₁₁H₁₉N₃OF₃ [M + H]⁺: 266.1480; found 266.1490.



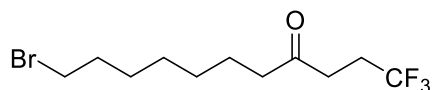
1,1,1-trifluoro-11-hydroxyundecan-4-one (Table 5.1, Entry 6): prepared according to general procedure 1. Purification by flash column chromatography (SiO₂) provided 50 mg (84% yield) in \geq 20:1 selectivity: **¹H NMR** (500 MHz, CDCl₃) δ = 3.64 (t, J =6.6, 2H), 2.67 (dd, J =8.6, 6.8, 2H), 2.47 – 2.34 (m, 4H), 1.58 (dddd, J =17.3, 13.0, 8.3, 6.9, 4H), 1.39 – 1.27 (m, 6H); **¹³C NMR** (126 MHz, CDCl₃) δ = 207.36, 127.10 (q, J =275.6), 63.09, 42.91, 35.01 (q, J =2.6), 32.80, 29.27, 29.21, 28.03 (q, J =29.8), 25.67, 23.77; **¹⁹F NMR** (376 MHz, CDCl₃) δ = -66.65 (t, J =10.9); **HRMS (FAB+):** Calcd. for C₁₁H₂₀O₂F₃ [M + H]⁺: 241.1415; found 241.1417.



12,12,12-trifluoro-9-oxododecanenitrile (Table 5.1, Entry 7): prepared according to general procedure 1. Purification by flash column chromatography (SiO₂) provided 47 mg (75% yield) in \geq 20:1 selectivity: **¹H NMR** (400 MHz, CDCl₃) δ = 2.66 (t, J =7.7, 2H), 2.47 – 2.29 (m, 6H), 1.62 (tt, J =14.5, 7.1, 4H), 1.44 (p, J =6.8, 2H), 1.31 (qd, J =10.3, 8.9, 5.5, 4H); **¹³C NMR** (126 MHz, CDCl₃) δ = 207.10, 127.07 (q, J =275.7), 119.87, 42.74, 35.00 (q, J =2.5), 28.90, 28.66, 28.56, 27.99 (q, J =29.8), 25.38, 23.59, 17.23; **¹⁹F NMR** (376 MHz, CDCl₃) δ = -66.66 (t, J =10.9); **HRMS (FAB+):** Calcd. for C₁₂H₁₉NOF₃ [M + H]⁺: 250.1419; found 250.1412.



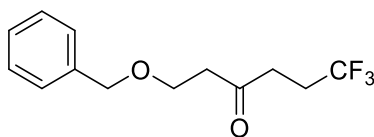
11,11,11-trifluoro-8-oxoundecyl 4-methylbenzenesulfonate (Table 5.1, Entry, 8): prepared according to general procedure 1. Purification by flash column chromatography (SiO₂) provided 81 mg (82% yield) in $\geq 20:1$ selectivity: **¹H NMR** (300 MHz, CDCl₃) δ = 7.78 (d, $J=8.2$, 2H), 7.35 (dt, $J=7.6$, 0.9, 2H), 4.01 (t, $J=6.4$, 2H), 2.66 (dd, $J=8.6$, 6.6, 2H), 2.49 – 2.31 (m, 7H), 1.70 – 1.48 (m, 4H), 1.26 (tq, $J=8.2$, 3.6, 6H); **¹³C NMR** (126 MHz, CDCl₃) δ = 207.03, 144.67, 133.14, 129.80, 127.85, 126.94 (q, $J=275.7$), 70.52, 42.63, 34.85 (q, $J=2.5$), 28.82, 28.72, 28.64, 27.86 (q, $J=29.8$), 25.15, 23.46, 21.62; **¹⁹F NMR** (282 MHz, CDCl₃) δ = -66.63 (t, $J=10.8$); **HRMS (FAB+):** Calcd. for C₁₈H₂₆O₄F₃S [M + H]⁺: 395.1504; found 395.1511.



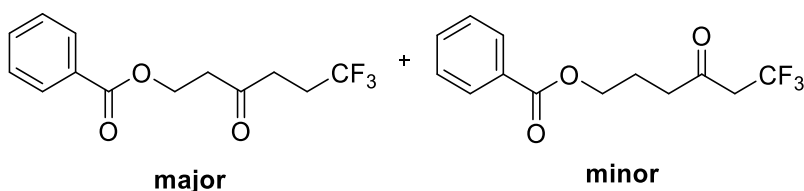
11-bromo-1,1,1-trifluoroundecan-4-one (Table 5.1, Entry 9): Compound **S10** was prepared according to general procedure 1. Purification by flash column chromatography (SiO₂) provided 47 mg (74% yield) in $\geq 20:1$ selectivity: **¹H NMR** (500 MHz, CDCl₃) δ = 3.40 (t, $J=6.8$, 2H), 2.67 (dd, $J=8.5$, 6.8, 2H), 2.47 – 2.35 (m, 4H), 1.88 – 1.81 (m, 2H), 1.63 – 1.56 (m, 2H), 1.43 (dtdd, $J=9.4$, 7.1, 5.5, 1.5, 2H), 1.36 – 1.24 (m, 4H); **¹³C NMR** (126 MHz, CDCl₃) δ = 207.22, 127.10 (q, $J=275.7$), 42.86, 35.04 (q, $J=2.4$), 34.03, 32.81, 29.07, 28.65, 28.08, 28.05 (q,

$J=29.8$), 23.71; ^{19}F NMR (376 MHz, CDCl_3) $\delta = -66.65$ (t, $J=10.9$); HRMS

(FAB+): Calcd. for $\text{C}_{11}\text{H}_{19}\text{BrOF}_3$ [$\text{M} + \text{H}$] $^+$: 303.0571; found 303.0581.

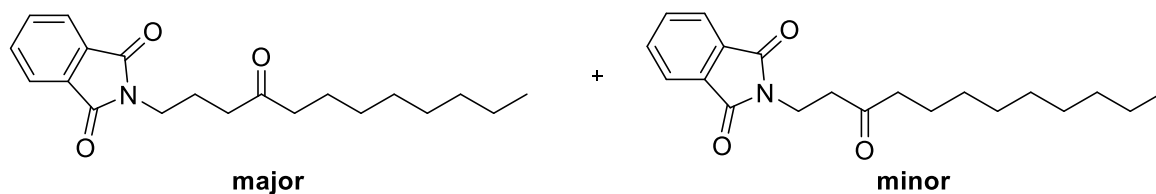


1-(benzyloxy)-6,6,6-trifluorohexan-3-one (Figure 5.2): prepared according to general procedure 1. Purification by flash column chromatography (SiO_2) provided 51 mg (79% yield) in $\geq 20:1$ selectivity (distal oxidation/proximal oxidation): ^1H NMR (300 MHz, CDCl_3) $\delta = 7.40 - 7.26$ (m, 5H), 4.51 (s, 2H), 3.75 (td, $J=6.1, 0.7$, 2H), 2.77 – 2.70 (m, 4H), 2.50 – 2.33 (m, 2H); ^{13}C NMR (126 MHz, CDCl_3) $\delta = 205.62, 138.00, 128.58, 127.92, 127.84, 127.07$ (q, $J=275.7$), 73.46, 65.25, 43.07, 35.77 (q, $J=2.5$), 27.89 (q, $J=29.8$); ^{19}F NMR (282 MHz, CDCl_3) $\delta = -66.61$ (t, $J=10.9$); HRMS (FAB+): Calcd. for $\text{C}_{13}\text{H}_{14}\text{O}_2\text{F}_3$ [($\text{M} + \text{H}$) – H_2] $^+$: 259.0947; found 259.0946.

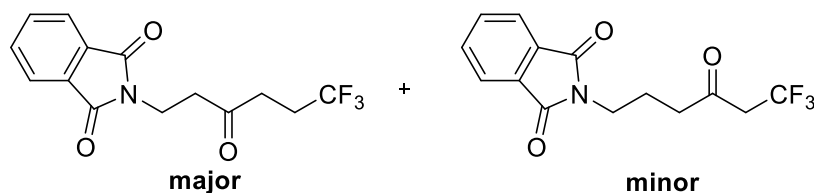


6,6,6-trifluoro-3-oxohexyl benzoate (Figure 5.2): prepared according to general procedure 1. Purification by flash column chromatography (SiO_2) provided 36 mg (53% yield) as a mixture of regioisomers in 15:1 selectivity (average selectivity of two experiments; distal oxidation/proximal oxidation). Only

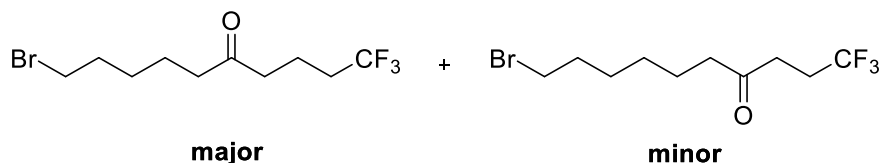
NMR-shifts of the major regioisomer are reported: **¹H NMR** (500 MHz, CDCl₃) δ = 8.01 – 7.98 (m, 2H), 7.59 – 7.54 (m, 1H), 7.46 – 7.41 (m, 2H), 4.61 (t, *J*=6.2, 2H), 2.93 (t, *J*=6.2, 2H), 2.77 (dd, *J*=8.4, 6.9, 2H), 2.51 – 2.40 (m, 2H); **¹³C NMR** (126 MHz, CDCl₃) δ = 204.08, 166.49, 133.31, 129.91, 129.71, 128.55, 126.95 (q, *J*=275.6), 59.72, 41.75; 35.62 (q, *J*=2.7), 27.90 (q, *J*=30.0); **¹⁹F NMR** (282 MHz, CDCl₃) δ = -66.64 (d, *J*=21.3); **HRMS (FAB+)**: Calcd. for C₁₃H₁₄O₃F₃ [M + H]⁺: 275.0895; found 275.0901.



2-(4-oxododecyl)isoindoline-1,3-dione (Figure 5.2): prepared according to general procedure 1. Purification by flash column chromatography (SiO₂) provided 63 mg (77% yield) as a mixture of regioisomers in 2:1 selectivity (distal oxidation/proximal oxidation). Only NMR-shifts of the major regioisomer are reported: **¹H NMR** (500 MHz, CDCl₃) δ = 7.86 – 7.81 (m, 2H), 7.73 – 7.68 (m, 2H), 3.70 (t, *J*=6.7, 2H), 2.46 (t, *J*=7.2, 2H), 2.38 (t, *J*=7.5, 2H), 1.95 (p, *J*=7.0, 2H), 1.59 – 1.49 (m, 2H), 1.31 – 1.20 (m, 10H), 0.89 – 0.84 (m, 3H); **¹³C NMR** (126 MHz, CDCl₃) δ = 209.99, 168.57, 134.07, 132.21, 123.36, 42.96, 39.81, 37.47, 31.95, 29.50, 29.35, 29.26, 23.89, 22.82, 22.78, 14.23; **HRMS (FAB+)**: Calcd. for C₂₀H₂₈O₃N [M + H]⁺: 330.2069; found 330.2074.

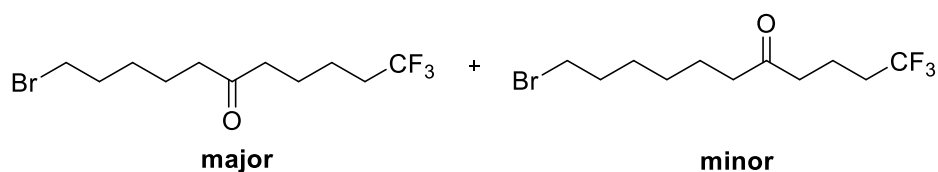


2-(6,6,6-trifluoro-3-oxohexyl)isoindoline-1,3-dione (Figure 5.2): prepared according to general procedure 1. Purification by flash column chromatography (SiO₂) provided 38 mg (51% yield) as a mixture of regioisomers in 18:1 selectivity (average selectivity of two experiments; distal oxidation/proximal oxidation). Only NMR-shifts of the major regioisomer are reported: **¹H NMR** (500 MHz, CDCl₃) δ = 7.86 – 7.82 (m, 2H), 7.76 – 7.68 (m, 2H), 3.98 (dd, *J*=7.5, 6.9, 2H), 2.89 (t, *J*=7.2, 2H), 2.75 – 2.71 (m, 2H), 2.47 – 2.37 (m, 2H); **¹³C NMR** (126 MHz, CDCl₃) δ = 204.30, 168.19, 134.24, 132.09, 126.96 (q, *J*=275.9), 123.49, 40.87, 35.11 (q, *J*=2.6), 32.99, 27.90 (q, *J*=30.0); **¹⁹F NMR** (376 MHz, CDCl₃) δ = -66.66 (t, *J*=10.8); **HRMS (FAB+):** Calcd. for C₁₄H₁₃O₃NF₃ [M + H]⁺: 300.0848; found 300.0834.



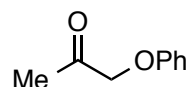
10-bromo-1,1,1-trifluorodecan-5-one and 10-bromo-1,1,1-trifluorodecan-4-one (Table 5.2, entry 2): prepared according to general procedure 1. Purification by flash column chromatography (SiO₂, Et₂O/pentane) provided 25 mg (86% yield) as a mixture of regioisomers in 5.5:1 selectivity (distal oxidation/proximal oxidation): **¹H NMR** (500 MHz, Chloroform-*d*) δ = 3.41 (t, *J*=6.7, 2H; major), 3.40

(t, $J=6.8$, 2H; minor), 2.69 – 2.64 (m, 2H; minor), 2.51 (t, $J=7.1$, 2H; major), 2.46 (t, $J=7.4$, 2H; minor), 2.43 (t, $J=7.3$, 2H; major), 2.44 – 2.35 (m, 2H; minor), 2.17 – 2.05 (m, 2H; major), 1.90 – 1.80 (m, major: 4H, minor 2H), 1.64 – 1.57 (m, 2H), 1.47 – 1.39 (m, 2H), 1.35 – 1.27 (m, 2H; minor); **^{13}C NMR** (126 MHz, CDCl_3) δ = 209.09 (major), 206.88 (minor), 127.18 (q, $J=276.7$; major), 127.11 (d, $J=275.8$; minor), 42.69 (minor), 42.66 (major), 41.04 (major), 35.02 (q, $J=2.5$; minor), 33.72 (minor), 33.50 (major), 33.03 (q, $J=28.7$; major), 32.68 (major), 32.63 (minor), 28.36 (minor), 28.08 (q, $J=29.8$; minor), 27.99 (minor), 27.88 (major), 23.59 (minor), 22.99 (major), 16.27 (q, $J=3.3$; major); **^{19}F NMR** (282 MHz, CDCl_3) δ = -66.21 (t, $J=10.8$, major), -66.65 (t, $J=10.9$, minor); **HRMS (FAB+)**: Calcd. for $\text{C}_{10}\text{H}_{16}\text{BrF}_3\text{O}$ [$\text{M} + \text{H}$] $^+$: 288.0337; found 288.0346.

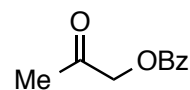


11-bromo-1,1,1-trifluoroundecan-6-one and 11-bromo-1,1,1-trifluoroundecan-5-one (Table 5.2, Entry 3): prepared according to general procedure 1. Purification by flash column chromatography (SiO_2 , Et_2O /pentane) provided 22 mg (74% yield) as a mixture of regioisomers in 1.9:1 selectivity (distal oxidation/proximal oxidation): **^1H NMR** (500 MHz, CDCl_3) δ = 3.41 (t, $J=6.7$, 2H; major), 3.40 (t, $J=6.8$, 2H; minor), 2.50 (t, $J=7.1$, 2H; minor), 2.43 (q, $J=7.3$, 4H; major), 2.43 – 2.39 (m, 2H; minor), 2.14 – 2.03 (m, 2H), 1.90 – 1.83 (m, 2H), 1.68 – 1.51 (m, major: 6H; minor: 4H), 1.47 – 1.40 (m, 2H), 1.34 – 1.27 (m, 2H);

minor); **¹³C NMR** (126 MHz, CDCl₃) δ = 209.79 (major), 209.31 (minor), 127.20 (q, *J*=276.3; major), 127.19 (q, *J*=276.4; minor), 42.76 (minor), 42.70 (major), 42.29 (major), 41.01 (minor), 33.84 (q, *J*=28.5; major), 33.76 (minor), 33.53 (major), 33.04 (q, *J*=28.7; minor), 32.71 (major), 32.68 (minor), 28.45 (minor), 28.04 (minor), 27.92 (major), 23.67 (minor), 23.03 (major), 22.89 (major), 21.75 (q, *J*=3.1; major), 16.28 (q, *J*=3.2; minor); **¹⁹F NMR** (282 MHz, CDCl₃) δ = -66.21 (t, *J*=10.8, minor); -66.41 (t, *J*=10.9, major); **HRMS (FAB+)**: Calcd. for C₁₁H₁₉F₃OBr [M + H]⁺: 303.0571; found (major) 303.0562; found (minor) 303.0565.

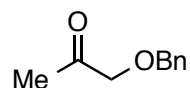


1-phenoxypropan-2-one (Table 5.3, Entry 1): prepared according to general procedure 3. Purification by flash column chromatography (SiO₂) provided 118 mg (88% yield) in ≥ 89:11 selectivity. **¹H NMR** (400 MHz, CDCl₃) δ 7.36 – 7.28 (m, 2H), 7.02 (tt, *J* = 7.3, 1.1 Hz, 1H), 6.91 (dt, *J* = 7.8, 1.0 Hz, 2H), 4.55 (s, 2H), 2.30 (s, 3H).

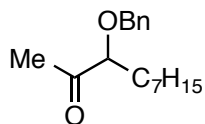


2-oxopropyl benzoate (Table 5.3, Entry 2): prepared according to general procedure 3. Purification by flash column chromatography (SiO₂) provided 118.5

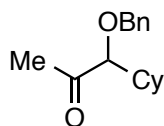
mg (83% yield) in \geq 80:20 selectivity. $^1\text{H NMR}$ (400 MHz, CDCl_3) δ 8.17 – 8.06 (m, 2H), 7.65 – 7.60 (m, 1H), 7.52 – 7.46 (m, 2H), 4.91 (s, 2H), 2.27 (s, 3H).



1-(benzyloxy)propan-2-one (Table 5.3, Entry 4): prepared according to general procedure 3. Purification by flash column chromatography (SiO_2) provided 142.9 mg (87% yield) in \geq 89:11 selectivity. $^1\text{H NMR}$ (300 MHz, CDCl_3) δ 7.41 – 7.28 (m, 5H), 4.60 (s, 2H), 4.06 (s, 2H), 2.17 (s, 3H).



3-(benzyloxy)decan-2-one (Table 5.3, Entry 6): prepared according to general procedure 3. Purification by flash column chromatography (SiO_2) provided 235.4 mg (90% yield) in 95:5 selectivity. $^1\text{H NMR}$ (400 MHz, CDCl_3) δ 7.41 – 7.31 (m, 3H), 4.64 – 4.57 (m, 1H), 4.48 – 4.42 (m, 1H), 3.78 (dd, $J = 7.8, 5.1$ Hz, 1H), 2.20 (s, 3H), 1.80 – 1.56 (m, 2H), 1.50 – 1.20 (m, 10H), 0.93 – 0.85 (m, 2H).



1-(benzyloxy)-1-cyclohexylpropan-2-one (Table 5.3, Entry 7): prepared according to general procedure 3. Purification by flash column chromatography

(SiO₂) provided 224.2 mg (91% yield) in \geq 94:6 selectivity. ¹H NMR (400 MHz, CDCl₃) δ 7.45 – 7.30 (m, 5H), 4.59 (d, *J* = 11.6 Hz, 1H), 4.39 (d, *J* = 11.7 Hz, 1H), 3.49 (d, *J* = 6.8 Hz, 1H), 2.18 (s, 3H), 1.89 (brd, 1H), 1.80 – 1.63 (m, 5H), 1.49 (dd, *J* = 12.6, 3.4 Hz, 1H), 1.39 – 1.04 (m, 5H).

References

- (1) Muzart, J. *Tetrahedron* **2007**, *63*, 7505.
- (2) Sigman, M. S.; Werner, E. W. **2012**, *45*, 874.
- (3) Takacs, J.; Jiang, X.-T. *Curr. Org. Chem.* **2003**, *7*, 369.
- (4) Choi, P. J.; Sperry, J.; Brimble, M. A. *J. Org. Chem.* **2010**, *75*, 7388.
- (5) Lai, J.; Shi, X.; Dai, L. *J. Org. Chem.* **1992**, *57*, 3485.
- (6) Tsuji, J.; Nagashima, H.; Hori, K. *Tetrahedron Letters* **1982**.
- (7) Michel, B. W.; Sigman, M. S.; McCombs, J. R.; Winkler, A. *Angew. Chem. Int. Ed.* **2010**, *49*, 7312.
- (8) Michel, B. W.; Camelio, A. M.; Cornell, C. N.; Sigman, M. S. *J. Am. Chem. Soc.* **2009**, *131*, 6076.
- (9) Mahatthananchai, J.; Dumas, A. M.; Bode, J. W. *Angew. Chem. Int. Ed.* **2012**, *51*, 10954.
- (10) Tsuji, J. *Synthesis* **1984**, 369.
- (11) Tsuji, J. *Palladium Reagents and Catalysts: New Perspectives for the 21st Century*, 2nd ed.; Wiley, **2004**.
- (12) Gaunt, M. J.; Yu, J.; Spencer, J. B. *Chem. Commun.* **2001**, 1844.
- (13) Wright, J. A.; Gaunt, M. J.; Spencer, J. B. *Chem. Eur. J.* **2006**, *12*, 949.

- (14) Trost, B. M.; Czabaniuk, L. C. *Angew. Chem. Int. Ed.* **2014**, *53*, 2826.
- (15) Mei, T.-S.; Patel, H. H.; Sigman, M. S. *Nature* **2014**, *508*, 340.
- (16) Sigman, M. S.; Mei, T.-S.; Werner, E. W.; Burckle, A. J. *J. Am. Chem. Soc.* **2013**, *135*, 6830.
- (17) Morandi, B.; Wickens, Z. K.; Grubbs, R. H. *Angew. Chem. Int. Ed.* **2013**, *52*, 2944.
- (18) Morandi, B.; Wickens, Z. K.; Grubbs, R. H. *Angew. Chem. Int. Ed. Engl.* **2013**, *52*, 9751.
- (19) Hansch, C.; Leo, A.; Taft, R. W. *Chem. Rev.* **1991**, *91*, 165.
- (20) Neuvonen, H.; Neuvonen, K.; Koch, A.; Kleinpeter, E.; Pasanen, P. *J. Org. Chem.* **2002**, *67*, 6995.
- (21) Verma, R. P.; Hansch, C. *Chem. Rev.* **2011**, *111*, 2865.
- (22) Rooke, D. A.; Ferreira, E. M. *Angew. Chem. Int. Ed.* **2012**, *51*, 3225.
- (23) Rooke, D. A.; Menard, Z. A.; Ferreira, E. M. *Tetrahedron* **2014**, *70*, 4232.
- (24) No significant variation in regioselectivity was observed between the Brønsted acid free and the HBF₄ Wacker oxidations discussed.
- (26) Chu, L.; Qing, F.-L. *Org. Lett.* **2012**, *14*, 2106-2109.
- (27) Wuts, P. G. M.; Greene, T. W. in *Greene's Protective Groups in Organic Synthesis*, John Wiley & Sons, Inc., **2006**, pp. 230.
- (28) Hester, J. B.; Gibson, J. K.; Buchanan, L. V.; Cimini, M. G.; Clark, M. A.; Emmert, D. E.; Glavanovich, M. A. I Imbordino, R. J.; LeMay, R. J.;

McMillan, M. W.; Perricone, S. C.; Squires, D. M.; Walters, R. R. *J. Med. Chem.* **2001**, *44*, 1099-1115.